MODELLING OF BOUYANCY-INDUCED HYDROMAGNETIC COUPLE STRESS FLUID FLOW WITH PERIODIC HEAT INPUT

by

CYNTHIA REITUMETSE MAKHALEMELE

THESIS Submitted in fulfilment of the requirements for the degree of

Doctor of Philosophy

in

Applied Mathematics

in the

FACULTY OF SCIENCE AND AGRICULTURE

(School of Mathematical and Computer Sciences)

at the

UNIVERSITY OF LIMPOPO

Supervisor: Dr. Lazarus Rundora

Co-Supervisor: Dr. S.O Adesanya (Redeemer's University, Nigeria)

2020

DECLARATION

I declare that the thesis hereby submitted to the University of Limpopo, for the degree of Doctor of Philosophy in Applied Mathematics has not previously been submitted by me for a degree at this or any other university; that it is my work in design and in execution, and that all material contained herein has been duly acknowledged.

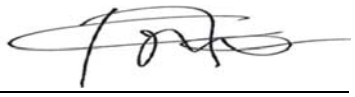

Makhalemele, CR (Mrs) 24 November 2020

ACKNOWLEDGEMENTS

I would like to express my sincere gratitude to my supervisor Dr. Lazarus Rundora and my co-supervisor Dr. Samuel Adesanya for the project, their assistance, patience and always encouraging me to work harder. My appreciation also goes to my employer the Vaal University of Technology for funding my studies and to the University of Limpopo for the opportunity to study for this degree. I also want to thank Dr. Zimba for encouraging me to study and Dr. Mahlobo for always allowing me time to go visit my supervisor. My colleagues in the Mathematics department I can't thank you enough for always making sure my classes are taken care of whenever I'm away. My husband Amulet Makhalemele and my kids, Thato and Tshiamo thank you so much for your love, patience and the support you gave me throughout my studies. Above all I give honour to the Almighty God for giving me strength to make it against all odds.

DEDICATION

To my mother Anna Ndaba, my husband and my kids, this is for you.

To God almighty and all people who played a major role in encouraging me to further my studies.

ABSTRACT

The flow of electrically conducting fluids in the presence of a magnetic field has wide applications in science, engineering and technology. Examples of the applications include industrial processes such as the cooling of reactors, extrusion of plastics, purification of crude oil, medical applications, aerodynamics and many more. The induced magnetic field usually act as a flow control mechanism, especially under intense heat. In this study a couple stress fluid in a channel will be used as the working fluid. Channel flow and heat transfer characteristics of couple stress fluids find applications in processes such as the extrusion of polymer fluids, solidification of liquid crystals, cooling of metallic plates in a bath, tribology of thrust bearings and lubrication of engine rod bearings. One major characteristic that distinguishes the couple stress fluid from other non-Newtonian fluids is the inclusion of size-dependent microstructure that is of mechanical significance. As such, the couple stress constitutive model is capable of describing the couple stresses, the effect of body couples and the non-symmetric tensors manifested in several real fluids of technological importance.

A fully developed laminar magnetohydrodynamic (MHD) flow of an incompressible couple stress fluid through a vertical channel due to a steady-periodic temperature on the channel plates is investigated. Specifically, the effects of couple stresses and internal heat generation on MHD natural convection flow with steady-periodic heat input, the impact of magnetic field induction on the buoyancy-induced oscillatory flow of couple stress fluid with varying heating and a mixed convective two dimensional flow of unsteady MHD couple stress fluid through a channel field with porous medium are studied. Analytical methods and the semi-analytic Adomian decomposition method will be used to solve the resulting non-linear differential equations governing the flow systems. Useful results for velocity, temperature, skin friction and Nusselt number are obtained and discussed quantitatively. The effects of the various flow governing parameters on the flow field are investigated.

NOMENCLATURE

T - Temperature of the fluid,

c_p - Specific heat at constant pressure,

g - Gravitational acceleration,

h - Half the channel width,

y - Horizontal coordinate,

t - Time,

T_0, T_1, T_2 - Fixed wall temperatures,

u' - Dimensional velocity,

u - Velocity,

β - Thermal expansion coefficient,

μ - Dynamic viscosity,

γ - The couple stress parameter

ν - Fluid kinematic viscosity,

ω - Heating frequency,

σ - Electrical conductivity,

B_0 - Constant magnetic field strength,

k - Thermal conductivity,

Q_0 - Internal heat loss,

ρ - Fluid density,

$A(\eta), B(\eta)$ - dimensionless steady and oscillatory velocity respectively,

$F(\eta), G(\eta)$ - dimensionless steady and periodic temperature respectively,

λ - viscous heating parameter,

Pr - Prandtl number,

St - Strouhal number,

Ha^2 - Hartmann number,

η - Couple stress coefficient,

δ - heat loss parameter/internal heat generation parameter

κ^2 - couple stress parameter.

a^2 - the inverse of couple stress parameter

TABLE OF CONTENTS PAGE

LIST OF FIGURES **PAGE**

LIST OF TABLES **PAGE**

CHAPTER ONE

INTRODUCTION

Chapter Abstract

In this chapter, essential terms used in the thesis are defined and discussed. Literature review, problem statement, aims and objectives of the study and the research methodology are outlined. Some important dimensionless parameters are also defined.

1.1. Definition of terms

1.1.1. Heat transfer

It has always been understood that there is something that flows from hot objects to cold objects, and it is called heat. For instance, heat flows constantly from the bloodstream to the ambient air. The warmed air lifts off the body to warm the room and whenever the body leaves the room, some tiny buoyancy driven motion of the air will continue because walls will not be perfectly isothermal. The driving force for the heat flow process is the cooling of the thermal gradients within our universe [75].

Heat transfer is described as the flow of heat due to temperature differences. It is further described as the process of the transfer of heat from high temperature reservoir to low temperature reservoir, and in terms of the thermodynamic system, it is the movement of heat across the boundary of the system because of temperature difference between the system and the surroundings. Heat transfer processes are classified into three types, namely, conduction, convection and radiation. In this study the focus is more on convection.

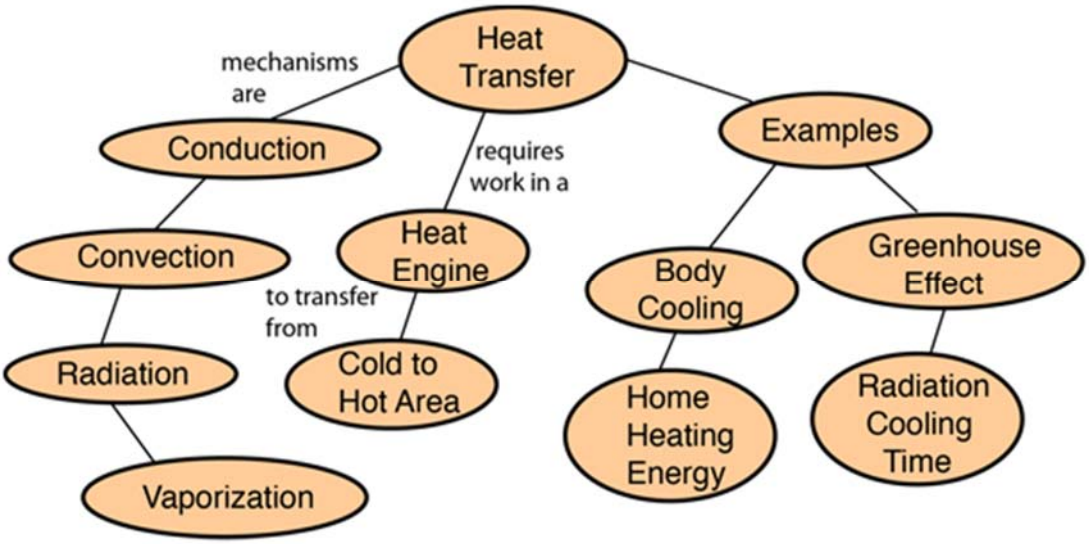

Figure 1.1: Heat transfer (Image source: hyperphysics.phy-astr.gsu.edu)

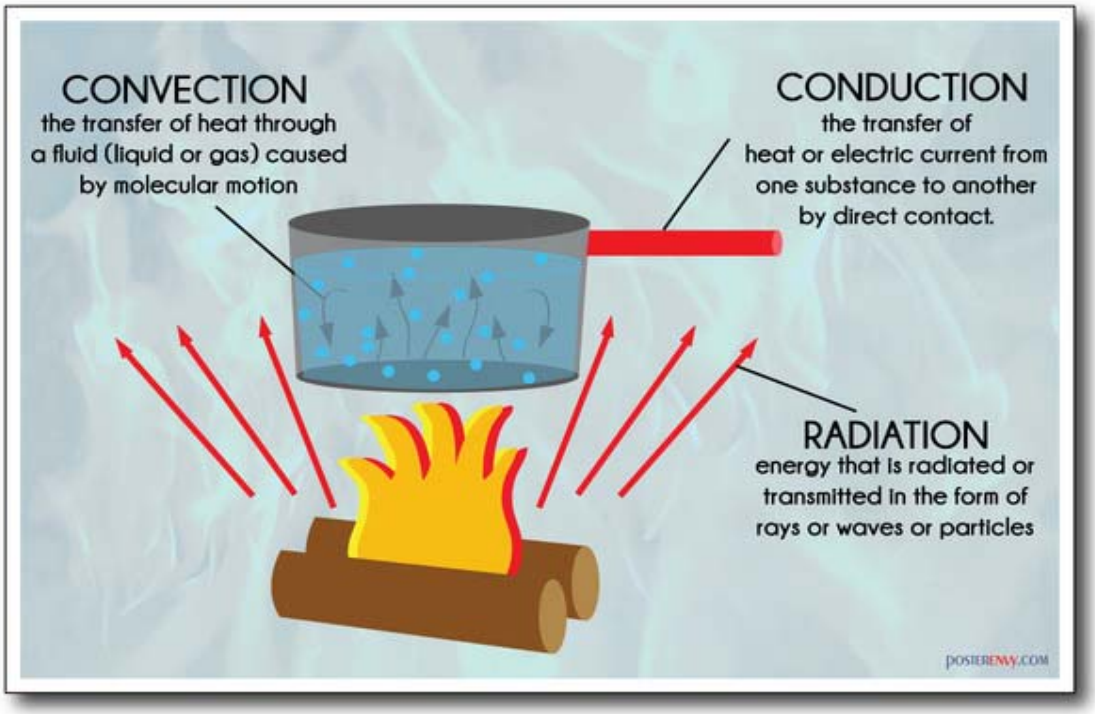

Figure 1.2: Modes of heat transfer (Image source: learnmechanical.com).

Convection is defined as the transfer of heat by circulation of movement of the heated parts of a liquid or a gas. It is also described as the heat transfer by mass motion of a fluid such as air or water when the heated fluid is caused to move away from the source of heat, carrying energy with it. Convection occurs when particles with a lot of heat energy in a liquid or gas move and take the place of particles with less heat energy. Heat energy is transferred from hot places to cooler places by convection. Liquids and gases expand when they are heated.

The transfer of heat occurs between the surface and a fluid in motion when their temperature is different. The rate of transfer is given by

$$q = h\left(T_{body} - T_{\infty}\right).$$

This is the steady-state form of Newton's law of cooling and h is the heat transfer coefficient [46].

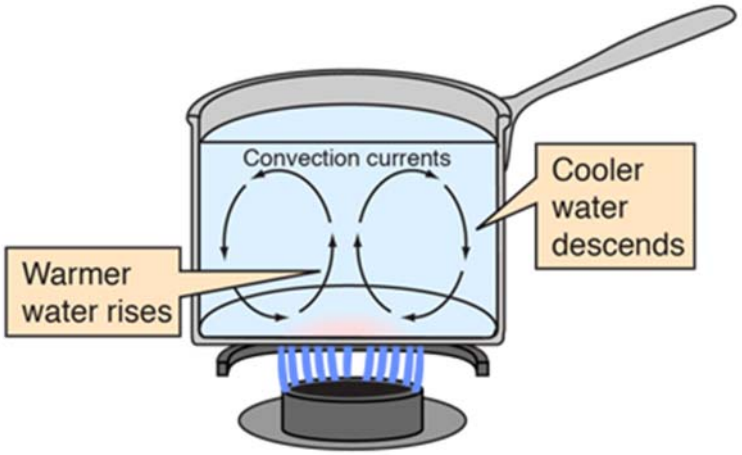

Figure 1.3: Convective heating (Image source: hyperphysics.phy-astr.gsu.edu)

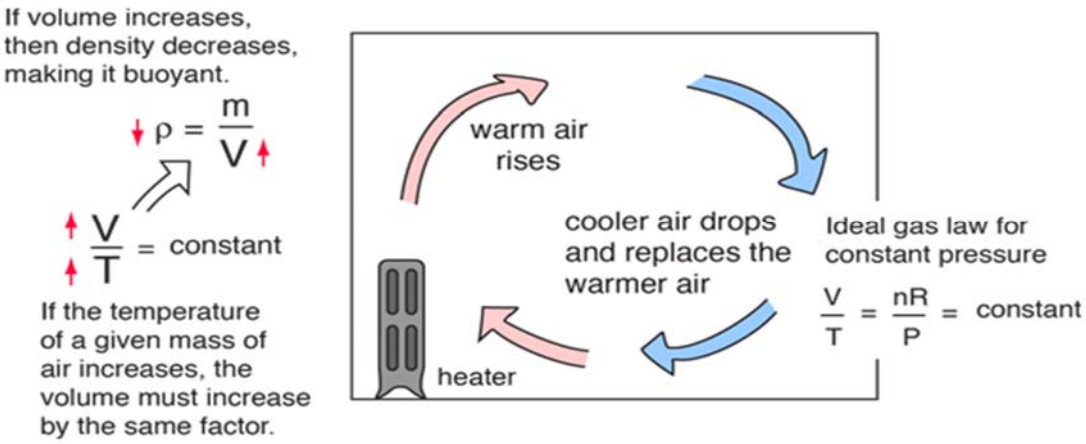

Figure 1.4: Convective heat transfer (Image source: hyperphysics.phy-astr.gsu.edu)

Convection is categorized into three types, namely, natural convection, forced convection and mixed convection. Natural convection is a type of mass and heat transport in which the fluid motion is generated only by density differences in the fluid occurring due to temperature gradients, not by external sources like a pump, fan, suction device, etc. Since the fluid velocity associated with natural convection is relatively low, the heat transfer coefficient encountered in natural convection is also low. The driving force for natural convection is gravity. The inception of natural convection is determined by the Rayleigh number (Ra), a dimensionless quantity given by

$$Ra = \frac{\Delta\rho g L^3}{D\mu},$$

where $\Delta\rho$ is the change in density, g is the local gravitational acceleration, L is the characteristic length-scale of convection, D is the coefficient of diffusion, and μ is the dynamic viscosity.

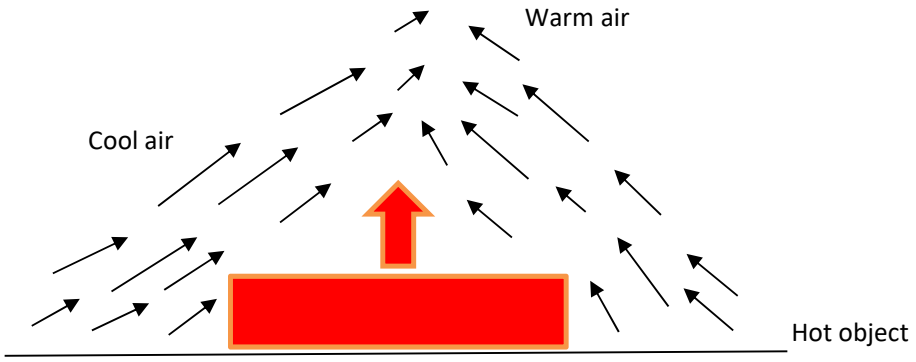

Figure 1.5: Natural convection heat transfer from a hot body (image source: studylib.net)

Forced convection is a mechanism that occurs when fluid flow is induced by an external force such as a pump, fan or a mixer in order to increase the heat transfer. Most engineers come across the forced convection when designing or analyzing heat exchangers. This mechanism is found mostly in everyday life including central heating, air conditioning, steam turbines and other numerous machines [58].

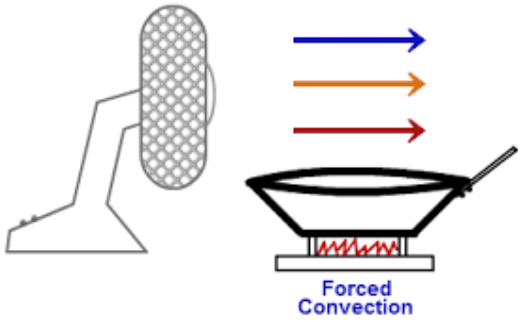

Figure 1.6: Forced convection heat transfer (image source: pinterest.com)

Mixed convection occurs when natural convection and forced convection mechanisms act together to transfer heat. In other words, this is a phenomenon where both pressure forces and buoyant forces interact.

1.1.2. Magnetohydrodynamics (MHD)

Magnetic fields inspire a lot of natural and induced flows. These flows are regularly used in industry to heat, pump, stir and soar liquid metals. The study of these flows is called the magnetohydrodynamics (MHD). MHD is the study of the flow of electrically conducting fluids in the presence of magnetic fields, either externally applied or generated within the fluid by inductive action. Examples of electrically conducting fluids include plasmas, liquid metals, salt water and electrolytes. The essential thought around MHD is that magnetic fields can induce currents in a flowing conductive fluid, which in turn polarizes the fluid and equally changes the magnetic field by itself.

The applications of MHD include boundary layer control in the field of aerodynamics, the cooling of nuclear reactors, the cooling of a metallic plate in a cooling bath, geothermal energy extraction, operation of MHD generators, plasma studies, etc.

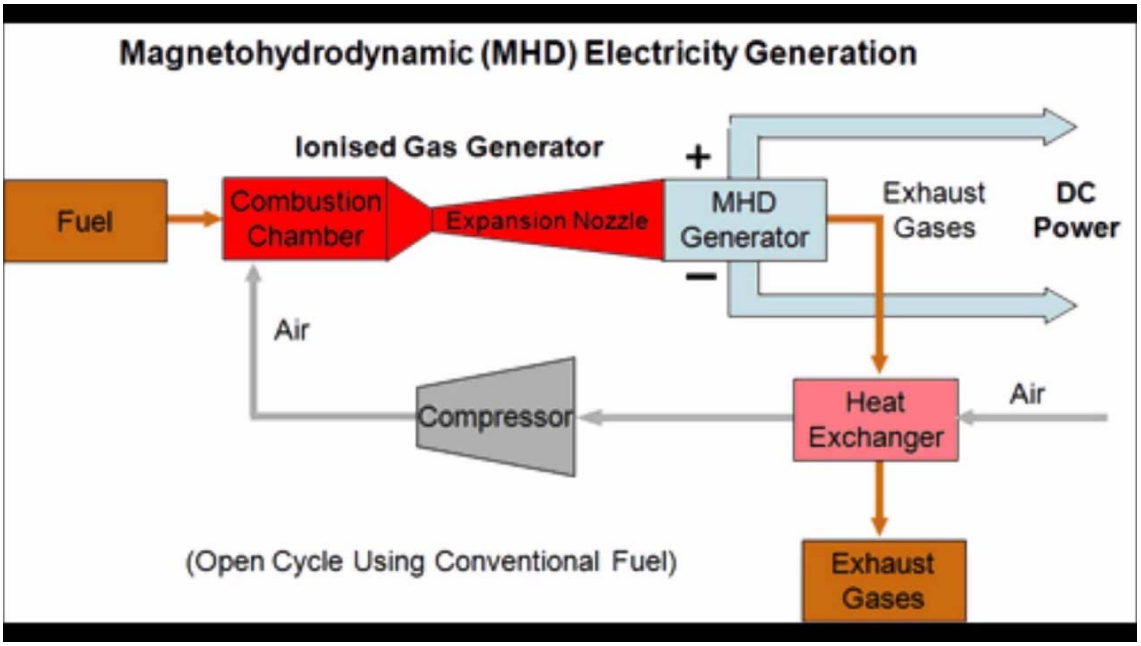

Figure 1.7: Magnetohydrodynamic electricity generation (Image source: gsupsc.blogspot.com)

1.1.2.1. MHD Equations

In the standard non-relativistic form the MHD equations consist of the basic conservation laws of mass, momentum and energy, together with the induction equation for the magnetic field. The equations written in international system of units (SI) according to [37] are:

$$\frac{\partial \rho_m}{\partial t} + \nabla . \rho_m \vec{v} = 0, \tag{1.1}$$

where ρ_m is the mass density and $\vec{v}$ is the fluid bulk velocity. The equation of motion is given as

$$\frac{\partial (\rho_m \vec{v})}{\partial t} + \nabla . \left(\rho_m \overrightarrow{v^2}\right) = -\nabla p + \vec{J} \times \vec{B} + \nabla . \sigma, \tag{1.2}$$

where p is the gas pressure, $\vec{B}$ the magnetic flux density, $\vec{J} = \nabla \times \frac{\vec{B}}{\mu_0}$ is the current density, μ_0 is the vacuum permeability, and σ is the viscous stress tensor.

The equation for internal energy, which is usually written as an equation for the pressure p, is given by

$$\frac{\partial p}{\partial t} + \vec{v}.\nabla p + \gamma p \nabla.\vec{v} = Q, \qquad (1.3)$$

where Q comprises the effects of heating and cooling as well as thermal conduction and γ is the adiabatic coefficient. Eqn. (3) implies the equation of state of the ideal ionized gas

$$p = 2\left(\frac{\rho_m}{m_i}\right) k_B T,$$

which is well satisfied for most dilute plasmas. T is the temperature, m_i the iron mass, k_B the Boltzmann constant and the factor 2 arises because irons and electrons contribute equally.

The induction equation or Faraday's law is given by

$$\frac{\partial \vec{B}}{\partial t} = -\nabla \times \vec{E} = \nabla \times \left(\vec{u} \times \vec{B}\right) + \eta \nabla^2 \vec{B}, \qquad (1.4)$$

where η is the magnetic diffusivity and

$$\vec{E} = -\vec{u} \times \vec{B} + \eta\, \vec{J}$$

is Ohm's law. The magnetic field is coupled to the fluid by the Lorentz force $\vec{J} \times \vec{B}$ in the equation of motion Eqn. (1.2).

In total the MHD equations thus consist of two vector and two scalar partial differential equations that are to be solved simultaneously, either analytically or numerically.

1.1.3. Non-Newtonian fluids

There are two ways of describing the behavior of fluids, namely, Newtonian and non-Newtonian fluids, depending on how they act when responding to shear stress. Most fluids are non-Newtonian in nature. A Newtonian fluid is a fluid in which the viscous stresses arising from its flow at every point are linearly correlated to the local strain (the rate of change of its deformation over time). Examples of Newtonian fluids are

gasoline, mineral oil, alcohol and glycerin. A non-Newtonian fluid is defined as a fluid whose viscosity changes due to stress or force applied on it. For a non-Newtonian fluid, shear stress is not directly proportional to the rate of strain. There are several types of non-Newtonian fluids, namely, shear thickening, bingham plastic, rheopectic or anti-thixotropic, couple stress, Casson and many more. A fluid is shear thickening if the viscosity of the fluid increases as the shear rate increases. A close example of shear thickening is mixing cornstarch with water. Examples of non-Newtonian fluids are blood, honey, grease, gels, oobleck and many more. Non-Newtonian fluids occur naturally and a few examples of their applications include reduction of fluid friction, surfactant applications to large scale heating and cooling systems, flow tracers and many more.

Figure 1.8: An example of a non-Newtonian fluid (image source: biocircuits.ucsd.edu)

1.1.4. Couple stress fluids

Couple stress fluid theory is a simple generalization of the classical theory of viscous Newtonian fluids that allow the sustenance of couple stresses and body couples in the fluid medium [34]. The concept of couple stresses arises due to the way in which the mechanical interactions in the fluid medium are modelled. When additives in the fluid are mixed, forces in the fluid oppose the forces generated by additives. This opposite force forms a couple force and a couple stress is induced in a fluid. Couple stresses

are an outcome of the supposition that the interaction of one part of a body on another across a surface is equivalent to a force and moment distribution. They consist of rigid, randomly oriented particles suspended in a viscous medium such as blood fluids, electro-rheological fluids and synthetic fluids. The main feature of a couple stress fluid is that the stress tensor is anti-symmetric [101]. The couple stress fluid theory is proficient for describing different types of lubricants, suspension fluids, blood, etc. These fluids have applications in various processes that take place in the industry, such as solidification of liquid crystals, extrusion of polymer fluids, colloidal solutions and cooling of metallic plate in a bath and so on [43].

1.1.5. Buoyancy

Buoyancy is defined as an upward force applied by a fluid on an immersed object in a gravity field and opposes the weight of an object [144]. In fluids, pressure increases with depth, hence when an object is dipped in a fluid, the pressure applied on the bottom surface is higher than the one applied on the top surface. Any object fully or partly immersed in a fluid is buoyed up by a force equal to the weight of the fluid displaced by an object. Buoyancy is caused by differences in pressure acting on opposite sides of an object dipped in a motionless fluid. Pressure differences in a fluid are caused by gravity. Generally, buoyant forces act opposite the direction of the frame of reference acceleration. Three types of buoyancy are positive, negative and neutral buoyancy.

Positive buoyancy takes place when an object is lighter than the fluid it displaces. In this case the object will float because the buoyant force is greater than the object's weight. Negative buoyancy happens when an object is denser than the fluid it displaces. In this case the object will sink because its weight is greater that the buoyant force. Neutral buoyancy occurs when an object's weight is equal to the fluid it displaces. Applications of buoyancy include staying afloat, ships at the sea, submarines, floating of balloons, airships and many more.

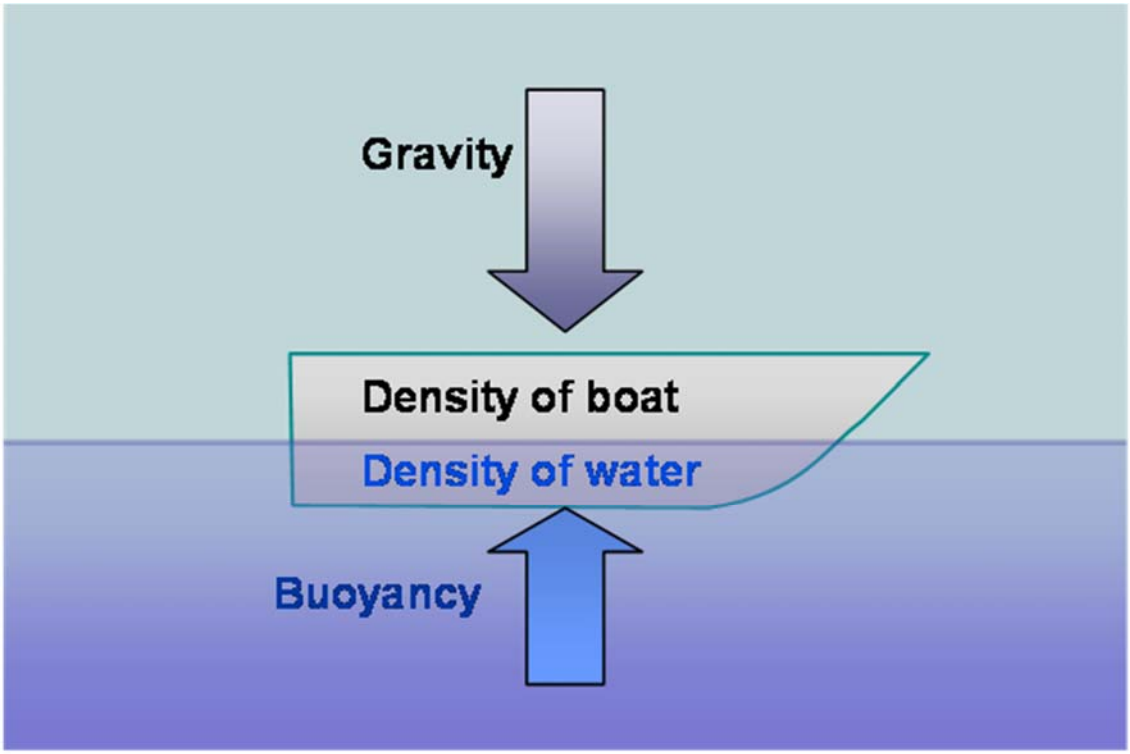

Figure 1.9: Buoyancy (Image source: mixandflowofmatter.weebly.com)

1.1.6. Oscillatory flow

The repetitive variation normally in time of some measure about a value or between two or more distinct states is called an oscillation. Oscillations do not only take place in mechanical systems, they also occur in all areas of science. For example the beating of human heart, business cycles in economics, geothermal geysers in geology, periodic firing of nerve cells in the brain, etc. Oscillations lead to momentous development of heat and mass transfer. Oscillatory flow is a physical occurrence encountered in internal combustion engines, stirling engines, cryogenic coolers and chemical processes. The fact that oscillating flow has two thermal entrance regions is one of the reasons why it enhances heat transfer.

Oscillatory flows have the potential of being used for heat spreading applications for cooling of high power electronics and electrical equipment.

1.1.7. Prandtl number (P_r)

The Prandtl number is a non-dimensional quantity that is responsible for setting viscosity of the fluid in association with the thermal conductivity. It consequently

measures the connection between momentum transport and thermal transport capacity of a fluid and it is mathematically defined as

$$P_r = \frac{v}{\alpha} = \frac{momentum\ transport}{heat\ transport} = \frac{{}^{\mu}/_{\rho}}{{}^{k}/_{c_p\rho}} = \frac{c_p\mu}{k},$$

where v is the momentum diffusivity, α is the thermal diffusivity, μ is the dynamic viscosity, k is the thermal conductivity, c_p is the specific heat and ρ is the density of the fluid. Prandtl number is important in displaying the relative thickness of the velocity boundary layer to the thermal boundary layer. In heat transfer problems, the Prandtl number controls the relative thickness of the momentum and thermal boundary layers, i.e. when P_r is small, the heat circulation becomes quicker as compared to the velocity, meaning that, for liquid metals the thickness of the thermal boundary layer is bigger than the velocity boundary layer.

1.1.8. Strouhal number (S_t)

The Strouhal number (S_t) is a dimensionless number describing the oscillating flow mechanism. The parameter is named after Vincene Strouhal, a Czech physicist who experimented in 1878 with wires experiencing vortex shedding and singing in the wind. The Strouhal number is defined as

$$S_t = \frac{FL}{U},$$

where F is the frequency of vortex shedding, L is the characteristic length and U is the flow velocity. In flows characterized by a periodic motion, a Strouhal number is associated with the oscillations of the flow due to the inertial forces relative to the changes in velocity due to the convective acceleration of the flow field. At high S_t oscillations dominate the flow, whereas at low S_t oscillations are swept by the fast moving fluid. The Strouhal number can be important when analyzing unsteady oscillating flow problems. It represents a measure of the ratio of inertial forces due to changes in velocity from one point to the other in the flow field.

1.1.9. Hartmann number (Ha)

The Hartmann number (Ha) is the ratio of the electromagnetic force to the viscous force. It was first introduced by Hartmann. It is frequently encountered in fluid flows through magnetic fields and it is defined as

$$H_a = BL\sqrt{\frac{\sigma}{\mu}}.$$

where B is the magnetic field intensity, L is the characteristic length scale, σ is the electrical conductivity and μ is the dynamic viscosity. From the practical point of view, the important range of Hartmann number is $102 < Ha < 106$. High values of the Hartmann number means that the magnetic field intensity is stronger.

1.1.10 Reynolds number (Re)

The Reynolds number (Re) is the ratio between the inertial and viscous forces in a fluid. A fluid in motion tends to behave as sheets or layers of infinitely small thicknesses sliding relative to each other. The Reynolds number is an important dimensionless quantity in fluid mechanics used to help predict flow patterns in different fluid flow situations. At low Reynolds number, flow tends to be dominated by laminar flow, while at high Reynolds number turbulence results from differences in the fluid's speed and direction, which may sometimes intersect or even move counter to the overall direction of the flow. The Reynolds number is expressed by

$$Re = \frac{\rho VL}{\mu},$$

where ρ is the density, V is the velocity, μ is the viscosity and L is the characteristic linear dimension.

1.1.11 Grashof number (Gr)

The Grashof number (Gr) is a non-dimensional parameter in fluid dynamics and heat transfer responsible for estimating the relation of the buoyancy to viscous forces acting on a fluid. It normally happens in studies of conditions relating natural convection and it is equivalent to the Reynolds number. The Grashof number is represented mathematically as follows

$$Gr = \frac{\text{buoyancy forces}}{\text{viscous forces}} = \frac{g\beta L^3(T_{wall} - T_\infty)}{v^2},$$

where g is the acceleration due to gravity, β is the thermal expansion coefficient, T_{wall} is the wall temperature, T_∞ is the bulk temperature, L is the vertical length and v is the kinematic viscosity. The importance of the Grashof number is that it represents the ratio between the buoyancy forces due to spatial variation in fluid density to the restraining force due to the viscosity of the fluid. Since Reynolds number, Re, represents the ratio of momentum to viscous forces, the relative magnitudes of Gr and

Re are an indication of the relative importance of natural and forced convection in determining heat transfer.

1.2. Literature review

Motivated by a plethora of wide applications in industry and contemporary technology, as well as the need for technological advancement in the improvement of life in general, an upsurge of research interest in studies of phenomena connected with hydromagnetic fluid flow has been witnessed. Recent findings on MHD have shown that the magnetic field produced by a simple magnet placed in a transverse direction to the channel interacts with the fluid flow [4]. This phenomenon plays an important role in the control of hot moving fluid in many metallurgical engineering applications, crystal growth, electrochemistry and other thermal processes occurring at high temperature [5]. Depending on the geometry of the medium, the mechanics of the fluid and other physical conditions, challenging fluid flow models arise [129].

Theoretical studies of Hartmann [50] on laminar flow of an electrically conducting liquid in a homogeneous magnetic field motivated scientists to engage in active research in hydromagnetic fluid flow and heat transfer. If the electrically conducting fluid involved is a non-Newtonian fluid the studies of the flow dynamics have an additional challenge in that the classical linear Navier-Stokes model breaks down. A diversity of models have been postulated depending on the nature of the departure from Newtonian behaviour. Amongst these models is the couple stress fluid theory [141].

The couple stress fluid may be considered as a special case of a non-Newtonian fluid which takes into account the particle size effects [82]. Recently, Kareem *et al*. [69] reported on the second law analysis for hydromagnetic couple stress fluid flow through a porous channel. In second law analysis or entropy generation studies the main focus is on how to minimise or control energy wastages in the form of heat dissipation. Kareem *et al*. [69] concluded that the magnetic field reduces the randomness in the fluid's particles, resulting in the lowering of the fluid's velocity and entropy generation. Makinde and Eegunjobi [78] studied the entropy generation in a couple stress fluid flow through a vertical channel filled with saturated porous media. In their study, entropy generation was observed to increase with the buoyancy force and pressure gradient, while the porous medium decreased it. Falade *et al.* [41] studied the entropy generation analysis for variable viscous couple stress fluid flow through a channel with

non-uniform wall temperature. An increase in the couple stress inverse (which represents a decrease in the dynamic fluid viscosity) was observed to enhance the dominance of fluid friction irreversibility over heat transfer.

Abbas *et al*. [1] presented the hydromagnetic mixed convective two-phase flow of couple stress and viscous fluids in an inclined channel. Nayak and Dash [89] investigated the MHD couple stress fluid flow through a porous medium in a rotating channel. They analysed the effect of couple stress as well as the case of steady and pulsatile pressure gradient on a flow through a porous saturated rotating channel. Adesanya *et al*. [12] presented the hydromagnetic natural convection flow between vertical parallel plates with time-periodic boundary conditions, and concluded that an increase in the magnetic field intensity decreases the flow velocity while it enhances fluid temperature owing to joule dissipation. Other related studies are found in [7,22,32 and 108].

MHD studies in various flow geometries are pertinent in that they lead to improvement of design of machinery and industrial processes as well as enhancement of energy efficiency of thermal systems. Efficient industrial flow processes contribute immensely to economic growth and improvement of life of citizens. Although several MHD studies have been undertaken to date, literature survey revealed that the present study has not been investigated in the previous models presented in the literature.

1.3. Problem statement

Fluid mechanics is concerned with the flow of fluids. It is one of the most important of all the areas of physics [32]. A fluid is a substance that deforms continuously under the application of a shear stress no matter how small the shear stress may be [46]. In the natural world, we frequently encounter transport processes in fluids, where the motion is driven by the interface of a difference in density in a gravitational field. Therefore the buoyancy force is the stimulus to the fluid flow [148]. Buoyancy forces arise as a result of variations of density in a fluid subject to gravity, and produce a wide range of phenomena of importance in many aspects of everyday life [144].

The study of flows in which the fluid is electrically conducting and moves in a magnetic field is known as magnetohydrodynamics (MHD) [27]. Hartmann [50] pioneered the study of such flows and following his ground breaking work, the rheological community

has undertaken to investigate hydromagnetic fluid flow and heat transfer in different geometries under varied physical effects. The fluid may be Newtonian or non-Newtonian. For the latter, complexities arising from the breakdown of the classical linear Navier-Stokes model has led to fascinating field of non-Newtonian rheology. Couple stress fluid theory was introduced by Stokes and is among the non-Newtonian fluid theory which considers couple stresses in addition to the classical Cauchy stresses in viscous fluid dynamics [16].

In recent times, studies have shown that magnetic nanoparticles suspended in base fluid have significant influence on many fluids of technological importance [61] and [151]. For instance, in hydraulic systems used in automobiles shock absorbers, the interactions between the electromagnetic fields produced by the dipolar Lorentz forces clamped transversely to the flow channel always interact with the ferrofluid particles to dampen the shock. The introduction of magnetic nanoparticles is also a useful means of controlling hot moving molten steel of commercial quantity in several metallurgical engineering applications. Moreover, the magnetic nanoparticles are used widely in electro-chemistry to agglomerate fluid particles due to interactions with the dipolar forces and lots more applications that are too numerous to be mentioned here.

Motivated by the few above-mentioned application areas, the study shall address several flow problems in magnetic nanoparticles flow and heat transfer characteristics by using the couple stress fluid model. A survey of the literature suggests that the study described here has not been investigated in the steady-periodic regimes despite its wide applications in a wide range of fluids flowing through parallel plates subjected to periodic heat input. We consider a fully developed laminar flow of an electrically conducting incompressible couple stress fluid through a vertical channel due to a steady-periodic temperature on the plates. The fluid is assumed to be under the influence of an externally applied homogeneous magnetic field. All fluid properties are assumed to be constant except for fluid density that varies with temperature. The fluid is assumed to have small electrical conductivity, and the electromagnetic force produced is very small.

1.4. Rationale

Studies related to channel flow and heat transfer characteristics of couple stress fluids do not only present theoretically challenging problems, but also find several applications in many industrial and chemical engineering processes such as the extrusion of polymer fluids, solidification of liquid crystals, cooling of metallic plates in a bath, colloidal solutions, etc. Couple stress fluids are also important in physiological fluid mechanics, tribology of thrust bearings and lubrication of engine rod bearings [16]. Couple stress fluid models are also capable of describing the characteristics and behaviour of blood and suspension fluids [78]. Many nanofluids of mechanical significance contain tiny magnetic colloidal additives that are suspended in the base fluid to form ferrofluid. The presence of these nano-materials suggest that the couple stress constitutive model can be used to describe the rheological properties of nanofluids. Meanwhile convective flows in the steady-periodic regimes have attracted considerable attention owing to their applicability in electrical and electronic devices and in the flow of fluids in human and animal bodies [65,149].

1.5. Aim of the study

The aim of this research work is to study the hydromagnetic couple stress fluid flow through vertical channel subjected to steady-periodic heating under various flow conditions.

1.6. Research objectives

The objectives of the study are:

(i) To formulate Mathematical models describing hydromagnetic couple stress fluid flow through vertical channel subjected to steady-periodic heating under various conditions.

(ii) To identify and/or develop analytical and numerical methods to solve the model problems.

(iii) To examine the effect of couple stresses on the buoyancy-induced flow.

(iv) To investigate the influence of viscous and Joule dissipation on the thermal structure.

(v) To analyse the effects of the various thermophysical parameters on the velocity and temperature fields, the skin friction and the rate of heat transfer.

1.7. Research methodology

Both analytical techniques and numerical methods will be used to solve the modelling equations. For most engineering and scientific applications numerical solutions are of particular interest due to the fact that exact solutions may not exist in closed form. In our study the partial differential equations that will be derived are coupled and nonlinear, and exact solutions may be impossible. For this reason numerical methods will need to be employed. The semi-analytical Adomian decomposition method (ADM) is envisaged to be utilised in solving the three variants of the problems to be formulated.

Three variations of the problem will be analysed, and these are:

i. In the first case, the hydromagnetic couple stress fluid flow through vertical channel subject to steady-periodic heating would be investigated.
ii. The second case will address the impact of magnetic field induction on the buoyancy-induced oscillatory flow of couple stress fluid with varying heating.
iii. Finally, the third case will investigate mixed convective three dimensional flow of unsteady hydromagnetic couple stress fluid through a vertical channel filled with porous medium.

The modelling equations will be formulated, non-dimensionalised and solved using analytical methods and/or the ADM.

1.7.1. The Adomian decomposition method (ADM)

ADM is a semi-analytical approach for obtaining solutions to functional problems. The method requires no linearisation, discretisation, use of initial guess or transformation to obtain the solution of any linear or nonlinear integral equations. One main advantage of ADM is that it can be coded on symbolic software packages like Mathematica, Maple or Matlab for high accuracy of the solution, and this ensures that human error will be completely eliminated. The method has been used by several researchers including [8]. One gets a convergent series solution with just a few iterations. The method of decomposition crumbles the linear term $u(x,t)$ into a non-ending sum of components $u_n(x,t)$ expressed as

$$u(x,t) = \sum_{n=0}^{\infty} u_n(x,t).$$

In addition, the method of decomposition do the identification of the nonlinear term $F\big(u(x,t)\big)$ applying the series of decomposition

$$F\big(u(x,t)\big) = \sum_{n=0}^{\infty} A_n,$$

where A_n are the Adomian polynomials obtained from the formula

$$A_n = \frac{1}{n!}\frac{d^n}{d\lambda^n}\left[F\left(\sum_{i=0}^{n}\lambda^i u_i\right)\right]_{\lambda=0}, \qquad n = 0,1,2,\ldots$$

The first few Adomian polynomials are obtained as:

$$A_0 = F(u_0),$$

$$A_1 = u_1 F'(u_0),$$

$$A_2 = u_2 F'(u_0) + \frac{1}{2!}{u_1}^2 F''(u_0),$$

$$A_3 = u_3 F'(u_0) + u_1 u_2 F''(u_0) + \frac{1}{3!}{u_1}^3 F'''(u_0),$$

$$A_3 = u_3 F'(u_0) + u_1 u_2 F''(u_0) + \frac{1}{3!}{u_1}^3 F'''(u_0)$$

$$A_4 = u_4 F'(u_0) + \left(\frac{1}{2!}{u_2}^2 + u_1 u_3\right) F''(u_0) + \frac{1}{2!}{u_1}^2 u_2 F'''(u_0) + \frac{1}{4!}{u_1}^4 F^{iv}(u_0).$$

The similar method can be applied to produce other polynomials.

1.8. Thesis outline

The thesis is organized as follows:

Chapter One

In Chapter one, the important terminology and expressions used in the study are defined and elaborated, literature review is presented together with the problem statement, aim of the study, research objectives, rationale and research methodology.

Chapter Two

Chapter two focuses on the derivation of basic equations of fluid dynamics, namely, the continuity, momentum and the energy equations.

Chapter Three

In Chapter three, the natural convection flow of heat generating hydromagnetic couple stress fluid with time periodic boundary conditions is investigated. Specific research objectives (i) – (v) are achieved in this chapter.

Chapter Four

In Chapter four, the convective flow of hydromagnetic couple stress fluid with varying heating through vertical channel is analysed and investigated. Specific research objectives (i) – (v) are achieved in this chapter.

Chapter Five

In Chapter five, the focus is on the investigation of the mixed convective flow of unsteady hydromagnetic couple stress fluid through a vertical channel filled with porous medium. Specific research objectives (i) – (v) are achieved in this chapter.

Chapter Six

This chapter concludes the thesis with a general discussion, conclusion, recommendations and future research work.

CHAPTER TWO

DERIVATION OF BASIC FLUID FLOW EQUATIONS

Chapter Abstract

In this chapter, the governing equations of computational fluid dynamics are derived and discussed.

2.1. Introduction

The basis of computational fluid dynamics is the essential governing equations of the fluid in motion, namely, the continuity, momentum and energy equations. The momentum equations are referred to as Navier-Stokes equations. Applying the laws of conservation of mass, momentum and energy balance to an infinitesimal volume element yields the equations in differential form, which assumes that the fluid particles are continuous and that derivatives exist [104].

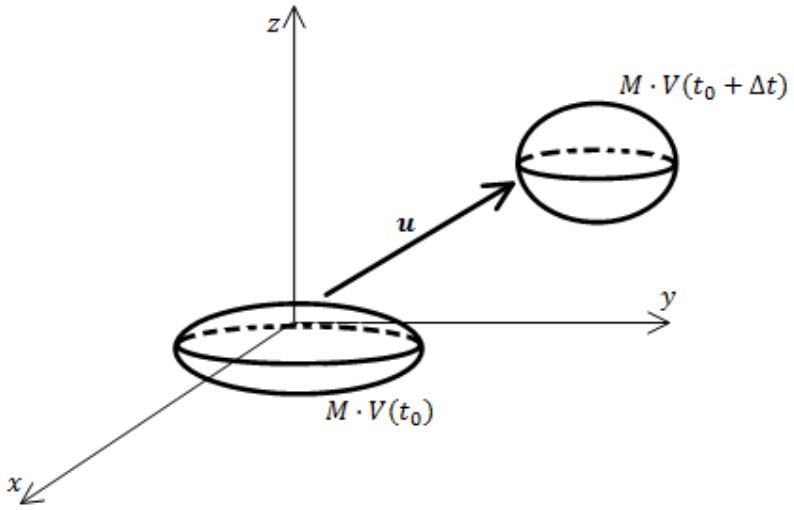

Figure 2.1. Fluid element moving in a flow field (image source: www.cfd-online.com)

2.2. The continuity equation

The continuity equation is developed simply by applying the law of conservation of mass to a small volume element within a flowing fluid [46].

The continuity equation is conveyed in a differential form for one dimensional setup as

$$\frac{\partial \rho}{\partial t} + \nabla . (\rho u) = 0, \qquad (2.1)$$

where ρ is the density of the fluid, t is time, and u is the fluid velocity. It can also be obtained in Cartesian tensor scheme as

$$\frac{\partial \rho}{\partial t} + \frac{\partial (\rho u_k)}{\partial x_k} = 0. \qquad (2.2)$$

In operator form it can be shown as

$$\nabla . u = 0. \qquad (2.3)$$

In a two dimensional setup, a small control volume of lengths Δx and Δy and depth of unity perpendicular to xy-plane is considered. Figure 2.2 shows the differential control volume $(dx. dy. 1)$ for mass conservation in two dimensional flow.

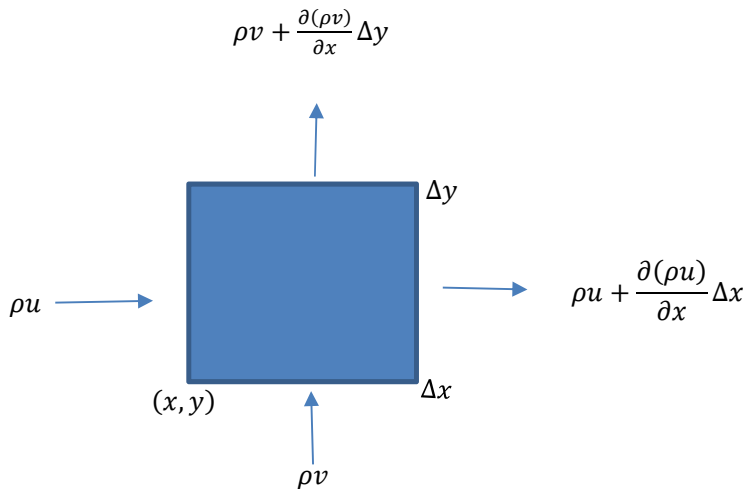

Figure 2.2. Control volume for mass conservation in two dimensional flow

The rate of mass entering a face is the product of the density, fluid velocity and the face area. For example, on the left face with area $A = \Delta y \Delta z$, the density ρ is multiplied by the velocity u in the x direction, so that the rate at which the mass enters the control volume is

$$\rho u \Delta y \Delta z. \qquad (2.4)$$

The mass leaving the volume is expressed in the same manner, but in this case the velocity and density may have changed as the fluid passes through the control volume. The small changes in velocity and density are respectively expressed as $u + \Delta u$ and $\rho + \Delta\rho$. Therefore the mass leaving the control volume, denoted by a negative sign, is expressed as

$$-(\rho + \Delta\rho)(u + \Delta u)\Delta y\Delta z. \tag{2.5}$$

Consideration of the other faces in the y and z directions, in the case of a three dimensional flow, gives expressions for the mass entering the control volume as

$$\rho v\Delta x\Delta z \text{ and } \rho w\Delta x\Delta z, \tag{2.6}$$

where v and w are velocities in the y and z directions respectively.

The masses leaving the respective sides are

$$-(\rho + \Delta\rho)(v + \Delta v)\Delta x\Delta z \text{ and } -(\rho + \Delta\rho)(w + \Delta w)\Delta x\Delta y. \tag{2.7}$$

The total rate of mass entering and leaving the volume $\Delta x\Delta y\Delta z$ is thus expressed as

$$\left(\frac{\Delta\rho}{\Delta t}\right)\Delta x\Delta y\Delta z = \rho u\Delta y\Delta z + \rho v\Delta x\Delta z + \rho w\Delta x\Delta y - (\rho + \Delta\rho)(u + \Delta u)\Delta y\Delta z - (\rho + \Delta\rho)(v + \Delta v)\Delta x\Delta z - (\rho + \Delta\rho)(w + \Delta w)\Delta x\Delta y. \tag{2.8}$$

Equation (2.8) simplifies to

$$\left(\frac{\Delta\rho}{\Delta t}\right)\Delta x\Delta y\Delta z = -\Delta(\rho u)\Delta y\Delta z - \Delta(\rho v)\Delta x\Delta z - \Delta(\rho w)\Delta x\Delta y. \tag{2.9}$$

Dividing both sides of Equation (2.9) by $\Delta x \Delta y \Delta z$ and rearranging the terms, we have

$$\frac{\Delta \rho}{\Delta t} + \frac{\Delta(\rho u)}{\Delta x} + \frac{\Delta(\rho v)}{\Delta y} + \frac{\Delta(\rho w)}{\Delta z} = 0. \tag{2.10}$$

Taking the limits as $\Delta t \to 0$, we have the following equation

$$\frac{\partial(\rho u)}{\partial x} + \frac{\partial(\rho v)}{\partial y} + \frac{\partial(\rho w)}{\partial z} = 0. \tag{2.11}$$

For incompressible fluid where density is constant, the simplified form of the continuity equation becomes

$$\frac{\partial u}{\partial x} + \frac{\partial v}{\partial y} + \frac{\partial w}{\partial z} = 0. \tag{2.12}$$

In two dimensions, the equation reduces to

$$\frac{\partial u}{\partial x} + \frac{\partial v}{\partial y} = 0. \tag{2.13}$$

2.3. The momentum equation

The physical principle applied in deriving the momentum equation is Newton's second law of motion which states that

$$\boldsymbol{F} = m\boldsymbol{a}, \tag{2.14}$$

where $\boldsymbol{F}$ is the force, m the mass and $\boldsymbol{a}$ the acceleration.

The derivation follows a three dimensional scheme, and Fig 2.3 illustrates the two dimensional setup.

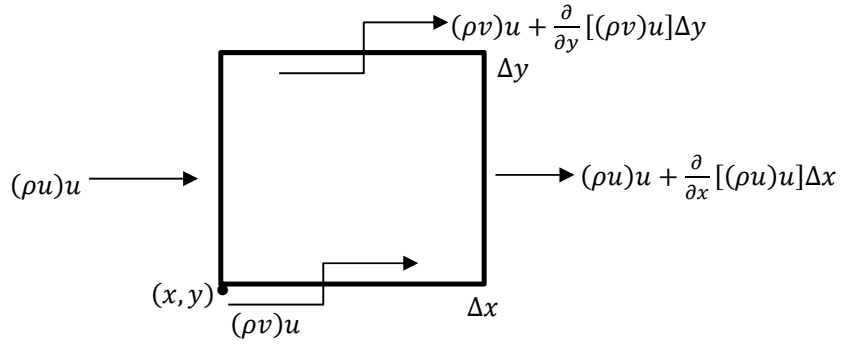

Figure 2.3. Control volume for momentum fluxes

The rate of change of momentum with respect to time, $\frac{\partial(momentum)}{\partial \bar{t}}$, inside the control volume is given as

$$\frac{\partial}{\partial t}(\rho u)\Delta x\Delta y\Delta z. \tag{2.15}$$

Therefore the momentum flux in the x direction is

$$(\rho u)u\Delta y\Delta z, \tag{2.16}$$

and the momentum flux out at the opposite side is given by

$$-\left[(\rho u)u + \frac{\partial}{\partial y}(\rho u)u\Delta x\right]\Delta y\Delta z. \tag{2.17}$$

The momentum flux in the y direction is given as

$$(\rho v)u\Delta x\Delta z\ , \tag{2.18}$$

and momentum flux out at the opposite side is expressed by

$$-\left[(\rho v)u + \frac{\partial}{\partial x}(\rho v)u\Delta y\right]\Delta x\Delta z. \tag{2.19}$$

Similarly, in the z direction we have

$$(\rho w)u\Delta\Delta x\Delta y \tag{2.20}$$

and

$$-\left[(\rho w)u+\frac{\partial}{\partial z}(\rho w)u\Delta x\right]\Delta x\Delta y. \quad (2.21)$$

Addition of the equations above from all directions, provides the equation for the change of momentum with respect to time as

$$\frac{\partial}{\partial t}(\rho u)\Delta x\Delta y\Delta z = -\left[(\rho u)u+\frac{\partial}{\partial y}(\rho u)u\Delta x\right]\Delta y\Delta z-\left[(\rho v)u+\frac{\partial}{\partial x}(\rho v)u\Delta y\right]\Delta x\Delta z-$$
$$\left[(\rho w)u+\frac{\partial}{\partial z}(\rho w)u\Delta x\right]\Delta x\Delta y+\sum F_x, \quad (2.22)$$

where $\sum F_x$ is the sum of all external forces in the x direction on the indicated control volume. After simplification, Equation (2.22) reduces to

$$\frac{\partial}{\partial t}(\rho u)\Delta x\Delta y\Delta z=-\frac{\partial}{\partial x}(\rho u)u\Delta x\Delta y\Delta z-\frac{\partial}{\partial y}(\rho v)u\Delta y\Delta x\Delta z-\frac{\partial}{\partial z}(\rho w)u\Delta x\Delta y\Delta z+\sum F_{x,} \quad (2.23)$$

Rearranging the terms in Equation (2.23), we have

$$\sum F_x=\left[\frac{\partial}{\partial t}(\rho u)+\frac{\partial}{\partial x}(\rho u)u+\frac{\partial}{\partial y}(\rho v)u+\frac{\partial}{\partial z}(\rho w)u\right]\Delta z\Delta x\Delta y. \quad (2.24)$$

Applying the product rule for the terms in square brackets, we obtain the following expression:

$$\sum F_x=\left[u\frac{\partial(\rho)}{\partial \bar{t}}+\rho\frac{\partial(u)}{\partial t}+u\frac{\partial(\rho u)}{\partial x}+\rho u\frac{\partial(u)}{\partial x}+u\frac{\partial(\rho v)}{\partial y}+\rho v\frac{\partial(u)}{\partial y}+u\frac{\partial(\rho w)}{\partial z}+\rho w\frac{\partial(u)}{\partial z}\right]\Delta z\Delta x\Delta y \quad (2.25)$$

The odd terms on the right hand side of the equation inside the square bracket are the continuity equation terms multiplied by u, where ρ is the density. The sum of the terms of the continuity equation must equal to zero, and Equation (2.25) then becomes

$$\sum F_x=\left[\rho\frac{\partial(u)}{\partial t}+\rho u\frac{\partial(u)}{\partial x}+\rho v\frac{\partial(u)}{\partial y}+\rho w\frac{\partial(u)}{\partial z}\right]\Delta z\Delta x\Delta y. \quad (2.26)$$

The external forces in the y and z directions are expressed similarly as

$$\sum F_y = \left[\rho \frac{\partial(v)}{\partial t} + \rho u \frac{\partial(v)}{\partial x} + \rho v \frac{\partial(v)}{\partial y} + \rho w \frac{\partial(v)}{\partial z}\right] \Delta z \Delta x \Delta y \quad (2.27)$$

and

$$\sum F_z = \left[\rho \frac{\partial(w)}{\partial t} + \rho u \frac{\partial(w)}{\partial x} + \rho v \frac{\partial(w)}{\partial y} + \rho w \frac{\partial(w)}{\partial z}\right] \Delta z \Delta x \Delta y. \quad (2.28)$$

For a two dimensional scheme, equations in the x and y directions are given as

$$\sum F_x = \left[\rho \frac{\partial(u)}{\partial t} + \rho u \frac{\partial(u)}{\partial x} + \rho v \frac{\partial(u)}{\partial y}\right] \Delta x \Delta y$$

and

$$\sum F_y = \left[\rho \frac{\partial(v)}{\partial t} + \rho u \frac{\partial(v)}{\partial x} + \rho v \frac{\partial(v)}{\partial y}\right] \Delta x \Delta y.$$

2.4. External forces

We now need to come up with formulae for external forces F_x, F_y and F_z. Forces acting on a fluid element maybe classified as body forces and surface forces [126].

The body forces act on the entire control volume. Examples are, the gravitational, centrifugal and magnetic or electric field forces. The body force due to gravity can be thought of acceleration due to gravity. In the directions of x, y and z the body force is expressed respectively as $g_x \rho \Delta x \Delta y \Delta z$, $g_y \rho \Delta x \Delta y \Delta z$ and $g_z \rho \Delta x \Delta y \Delta z$.

The surface forces arise due to pressure and viscous stresses on the surfaces of the control volume. The viscous stress may be resolved into two perpendicular components given by normal stress σ_{ij} and shear or tangential stress τ_{ij}. Figure 2.4 indicates the nine stress components working on the surfaces of the control volume in the x, y and z directions.

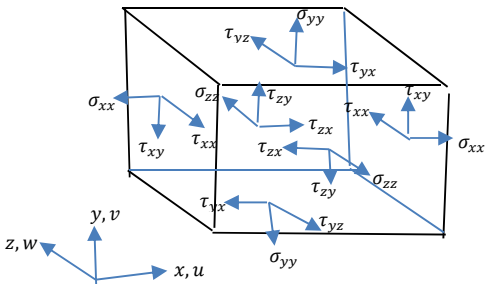

Figure 2.4. Nine stress components

The normal stresses σ_{xx}, σ_{yy} and σ_{zz} correspond to the force components that are normal to the x, y and z surfaces respectively. The shear stress τ_{xy} corresponds to the force in the y direction along the x surface, τ_{yx} to the force in the x direction along the y surface and τ_{zx} to the force in the x direction along the z surface. The symbols $F_{s(x)}$, $F_{s(y)}$ and $F_{s(z)}$ will be used for the derivation of the formulae for the net surface force for each of the three x, y, z directions. The external force can thus be expressed as $\sum F_x = F_{b(x)} + F_{s(x)}$, where $F_{b(x)}$ and $F_{s(x)}$ are body and surface forces in the x direction. The approach is first to concentrate on the x surface. The force due to stress is expressed in terms of the product of the stress and the surface area over which it acts [28]. Therefore, for the face with normal in the x direction where the surface area is $\Delta y \Delta z$, the stress in the x direction due to direct stresses are given by

$$-F_{s,(xx)} \Delta y \Delta z \tag{2.29}$$

and

$$\left(F_{s,(xx)} + \frac{\partial F_{s,(xx)}}{\partial x} \Delta x\right) \Delta y \Delta z. \tag{2.30}$$

Adding the forces, we have

$$-F_{s,(xx)} \Delta y \Delta z + F_{s,(xx)} \Delta y \Delta z + \frac{\partial F_{s,(xx)}}{\partial x} \Delta x \Delta y \Delta z = \frac{\partial F_{s,(xx)}}{\partial x} \Delta x \Delta y \Delta z \tag{2.31}$$

Following the same procedure for the face with normal in the y and z direction where the surface area is $\Delta x \Delta z$ and $\Delta x \Delta y$ respectively, the forces acting in the x direction due to direct stresses will be given by

$$\frac{\partial F_{s,(yx)}}{\partial y}\Delta x\Delta y\Delta z \tag{2.32}$$

and

$$\frac{\partial F_{s,(zx)}}{\partial z}\Delta x\Delta y\Delta z. \tag{2.33}$$

Adding all the surface forces in the x direction, we have

$$\left(\frac{\partial F_{s,(xx)}}{\partial x}+\frac{\partial F_{s,(yx)}}{\partial y}+\frac{\partial F_{s,(zx)}}{\partial z}\right)\Delta x\Delta y\Delta z. \tag{2.34}$$

Following the same procedure, the sum of all surface forces in the y direction, normal to the face $\Delta x\Delta z$ is

$$\left(\frac{\partial F_{s,(xy)}}{\partial x}+\frac{\partial F_{s,(yy)}}{\partial y}+\frac{\partial F_{s,(zy)}}{\partial z}\right)\Delta x\Delta y\Delta z, \tag{2.35}$$

and the sum of all forces in the z direction, normal to the face $\Delta y\Delta z$ is

$$\left(\frac{\partial F_{s,(xz)}}{\partial x}+\frac{\partial F_{s,(yz)}}{\partial y}+\frac{\partial F_{s,(zz)}}{\partial z}\right)\Delta x\Delta y\Delta z. \tag{2.36}$$

The stress $F_{s,(xx)}$ includes the negative static pressure and the normal stress σ_{xx}, and also that $F_{s,(yx)}$ and $F_{s,(zx)}$ include shearing stresses τ_{yx} and τ_{zx}, respectively. Therefore the forces normal to face $\Delta y\Delta z$ in the x direction are expressed as

$$\left(-\frac{\partial \rho}{\partial x}+\frac{\partial \sigma_{xx}}{\partial x}+\frac{\partial \tau_{yx}}{\partial y}+\frac{\partial \tau_{zx}}{\partial z}\right)\Delta x\Delta y\Delta z \tag{2.37}$$

Similarly, the forces normal to the faces $\Delta x\Delta z$ and $\Delta x\Delta y$ in the y and z directions are expressed respectively as

$$\left(\frac{\partial \tau_{xy}}{\partial x}-\frac{\partial \rho}{\partial y}+\frac{\partial \sigma_{yy}}{\partial y}+\frac{\partial \tau_{zy}}{\partial z}\right)\Delta x\Delta y\Delta z \tag{2.38}$$

and

$$\left(\frac{\partial \tau_{xz}}{\partial x}+\frac{\partial \tau_{yz}}{\partial y}-\frac{\partial \rho}{\partial z}+\frac{\partial \sigma_{zz}}{\partial z}\right)\Delta x\Delta y\Delta z. \tag{2.39}$$

The viscous stresses are associated with the deformation of the fluid and are also a function of fluid viscosity and velocity gradient [74]. It is expected that the normal stress should deform the fluid linearly, while the shear stress should result with angular

deformation. Figures 2.5 and 2.6 illustrate the effects of the normal and shear stress of the fluid deformation.

Figure 2.5: Linear deformation of a fluid element due to normal stress

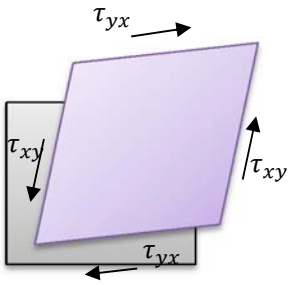

Figure 2.6: Angular deformation of a fluid element due to shear stress

A Newtonian fluid is one in which the viscous stress is linearly proportional to the rate of deformation, which is $\tau = \mu \frac{\partial u}{\partial x}$ in one dimension, where μ is the proportionality constant and also the fluid viscosity. Stokes extended the result into multidimensional flows. Stokes' extension describes the fact that the fluid element may undergo a strain due to gradients such as $\frac{\partial u}{\partial x}, \frac{\partial v}{\partial y}$ and $\frac{\partial w}{\partial z}$. The formulae developed by Stokes are called Stokes relations, and they are expressed as follows:

$$\sigma_{xx} = 2\mu \frac{\partial u}{\partial x} - \frac{2}{3}\mu \left(\frac{\partial u}{\partial x} + \frac{\partial v}{\partial y} + \frac{\partial w}{\partial z}\right) = 2\mu \frac{\partial u}{\partial x} \tag{2.40}$$

$$\sigma_{yy} = 2\mu \frac{\partial v}{\partial y} - \frac{2}{3}\mu \left(\frac{\partial u}{\partial x} + \frac{\partial v}{\partial y} + \frac{\partial w}{\partial z}\right) = 2\mu \frac{\partial v}{\partial y} \tag{2.41}$$

$$\sigma_{zz} = 2\mu \frac{\partial w}{\partial z} - \frac{2}{3}\mu \left(\frac{\partial u}{\partial x} + \frac{\partial v}{\partial y} + \frac{\partial w}{\partial z}\right) = 2\mu \frac{\partial w}{\partial z} \tag{2.42}$$

$$\tau_{xy} = \tau_{yx} = \mu\left(\frac{\partial u}{\partial x} + \frac{\partial v}{\partial y}\right) \quad (2.43)$$

$$\tau_{xz} = \tau_{zx} = \mu\left(\frac{\partial u}{\partial x} + \frac{\partial w}{\partial z}\right) \quad (2.44)$$

$$\tau_{yz} = \tau_{zy} = \mu\left(\frac{\partial v}{\partial y} + \frac{\partial w}{\partial z}\right) \quad (2.45)$$

The second terms or normal expressions on the right become zero, due to using the continuity equations. Substituting Equations (2.40)-(2.45) into (2.37)-(2.39) and with the addition of the body forces equations, we obtain the following results in the x, y and z directions, respectively:

$$\sum F_x = \left[\rho g_x - \frac{\partial \rho}{\partial x} + \mu\left(\frac{\partial^2 u}{\partial x^2} + \frac{\partial^2 v}{\partial y^2} + \frac{\partial^2 w}{\partial z^2}\right)\right]\Delta x \Delta y \Delta z \quad (2.46)$$

$$\sum F_y = \left[\rho g_y - \frac{\partial \rho}{\partial y} + \mu\left(\frac{\partial^2 u}{\partial x^2} + \frac{\partial^2 v}{\partial y^2} + \frac{\partial^2 w}{\partial z^2}\right)\right]\Delta x \Delta y \Delta z \quad (2.47)$$

$$\sum F_z = \left[\rho g_z - \frac{\partial \rho}{\partial z} + \mu\left(\frac{\partial^2 u}{\partial x^2} + \frac{\partial^2 v}{\partial y^2} + \frac{\partial^2 w}{\partial z^2}\right)\right]\Delta x \Delta y \Delta z \quad (2.48)$$

Substituting Equations (2.46) – (2.48) into equations (2.26) – (2.28) we have the following equations in the x, y and z directions, respectively:

$$\rho g_x - \frac{\partial \rho}{\partial x} + \mu\left(\frac{\partial^2 u}{\partial x^2} + \frac{\partial^2 v}{\partial y^2} + \frac{\partial^2 w}{\partial z^2}\right) = \rho\left(\frac{\partial u}{\partial t} + u\frac{\partial u}{\partial x} + v\frac{\partial u}{\partial y} + w\frac{\partial u}{\partial z}\right) \quad (2.49)$$

$$\rho g_y - \frac{\partial \rho}{\partial y} + \mu\left(\frac{\partial^2 u}{\partial x^2} + \frac{\partial^2 v}{\partial y^2} + \frac{\partial^2 w}{\partial z^2}\right) = \rho\left(\frac{\partial u}{\partial t} + u\frac{\partial v}{\partial x} + v\frac{\partial v}{\partial y} + w\frac{\partial v}{\partial z}\right) \quad (2.50)$$

and

$$\rho g_z - \frac{\partial \rho}{\partial z} + \mu\left(\frac{\partial^2 u}{\partial x^2} + \frac{\partial^2 v}{\partial y^2} + \frac{\partial^2 w}{\partial z^2}\right) = \rho\left(\frac{\partial w}{\partial t} + u\frac{\partial w}{\partial x} + v\frac{\partial w}{\partial y} + w\frac{\partial w}{\partial z}\right) \quad (2.51)$$

Equations (2.49) – (2.51) are called the x-momentum, y-momentum and the z-momentum equations.

2.5. The energy equation

One of the most fundamental laws in nature is the first law of thermodynamics, also known as the conservation of energy principle. It states that the rate of change of energy of a fluid particle is equal to the rate of heat addition plus the rate of work done.

This implies that energy can neither be created nor destroyed during a process, it can only change form [23].

Therefore,

$$\begin{Bmatrix} Rate\ of\ change\ of \\ energy\ inside\ the \\ fluid\ element \end{Bmatrix} = \begin{Bmatrix} Net\ flux\ of\ the \\ heat\ into\ the \\ fluid\ element \end{Bmatrix} + \begin{Bmatrix} Rate\ of\ work\ done\ on \\ the\ element\ due\ to\ body \\ and\ surface\ forces \end{Bmatrix}$$

The conservation of energy principle for any system can be expressed simply as

$$E_{in} - E_{out} = \Delta E.$$

The Energy equation will be derived by setting the total derivative to be equal to the change in energy as a result of the work done by viscous stresses and the net heat conduction in the control volume.

The energy per unit mass of the fluids includes internal energy e and kinetic energy $\frac{V^2}{2}$, where V, the magnitude of the velocity vector in the x, y and z directions, is given by $V^2 = u^2 + v^2 + w^2$ [62]. Thus

$$E = e + \frac{1}{2}(u^2 + v^2 + w^2). \tag{2.52}$$

The following expression describes the rate of change of total energy in the control volume:

$$\frac{\partial(\rho E)}{\partial \bar{t}} \Delta x \Delta y \Delta z. \tag{2.53}$$

The first law of thermodynamics can also be written in the form

$$internal\ energy\ increase\ rate = heat\ transfer\ rate - surface\ forces\ work\ rate. \tag{2.54}$$

The rate of net transfer of energy through the control volume is parallel to the momentum flux transfer into and out of the control volume. As a result, the use of the momentum conservation expression

$$\frac{\partial}{\partial \bar{t}}(\rho u) + \frac{\partial}{\partial x}(\rho u)u + \frac{\partial}{\partial y}(\rho v)u + \frac{\partial}{\partial z}(\rho w)u \qquad (2.55)$$

is applied.

Note that $(\rho u)u, (\rho v)u$ and $(\rho w)u$ represent the momentum flux through the $\Delta y \Delta z$ face, $\Delta x \Delta z$ face and $\Delta x \Delta y$ face in the x direction. Applying the expression in (2.55), the total transfer of energy per unit volume through the control volume in the x direction is

$$\frac{\partial}{\partial \bar{t}}\rho\left(e + \frac{1}{2}V^2\right) + \frac{\partial}{\partial x}\rho u\left(e + \frac{1}{2}V^2\right) + \frac{\partial}{\partial y}\rho v\left(e + \frac{1}{2}V^2\right) + \frac{\partial}{\partial z}\rho w\left(e + \frac{1}{2}V^2\right), \qquad (2.56)$$

where (2.55) is obtained by replacing u in Equation (2.54) by the sum of internal and kinetic energies. Then (2.55) can be shortened as

$$\frac{\partial(\rho E)}{\partial \bar{t}}\Delta y \Delta z. \qquad (2.57)$$

The second task is to look at the work done per unit volume by the surface forces in the control volume. Figure 2.7 illustrates the external forces working on the volume surfaces in the x direction:

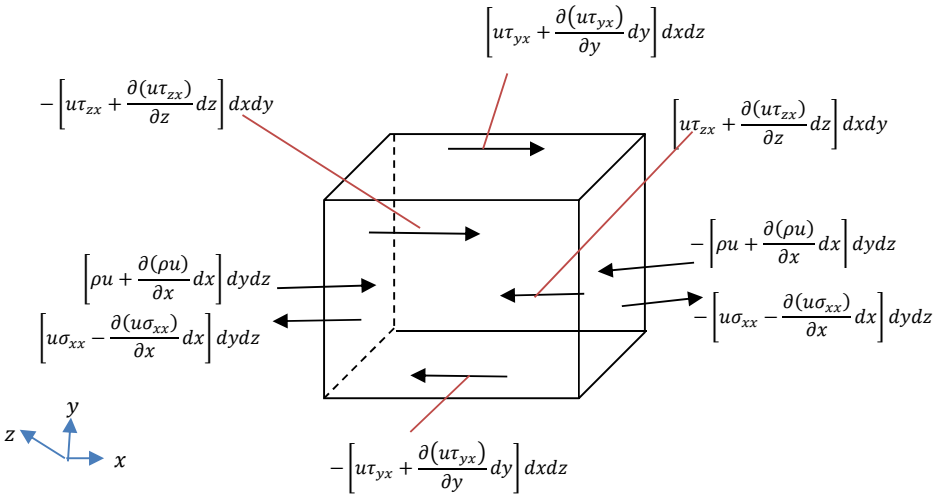

Figure 2.7: Work done by surface stresses (external forces)

It should be noted that in this case external forces are the same as in the case of momentum. The forces are multiplied by the velocity u, in the x direction. Summing all the external forces as shown in Fig. 2.7, and dividing by $2\Delta x\Delta y\Delta z$, we obtain the expression

$$-\frac{\partial(\rho u)}{\partial x}+\frac{\partial(u\sigma_{xx})}{\partial x}+\frac{\partial(u\tau_{yx})}{\partial y}+\frac{\partial(u\tau_{zx})}{\partial z}. \tag{2.58}$$

Considering the surface stresses acting on other faces, that is, the $\Delta x\Delta z$ and $\Delta x\Delta y$, in the y and z directions respectively, the expressions

$$-\frac{\partial(\rho v)}{\partial y}+\frac{\partial(v\sigma_{yy})}{\partial y}+\frac{\partial(v\tau_{xy})}{\partial x}+\frac{\partial(u\tau_{zy})}{\partial z} \tag{2.59}$$

and

$$-\frac{\partial(\rho w)}{\partial z}+\frac{\partial(w\sigma_{zz})}{\partial z}+\frac{\partial(w\tau_{xz})}{\partial x}+\frac{\partial(w\tau_{yz})}{\partial y} \tag{2.60}$$

are obtained. Adding the three expressions (2.58)-(2.60), the net expression for the work done by surface stresses becomes

$$-\frac{\partial(\rho u)}{\partial x}-\frac{\partial(\rho v)}{\partial y}-\frac{\partial(\rho w)}{\partial z}+\frac{\partial(u\sigma_{xx})}{\partial x}+\frac{\partial(u\tau_{yx})}{\partial y}+\frac{\partial(u\tau_{zx})}{\partial z}+\frac{\partial(v\sigma_{yy})}{\partial y}+\frac{\partial(v\tau_{xy})}{\partial x}+\frac{\partial(u\tau_{zy})}{\partial z}+$$
$$\frac{\partial(w\sigma_{zz})}{\partial z}+\frac{\partial(w\tau_{xz})}{\partial x}+\frac{\partial(w\tau_{yz})}{\partial y}. \qquad (2.61)$$

(2.61) can be expressed as

$$-div(\rho\boldsymbol{U})+\frac{\partial(\rho u)}{\partial x}+\frac{\partial(u\sigma_{xx})}{\partial x}+\frac{\partial(u\tau_{yx})}{\partial y}+\frac{\partial(u\tau_{zx})}{\partial z}+\frac{\partial(v\sigma_{yy})}{\partial y}+\frac{\partial(v\tau_{xy})}{\partial x}+\frac{\partial(u\tau_{zy})}{\partial z}+$$
$$\frac{\partial(w\sigma_{zz})}{\partial z}+\frac{\partial(w\tau_{xz})}{\partial x}+\frac{\partial(w\tau_{yz})}{\partial y}, \qquad (2.62)$$

where

$$-div(\rho\boldsymbol{U})=\frac{\partial(\rho u)}{\partial x}+\frac{\partial(\rho v)}{\partial y}+\frac{\partial(\rho w)}{\partial z} \qquad (2.63)$$

The final task in Equations (2.54) is to come up with the expression for the total heat per unit volume transferred into the control volume. This is determined by the heat flux q_i. The heat flux will be regarded as positive for heat going out of the control volume to the surrounding x, y and z directions. Figure 2.8 illustrates the heat flux as a result of the heat energy transfer through the control volume.

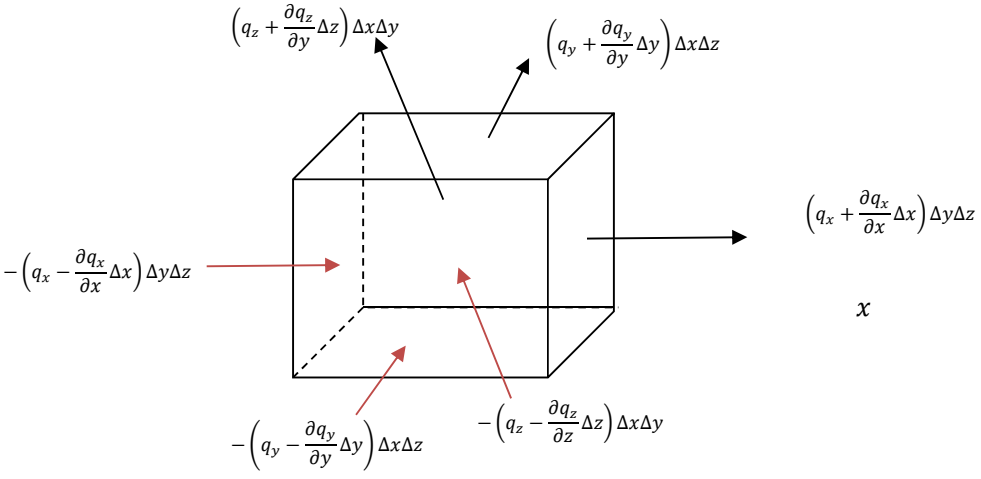

Figure 2.8: Heat flux due to heat energy transfer

Adding the heat flux components in Fig. 2.8 and dividing by $2\Delta x\Delta y\Delta z$, we obtain the result

$$\frac{\partial q_x}{\partial x}+\frac{\partial q_y}{\partial y}+\frac{\partial q_z}{\partial z}. \tag{2.64}$$

Figure 2.8 shows that the heat conduction effects are associated with the motion of gas molecules which randomly move in and out of the control volume. The gas motion gradually brings the energy in and out of the control volume, and there is also a heat exchange of the heat energy at the surface boundaries without any exchange in mass [36]. Fourier's law is applied to relate the heat flow in the x, y and z directions to the rate of change of temperature in the x, y and z directions.

Fourier's law states that the rate at which heat flows across the surface of unit area is proportional to the negative of the temperature gradient normal to the surface [42]. This law is expressed as follows in the x direction normal to the $\Delta y\Delta z$ face:

$$q_x = -k\frac{\partial T}{\partial x} \tag{2.65}$$

It follows that

$$q_y = -k\frac{\partial T}{\partial y} \tag{2.66}$$

and

$$q_z = -k\frac{\partial T}{\partial z}. \tag{2.67}$$

k is the proportionality constant and T is the temperature of the fluid element. The negative sign indicates that heat flows from hot to cold region. Therefore, (2.64) can be expressed as

$$\frac{\partial}{\partial x}\left(k\frac{\partial T}{\partial x}\right)+\frac{\partial}{\partial y}\left(k\frac{\partial T}{\partial y}\right)+\frac{\partial}{\partial z}\left(k\frac{\partial T}{\partial z}\right), \tag{2.68}$$

which can be simplified to

$$k\left(\frac{\partial^2 T}{\partial x^2}+\frac{\partial^2 T}{\partial y^2}+\frac{\partial^2 T}{\partial z^2}\right). \tag{2.69}$$

The sum of (2.56), (2.62) and (2.69) gives the following expression

$$\frac{\partial}{\partial \bar{t}}\rho\left(e+\frac{1}{2}V^2\right)+\frac{\partial}{\partial x}\rho u\left(e+\frac{1}{2}V^2\right)+\frac{\partial}{\partial y}\rho v\left(e+\frac{1}{2}V^2\right)+\frac{\partial}{\partial z}\rho w\left(e+\frac{1}{2}V^2\right)=$$
$$-div(\rho\boldsymbol{U})+\frac{\partial(\rho u)}{\partial x}+\frac{\partial(u\sigma_{xx})}{\partial x}+\frac{\partial(u\tau_{yx})}{\partial y}+\frac{\partial(u\tau_{zx})}{\partial z}+\frac{\partial(v\sigma_{yy})}{\partial y}+\frac{\partial(v\tau_{xy})}{\partial x}+\frac{\partial(u\tau_{zy})}{\partial z}+$$
$$\frac{\partial(w\sigma_{zz})}{\partial z}+\frac{\partial(w\tau_{xz})}{\partial x}+\frac{\partial(w\tau_{yz})}{\partial y}+k\left(\frac{\partial^2 T}{\partial x^2}+\frac{\partial^2 T}{\partial y^2}+\frac{\partial^2 T}{\partial z^2}\right)+R_E \tag{2.70}$$

R_E represents the energy term that may include the potential energy or heat production from nuclear or chemical reactions. The work done due to gravity is included as in the case of momentum equations. Using body forces in the x, y and z directions respectively represented by $g_x\rho\Delta x\Delta y\Delta z$, $g_y\rho\Delta x\Delta y\Delta z$ and $g_z\rho\Delta x\Delta y\Delta z$, the work done by gravity forces in the respective directions are $\rho u g_x$, $\rho v g_y$ and $\rho w g_z$. Equation (2.70) can be expressed as

$$\frac{\partial(\rho E)}{\partial \bar{t}}=k\left(\frac{\partial^2 T}{\partial x^2}+\frac{\partial^2 T}{\partial y^2}+\frac{\partial^2 T}{\partial z^2}\right)-\left[-div(\rho\boldsymbol{U})+\frac{\partial(\rho u)}{\partial x}+\frac{\partial(u\sigma_{xx})}{\partial x}+\frac{\partial(u\tau_{yx})}{\partial y}+\frac{\partial(u\tau_{zx})}{\partial z}+\right.$$
$$\left.\frac{\partial(v\sigma_{yy})}{\partial y}+\frac{\partial(v\tau_{xy})}{\partial x}+\frac{\partial(u\tau_{zy})}{\partial z}+\frac{\partial(w\sigma_{zz})}{\partial z}+\frac{\partial(w\tau_{xz})}{\partial x}+\frac{\partial(w\tau_{yz})}{\partial y}\right]+\rho u g_x+\rho v g_y+\rho w g_z+$$
$$R_E \tag{2.71}$$

Equation (2.71) is the energy conservation equation and it is a mathematical expression for (2.54).

CHAPTER THREE

NATURAL CONVECTION FLOW OF HEAT GENERATING HYDROMAGNETIC COUPLE STRESS FLUID WITH TIME PERIODIC BOUNDARY CONDITIONS

Chapter Abstract

In this chapter, analysis has been conducted to investigate the effects of couple stresses and internal heat generation on the magnetohydrodynamic (MHD) natural convection channel flow with steady-periodic heat input. By applying the steady-periodic heating assumptions, the flow governing equations driving the fluid system are reduced to boundary-value problems and solved by a convergent successive approximation. The result of the computation shows that the skin friction at the lower wall decreases with increasing values of the couple stress parameter while it enhances the heat transfer rate.

3.1. Introduction

Free convention flow through a vertical channel has been an active research area in heat transfer processes because of its usefulness in several thermal, industrial and mechanical engineering applications. Few practical applications of convective flows are seen in the cooling of electronic and electrical devices, cooling and heating of nuclear reactors for power generation, automated cooling in heat exchangers and lots more. To address this in oscillatory flows, Wang [149] implemented a technique to separate the energy and momentum equations into steady and oscillatory flows. Jha and Ajibade [65] examined the free convective oscillatory flow through a vertical wall, noting the influence of viscous dissipation on the fluid. Moreover, Jha and Ajibade [63] investigated the combination of temperature dependent internal heat generation and leaky walls on buoyancy-induced flow subjected to oscillatory heat condition. Adesanya [3] reported the transient natural convection heat generating buoyancy-induced flow in a porous micro-channel with slippage and temperature jump. Adesanya *et al.* [12] examined the hydromagnetic natural convective flow with heat source through an impervious parallel plate with periodic heating. Other relevant results on free convection flow in the steady-periodic regime include the following [2, 55, 56, 64, 80, 150] and references therein.

All the above studies are only applicable to purely Newtonian fluids, however, in many practical applications, many real fluids of industrial and medical importance contain tiny microstructures of mechanical significance which could enhance heat transfer, drug delivery processes and conserve energy. Some of these fluids are used as surfactants, coolants used in radiators, lubricating fluids or synthetic oil containing size-dependent polymer additives, blood containing red blood cells and other nano components, tooth paste and gels which are mixtures of nanoparticles, pharmaceutical mixtures, paints, ferrofluid used in car shock absorber and many more. In view of the wide range of application, it is very clear that the Newtonian constitutive model cannot capture the rheological properties of these fluids, in particular, when handling size-dependent microstructures. To account for these, Stokes [141] noted this all-important-effect and formulated a Couple stress model which could account for the presence of non-symmetric stress tensor, couple stresses and body couples. In view of his formulations, Srinivasacharya and Rao [137], proposed a couple stress model to examine the MHD pulsatile blood flow in a bifurcated stenosed artery. Akhtar and Shah [19] presented an analytical solution for unsteady couple stress fluid flow. Aksoy [21], studied the irreversibility analysis for couple stress fluid with constant heat flux. Ahmed *et al* [16] focused on the analytical approach for the oscillatory MHD couple stress fluid flow in rotating channel. Beg et al [26], analysed the oscillatory flow of hydromagnetic non-Newtonian bio-couple stress fluid. Other interesting works on the flows with microstructure can be found in [5, 8, 10, 11, 16, 19, 33, 34, 39, 53, 57, 78, 84, 127, 135, 138, 139,140,152].

In the handling viscous fluids, one of the easiest ways to enhance flow is by in situ combustion when fluids are made to undergo chemical reactions. By doing this, internal heat generation will grossly affect the volumetric temperature in the flow domain by either conduction or convection. Recently, Ali *et al.* [22] investigated the oscillatory hydromagnetic couple stress heat generating fluid flow through a porous medium with heat source by using Foraboschi and Federico [44] model. Similarly, Makinde [77] reported the effect of buoyancy-induced flow. Saravanan and Brindha [110] examined the stability of convective flow of problem in the presence of heat generation and other related literature can be found in [4, 17, 105, 143] and references therein.

Studies related to hydromagnetic flow problems have quite a number of applications in engineering, for instance, flow control, agglomeration of fluid particles and damping of shocks in car absorbers to mention just a few. In view of these Sheikholeslami and Rokni [123] reported a developing nanofluid flow with induced magnetic field. Sheikholeslami [112] reported the MHD effect on the radiative variable viscous flow of Fe_3O_4 −water nanofluid. Sheikholeslami and Shehzad [124] analysed the influence of magnetic field on the flow of CuO-water nanofluid through a leaky semi-annulus. Sheikholeslami *et al*. [122] examined the effect of the dependence of viscosity on magnetic field in a nanofluid flow. Sheikholeslami and Ganji [114] investigated MHD nanofluid channel flow using Buongiorno model. Sheikholeslami and Chamkha [113] examined the MHD Marangoni convective flow of a two-phase nanofluid. Other recent work on the convective flow of electrically conducting fluid in several geometries can be found in [115, 116, 117,120,121].

Motivated by the studies described above, the present work addresses the combined effect of couple stresses and internal heat generation on free convective flow of electrically conducting fluid with periodic heat input which have not been considered in previous models to the best of our knowledge. In the following sections: the problem is formulated and resolved by semi-analytical means [13, 14, 38, 95, 96, 97, 118,119]. Variations of pertinent fluid parameters are presented graphically and discussed extensively. Concluding remarks will be given in the last section.

3.2. Mathematical formulation

Consider the fully developed flow of an incompressible couple stress fluid via a channel positioned vertically and subjected to steady-periodic heating at the walls as shown in Figure 3.1. The couple stress fluid is subjected to magnetic field of constant intensity of small electrical conductivity and negligible induced magnetic field.

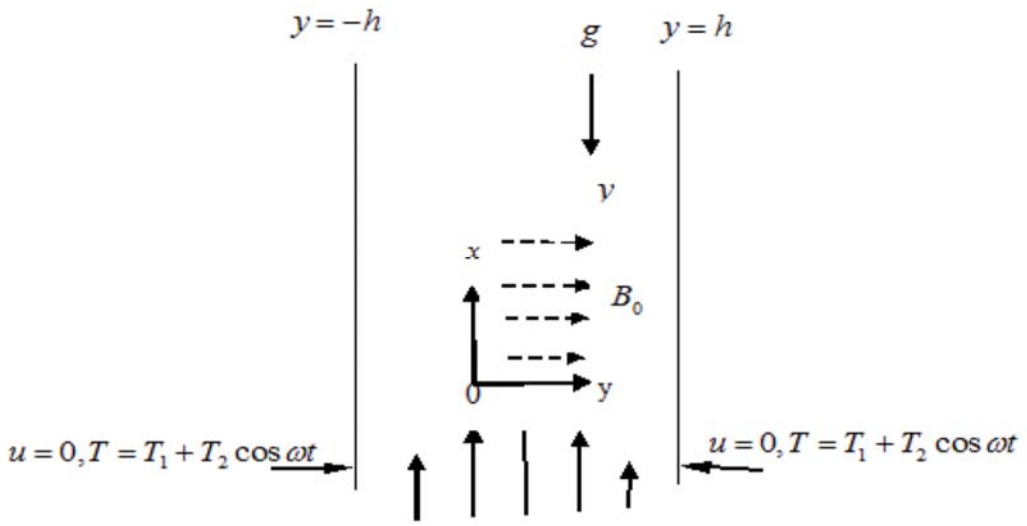

Figure 3.1 Physical model of the problem

We further assumed that all fluid properties are constant except the fluid density and internal heat generation that are temperature-dependent. As shown in the problem geometry, we take a Cartesian coordinate system (x, y) and the channel walls are taken at $y = \pm h$. Under Boussinesq approximations, the flow-governing-equations can be written as [12]:

$$\frac{\partial u}{\partial t} = \nu \frac{\partial^2 u}{\partial y^2} - \frac{\sigma B_0^2}{\rho} u + g\beta(T - T_0) - \frac{\gamma}{\rho} \frac{\partial^4 u}{\partial y^4} \tag{3.1}$$

$$\frac{\partial T}{\partial t} = \frac{k}{\rho c_p} \frac{\partial^2 T}{\partial y^2} + \frac{\mu}{\rho c_p} \left(\frac{\partial u}{\partial y} \right)^2 + \frac{\sigma B_0^2}{\rho c_p} u^2 + \frac{Q_0}{\rho c_p} (T - T_0) + \frac{\gamma}{\rho c_p} \left(\frac{\partial^2 u}{\partial y^2} \right)^2 \tag{3.2}$$

Other terms in equations (3.1) and (3.2) are due to the effect of couple stresses, dissipation due to couple stresses [5, 8, 10, 11, 16, 19, 33, 34, 39, 53, 57, 78, 84, 127, 135, 138, 139,140,152] and linear internal heat generation [17, 44, 77, 88, 105, 110, 143]. Together with the following initial and boundary conditions:

$$u(0, y) = 0, T(0, y) = T_0 \tag{3.3}$$

$$u(t, \pm h) = 0 = \frac{\partial^2 u}{\partial y^2}(t, \pm h), T(t, \pm h) = T_1 + T_2 \cos(\omega t), y = \pm h, t > 0 \tag{3.4}$$

Following [3, 12, 64, 65, 149], we introduce the following,

$$u(t,y)=\frac{g\beta h^2}{\nu}\left[(T_1-T_0)A(y)+T_2B(y)e^{i\omega t}\right] \tag{3.5}$$

$$T(t,y)=T_0+(T_1-T_0)F(y)+T_2G(y)e^{i\omega t} \tag{3.6}$$

Equations (3.1) and (3.2) become

$$\begin{aligned}\frac{g\beta h^2}{\nu}T_2 i\omega B(y)e^{i\omega t}=&\,g\beta h^2(T_1-T_0)A''(y)+g\beta h^2T_2B''(y)e^{i\omega t}-\frac{\sigma B_0^2}{\rho}\frac{g\beta h^2}{\nu}(T_1-T_0)A(y)\\&-\frac{\sigma B_0^2}{\rho}\frac{g\beta h^2}{\nu}T_2B(y)e^{i\omega t}+g\beta\left[(T_1-T_0)F(y)+T_2G(y)e^{i\omega t}\right]\\&-\frac{\gamma}{\rho}\frac{g\beta h^2}{\nu}(T_1-T_0)A^{(4)}(y)-\frac{\gamma}{\rho}\frac{g\beta h^2}{\nu}T_2B^{(4)}(y)e^{i\omega t}\end{aligned} \tag{3.7}$$

and

$$\begin{aligned}T_2 i\omega G(y)e^{i\omega t}=&\frac{k}{\rho c_p}\left[(T_1-T_0)F''(y)+T_2G''(y)e^{i\omega t}\right]\\&+\frac{\mu}{\rho c_p}\left(\frac{g\beta h^2}{\nu}\right)^2\left[(T_1-T_0)^2(A'(y))^2+2(T_1-T_0)T_2A'(y)B'(y)e^{i\omega t}+T_2^2(B'(y))^2e^{2i\omega t}\right]\\&+\frac{\sigma B_0^2}{\rho c_p}\left(\frac{g\beta h^2}{\nu}\right)^2\left[(T_1-T_0)^2(A'(y))^2+2(T_1-T_0)T_2A'(y)B'(y)e^{i\omega t}+T_2^2(B'(y))^2e^{2i\omega t}\right]\\&+\frac{\gamma}{\rho c_p}\left(\frac{g\beta h^2}{\nu}\right)^2+\left[(T_1-T_0)^2(A''(y))^2+2(T_1-T_0)T_2A''(y)B''(y)e^{i\omega t}+T_2^2(B''(y))^2e^{2i\omega t}\right]\\&+\frac{Q_0}{\rho c_p}\left[(T_1-T_0)F(y)+T_2G(y)e^{i\omega t}\right]\end{aligned} \tag{3.8}$$

Introducing the dimensionless quantities

$$\eta=\frac{y}{h},\lambda=\frac{\mu}{k}\left(\frac{g\beta h^2}{\nu}\right)^2(T_1-T_0),St=\frac{h^2\omega}{\nu},\Pr=\frac{\mu c_p}{k},Ha^2=\frac{\sigma B_0^2h^2}{\mu},a^2=\frac{h^2\mu}{\gamma},\delta=\frac{Q_0h^2}{k}, \tag{3.9}$$

gives rise to the coupled system:

$$iStT_2B(\eta)e^{i\omega t} = (T_1 - T_0)A''(\eta) + T_2B''(\eta)e^{i\omega t} - Ha^2\left[(T_1 - T_0)A(\eta) + T_2B(\eta)e^{i\omega t}\right] + (T_1 - T_0)F(\eta) + T_2G(\eta)e^{i\omega t} - \frac{1}{a^2}\left[(T_1 - T_0)A^{(4)}(\eta) + T_2B^{(4)}(\eta)e^{i\omega t}\right] \tag{3.10}$$

and

$$\begin{aligned} i\,\mathrm{Pr}\,StT_2G(\eta)e^{i\omega t} &= (T_1 - T_0)F''(\eta) + T_2G''(\eta)e^{i\omega t} \\ &+ \lambda\left[(T_1 - T_0)^2(A'(\eta))^2 + 2(T_1 - T_0)A'(\eta)T_2B'(\eta)e^{i\omega t} + T_2^2(B'(\eta))^2e^{2i\omega t}\right] \\ &+ \lambda Ha^2\left[(T_1 - T_0)^2(A(\eta))^2 + 2(T_1 - T_0)A(\eta)T_2B(\eta)e^{i\omega t} + T_2^2(B(\eta))^2e^{2i\omega t}\right] \\ &+ \frac{\lambda}{a^2}\left[(T_1 - T_0)^2(A''(\eta))^2 + 2(T_1 - T_0)A''(\eta)T_2B''(\eta)e^{i\omega t} + T_2^2(B''(\eta))^2e^{2i\omega t}\right] \\ &+ \delta\left[(T_1 - T_0)F(\eta) + T_2G(\eta)e^{i\omega t}\right] \end{aligned} \tag{3.11}$$

If we equate the orders of $e^{i\omega t}$, we get the following steady state system of coupled ordinary differential equations along with the appropriate boundary conditions

$$A^{(4)}(\eta) = a^2\left(A''(\eta) - H^2A(\eta) + F(\eta)\right);\quad A(\pm1) = 0, A''(\pm1) = 0 \tag{3.12}$$

$$B^{(4)}(\eta) = a^2\left(B''(\eta) - \left(iSt + H^2\right)B(\eta) + G(\eta)\right);\quad B(\pm1) = 0, B''(\pm1) = 0 \tag{3.13}$$

$$F''(\eta) + \lambda\left[(A'(\eta))^2 + H^2(A(\eta))^2 + \frac{1}{a^2}(A''(\eta))^2\right] + \delta F(\eta) = 0;\ F(\pm1) = 1 \tag{3.14}$$

$$G''(\eta) - iSt\,\mathrm{Pr}\,G(\eta) + 2\lambda\left[A'(\eta)B'(\eta) + H^2A(\eta)B(\eta) + \frac{1}{a^2}A''(\eta)B''(\eta)\right] + \delta G(\eta) = 0;\quad G(\pm1) = 1 \tag{3.15}$$

It is important to note that, in the asymptotic case as $a \to \infty, \delta \to 0$ the solutions of Equations (3.12) – (3.15) reduce to that reported in Adesanya *et al*. [5].

3.3. Method of Solution

In order to tackle the nonlinearity associated with the coupled model by Adomian decomposition method, the boundary value problem (3.12) - (3.15) would be converted into its equivalent integral equations. Integrating (3.12) - (3.15) together with the boundary conditions gives the following:

$$A(\eta)=\int_{-1}^{\eta}\frac{dA(-1)}{dY}dY+\int_{-1}^{\eta}\int_{-1}^{\eta}\int_{-1}^{\eta}\left(\frac{d^3A(-1)}{dY^3}\right)dYdYdY + \int_{-1}^{y}\int_{-1}^{y}\int_{-1}^{y}\int_{-1}^{y}\left(a^2\left(A''(Y)-H^2A(Y)+F(Y)\right)\right)dYdYdYdY \tag{3.16}$$

$$B(\eta)=\int_{-1}^{\eta}\frac{dB(-1)}{dY}dY+\int_{-1}^{\eta}\int_{-1}^{\eta}\int_{-1}^{\eta}\left(\frac{d^3B(-1)}{dY^3}\right)dYdYdY + \int_{-1}^{\eta}\int_{-1}^{\eta}\int_{-1}^{\eta}\int_{-1}^{\eta}\left(a^2\left(B''(Y)-\left(iSt+H^2\right)B(Y)+G(Y)\right)\right)dYdYdYdY \tag{3.17}$$

$$F(\eta)=1+\int_{0}^{y}\frac{dF(-1)}{dY}dY-\int_{-1}^{\eta}\int_{-1}^{\eta}\left(\lambda\left[\left(A'(Y)\right)^2+Ha^2\left(A(Y)\right)^2+\frac{1}{a^2}\left(A''(Y)\right)^2\right]-\delta F(Y)\right)dYdY\Bigg\} \tag{3.18}$$

$$G(\eta)=1+\int_{0}^{y}\frac{dG(-1)}{dY}dY-\int_{-1}^{\eta}\int_{-1}^{\eta}\left(\lambda\left[\left(B'(Y)\right)^2+H^2\left(B(Y)\right)^2+\frac{1}{a^2}\left(B''(Y)\right)^2\right]-\left(\delta+iSt\,\mathrm{Pr}\right)G(Y)\right)dYdY\Bigg\} \tag{3.19}$$

Let us now define Adomian series of the form:

$$A(\eta)=\sum_{n=0}^{\infty}A_n(\eta),\ B(\eta)=\sum_{n=0}^{\infty}B_n(\eta),\ \ F(\eta)=\sum_{n=0}^{\infty}F_n(\eta),\quad G(\eta)=\sum_{n=0}^{\infty}G_n(\eta) \tag{3.20}$$

Substituting (3.20) in (3.16)-(3.19), we obtain

$$\sum_{n=0}^{\infty}A_n(\eta)=\int_{-1}^{\eta}\frac{dA(-1)}{dY}dY+\int_{-1}^{\eta}\int_{-1}^{\eta}\int_{-1}^{\eta}\left(\frac{d^3A(-1)}{dY^3}\right)dYdYdY + \int_{-1}^{y}\int_{-1}^{y}\int_{-1}^{y}\int_{-1}^{y}\left(a^2\left(\left(\sum_{n=0}^{\infty}A_n(\eta)\right)''(Y)-H^2\sum_{n=0}^{\infty}A_n(\eta)+\sum_{n=0}^{\infty}F_n(Y)\right)\right)dYdYdYdY \tag{3.21}$$

$$\sum_{n=0}^{\infty}B_n(\eta)=\int_{-1}^{\eta}\frac{dB(-1)}{dY}dY+\int_{-1}^{\eta}\int_{-1}^{\eta}\int_{-1}^{\eta}\left(\frac{d^3B(-1)}{dY^3}\right)dYdYdY + \int_{-1}^{\eta}\int_{-1}^{\eta}\int_{-1}^{\eta}\int_{-1}^{\eta}\left(a^2\left(\left(\sum_{n=0}^{\infty}B_n\right)''(Y)-\left(iSt+H^2\right)\sum_{n=0}^{\infty}B_n(Y)+\sum_{n=0}^{\infty}G_n(Y)\right)\right)dYdYdYdY \tag{3.22}$$

With

$$\left.\begin{aligned}\sum_{n=0}^{\infty}F_n(\eta)&=1+\int_{-1}^{y}\frac{dF(-1)}{dY}dY\\&\quad-\int_{-1}^{\eta}\int_{-1}^{\eta}\left(\lambda\left[\left(\left(\sum_{n=0}^{\infty}A_n\right)'(Y)\right)^2+H^2\left(\sum_{n=0}^{\infty}A_n(Y)\right)^2+\frac{1}{a^2}(A''(Y))^2\right]-\delta\sum_{n=0}^{\infty}F_n(Y)\right)dYdY\end{aligned}\right\}$$

(3.23)

$$\left.\begin{aligned}\sum_{n=0}^{\infty}G_n(\eta)&=1+\int_{-1}^{y}\frac{dG(-1)}{dY}dY\\&-\int_{-1}^{\eta}\int_{-1}^{\eta}\left(2\lambda\left[\sum_{n=0}^{\infty}A_n'(Y)\sum_{n=0}^{\infty}B_n'(Y)+H^2\sum_{n=0}^{\infty}A_n(Y)\sum_{n=0}^{\infty}B_n(Y)+\frac{1}{a^2}\sum_{n=0}^{\infty}A_n''(Y)\sum_{n=0}^{\infty}B_n''(Y)\right]-(\delta+iSt\,\mathrm{Pr})G(Y)\right)dYdY\end{aligned}\right\}$$

(3.24)

In view of the afore-going, we get the following zeroth order

$$\left.\begin{aligned}A_0(\eta)&=\int_{-1}^{\eta}\frac{dA(-1)}{dY}dY+\int_{-1}^{\eta}\int_{-1}^{\eta}\int_{-1}^{\eta}\left(\frac{d^3A(-1)}{dY^3}\right)dYdYdY\\B_0(\eta)&=\int_{-1}^{\eta}\frac{dB(-1)}{dY}dY+\int_{-1}^{\eta}\int_{-1}^{\eta}\int_{-1}^{\eta}\left(\frac{d^3B(-1)}{dY^3}\right)dYdYdY\\F_0(\eta)&=1+\int_{-1}^{y}\frac{dF(-1)}{dY}dY\\G_0(\eta)&=1+\int_{-1}^{y}\frac{dG(-1)}{dY}dY\end{aligned}\right\}$$

(3.25)

and the recursive schemes

$$\left.\begin{aligned}A_{n+1}(\eta)&=\int_{-1}^{y}\int_{-1}^{y}\int_{-1}^{y}\int_{-1}^{y}a^2\left(A_n''(Y)-H^2A_n(\eta)+F_n(Y)\right)dYdYdYdY\\B_{n+1}&\int_{-1}^{\eta}\int_{-1}^{\eta}\int_{-1}^{\eta}\int_{-1}^{\eta}a^2\left(\left(\sum_{n=0}^{\infty}B_n(\eta)\right)''(Y)-(iSt+H^2)\sum_{n=0}^{\infty}B_n(Y)+\sum_{n=0}^{\infty}G_n(Y)\right)dYdYdYdY\\F_{n+1}(\eta)&=-\int_{-1}^{\eta}\int_{-1}^{\eta}\left(\lambda\left[L_n+H^2M_n+\frac{1}{a^2}K_n\right]-\delta F_n(Y)\right)dYdY\\G_{n+1}(\eta)&=-\int_{-1}^{\eta}\int_{-1}^{\eta}\left(2\lambda\left[C_n+H^2W_n+\frac{p_n}{a^2}\right]-(\delta+iSt\,\mathrm{Pr})G_n(Y)\right)dYdY\end{aligned}\right\}$$

(3.26)

The nonlinear terms represented by

$$L_n = \left(\frac{dA_n}{dY}\right)^2, \quad M_n = A_n^2(Y), \quad K_n = \left(\frac{d^2A_n}{dY^2}\right)^2$$
$$C_n = \left(\frac{dA_n}{dY}\right)\left(\frac{dB_n}{dY}\right), \quad W_n = A_n(Y)B_n(Y), \quad P_n = \left(\frac{d^2A_n}{dY^2}\right)\left(\frac{d^2B_n}{dY^2}\right) \tag{3.27}$$

are Taylor's series expanded and decomposed into Adomian polynomials using (3.20)

where $\frac{dA(-1)}{dY}, \frac{d^3A(-1)}{dY^3}, \frac{dB(-1)}{dY}, \frac{d^3B(-1)}{dY^3}, \frac{dF(-1)}{dY}, \frac{dG(-1)}{dY}$ are determined using $A(1) = 0 = A''(1) = B(1) = B''(1), F(1) = 1 = G''(1)$.

Equations (3.25) - (3.27) are carefully coded in a computer symbolic package for successive iteration of the tedious computation giving out a huge symbolic solution in the form of a truncated series

$$A(\eta) = \sum_{n=0}^{r} A_n(\eta), B(\eta) = \sum_{n=0}^{r} B_n(\eta), \quad F(\eta) = \sum_{n=0}^{r} F_n(\eta), \quad G(\eta) = \sum_{n=0}^{r} G_n(\eta) \tag{3.28}$$

The wall shear stress for the unsteady flow becomes

$$S_f = \frac{du}{dy} - \frac{1}{a^2}\frac{d^3u}{dy^3} \tag{3.29}$$

While the rate of heat transfer becomes

$$Nu = -\frac{dG}{dy} \tag{3.30}$$

Table 3.1 Convergence of steady state solution (3.28) at $\lambda = 0.1 = H = a = St = \delta, Pr = 0.71$

n	b_0	b_1	f_0
1	0.00363603	−0.0106486	0.107955
2	0.00345472	−0.010306	0.103252
3	0.00345884	−0.0103135	0.103635
4	0.00345865	−0.0103131	0.103623
5	0.00345866	−0.0103131	0.103623

Table 3.2 Comparison of the present result obtained in [12] when

$a \to \infty, \delta \to 0, \lambda = 0.1 = H$

η	F_{PER}	F_{ADM}	$\lvert F_{PER} - F_{ADM} \rvert$	A_{PER}	A_{ADM}	$\lvert A_{PER} - A_{ADM} \rvert$
−1	1.00000	1.00000	1.62912×10^{-9}	0	0	6.8923×10^{-7}
−0.8	1.00498	1.00498	1.88703×10^{-6}	0.180659	0.18066	7.85194×10^{-7}
−0.6	1.00736	1.00736	2.98225×10^{-6}	0.321199	0.3212	9.67417×10^{-7}
−0.4	1.00825	1.00826	3.59368×10^{-6}	0.421576	0.421578	1.69512×10^{-6}
−0.2	1.00847	1.00847	3.97457×10^{-6}	0.481794	0.481795	1.13009×10^{-6}
0	1.00849	1.00849	4.28825×10^{-6}	0.501863	0.501865	1.5934×10^{-6}
0.2	1.00847	1.00847	4.58461×10^{-6}	0.481794	0.481795	1.32165×10^{-6}
0.4	1.00825	1.00826	4.78536×10^{-6}	0.421577	0.421578	1.31444×10^{-6}
0.6	1.00736	1.00736	4.63599×10^{-6}	0.321200	0.32120	6.79332×10^{-7}
0.8	1.00498	1.00499	3.52411×10^{-6}	0.180660	0.18066	4.95768×10^{-7}
1	1.00000	1.00000	2.37204×10^{-9}	0	0	6.29913×10^{-7}

3.4. Results and Discussion

In this section, the effect of the various thermo-physical parameters on the steady and unsteady flow regimes are investigated. Table 3.1 shows the rapid convergence of the Adomian series solution. It is interesting to note that the convergence is reached when $n = 5$. In Table 3.2, the result of the asymptotic case is presented and validated by using Pertubation method of solution. As observed from the table the uniqueness of the solution is achieved. Figure 3.2 to Fig.3.11 are graphs of velocity and temperature distribution plotted against position η for $t = 0$. The effects of the Hartmann's number and the viscous heating parameter on the steady velocity field are illustrated in Fig.3.2 (a) and (b) respectively. Increasing the Hartmann's number means boosting the strength of the externally applied magnetic field. Figure 3.2(a) shows that the flow velocity is retarded by the increasing strength of the magnetic field dipolar forces. This phenomenon can be explained by the agglomeration property the Lorentz forces have on the ferrofluid. In Fig. 3.2(b), the steady state velocity field is seen to increase with increasing viscous heating parameter. Increasing the viscous heating parameter means that the dynamic viscosity of the fluid is decreasing and this renders reduced resistance to flow, resulting in increased flow velocity. Figure 3.3 (a) and (b) display the effects of the internal heat generation parameter and the couple stress inverse parameter on the steady fluid velocity regime. Both parameters increase the flow velocity. The physical explanation of this flow behaviour is that when the heat of the chemical reaction increases, the fluid particles are excited and their kinetic energy increase. On the other hand, the increase of fluid velocity due to an increase in the

couple stress inverse parameter means that the couple stresses will decrease the flow velocity. Figure 3.4 (a) and (b) and Fig. 3.5 (a) and (b) represent the effects of the Hartmann's number, the viscous heating parameter, the internal heat generation parameter and the couple stress inverse parameter on the unsteady velocity field. The effects are seen to be a mirror image of those for the steady velocity field except that the magnitude of the unsteady flow is much higher than the steady flow. This is true due to increased heating frequency. Similarly, effects of these parameters on the steady temperature distribution are shown in Figs. 3.6 (a), 3.6 (b), 3.7 (a) and 3.7 (b). Interestingly, in Fig. 3.6 (a) and (b) the Hartmann's number is observed to decrease the steady state temperature within the channel while the viscous heating parameter increases it. This diminishing effect of the Hartmann's number on fluid temperature can be explained by the augmentation effect. When the Lorentz forces damp the flow velocity, the strength of the heating source terms is reduced and thus a cooling effect is witnessed. On the other hand, the enhancement of the fluid temperature by an increase in the viscous heating parameter can be due to the convection rolls emanating from the buoyancy effects. The internal heat generation parameter inevitably increases the fluid temperature (Fig. 3.7 (a)). In Fig. 3.7 (b), the couple stress inverse parameter is seen to enhance the fluid temperature. The fluid temperature will therefore be lowered by the couple stresses as the magnitude of the ferrofluid increases. Similar effects are seen as the viscous heating parameter, the internal heat generation parameter and the inverse of the couple stress parameter increases, as shown in (Figs. 3.8 (b), 3.9 (a), 3.9 (b)). However, in Fig 3.8 (a), the Hartmann's number drastically enhances the fluid temperature distribution in the core area of the channel due to Ohmic heating.

Figure 3.10 (a) and (b) represent the effects of the Prandtl number on unsteady velocity field and unsteady temperature field respectively. The Prandtl number (Pr) is the ratio of momentum diffusivity to thermal diffusivity. Thus if $\mathrm{Pr} << 1$, thermal diffusivity dominates and if $\mathrm{Pr} >> 1$, momentum diffusivity will be dominant. We observe from both figures that an increase in the Prandtl number leads to a decrease in both the unsteady velocity and temperature fields. The diminishing temperature suggests a decrease in the fluid thermal conductivity. The corresponding lowering of the velocity can be explained by the thickening of the fluid due to increasing fluid dynamic viscosity. The effect of the Strouhal number (St) on unsteady velocity and temperature fields is

described in Fig. 3.11 (a) and (b) respectively. The Strouhal number is a parameter that describes oscillating flow dynamics. If Strouhal numbers are large, viscous forces dominate the fluid flow resulting in collective oscillating movement of the fluid, a phenomenon known as the “plug”. Otherwise low Strouhal numbers are associated with high velocity steady state part motion dominance. As Fig. 3.11 (a) and (b) depicts, increasing Strouhal number diminishes the magnitude of unsteady flow fields suggesting in this case that the steady state portion of the flow may be dominant.

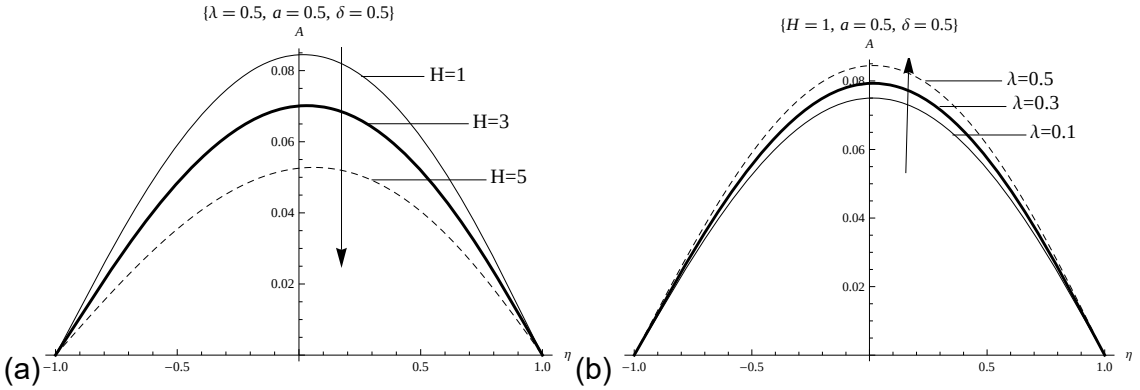

Figure 3.2. Effects of (a) Hartmann number and (b) viscous heating parameter on steady velocity fields.

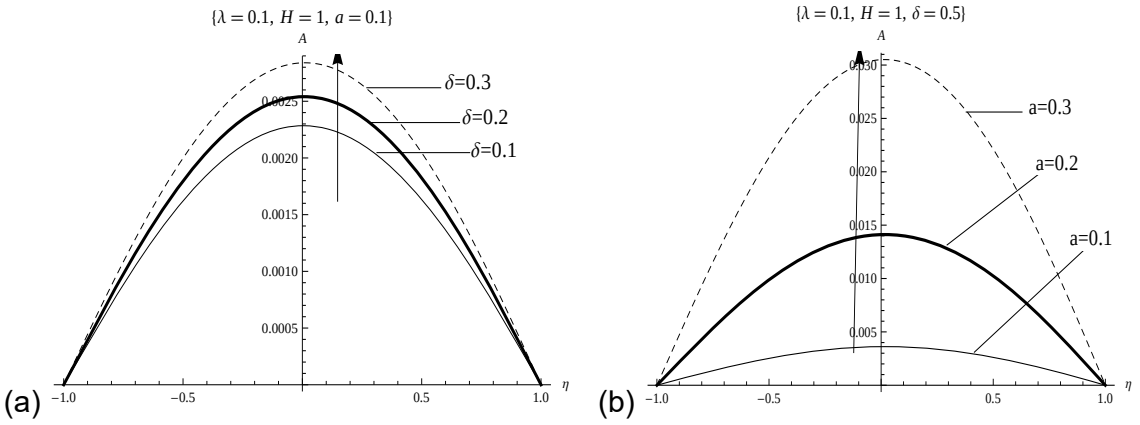

Figure 3.3. Effects of (a) internal heat generation parameter and (b) inverse of couple stress parameter on steady velocity fields.

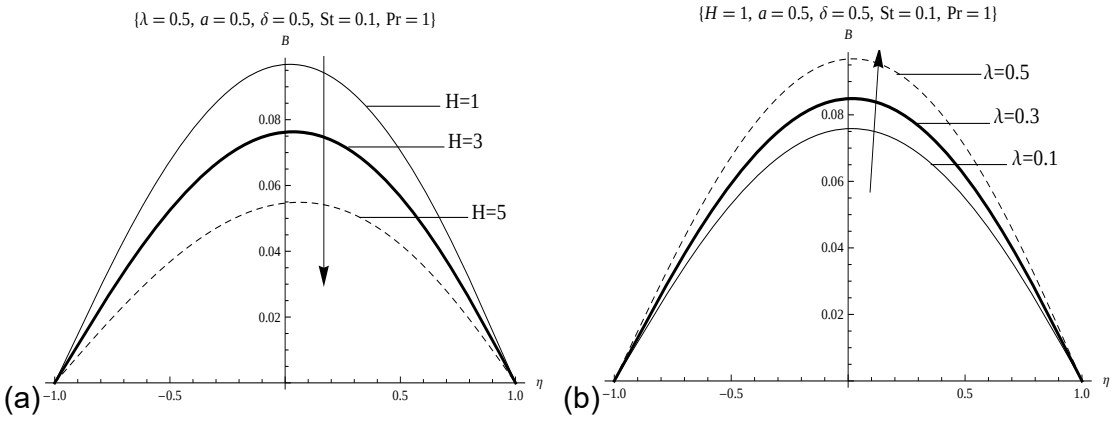

Figure 3.4. Effects of (a) Hartmann number and (b) viscous heating parameter on unsteady velocity fields.

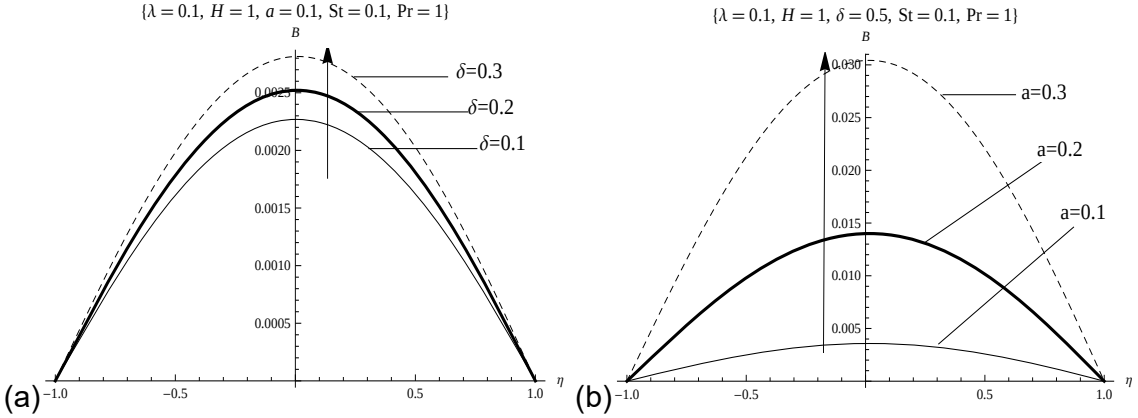

Figure 3.5. Effects of (a) internal heat generation parameter and (b) inverse of couple stress parameter on unsteady velocity fields

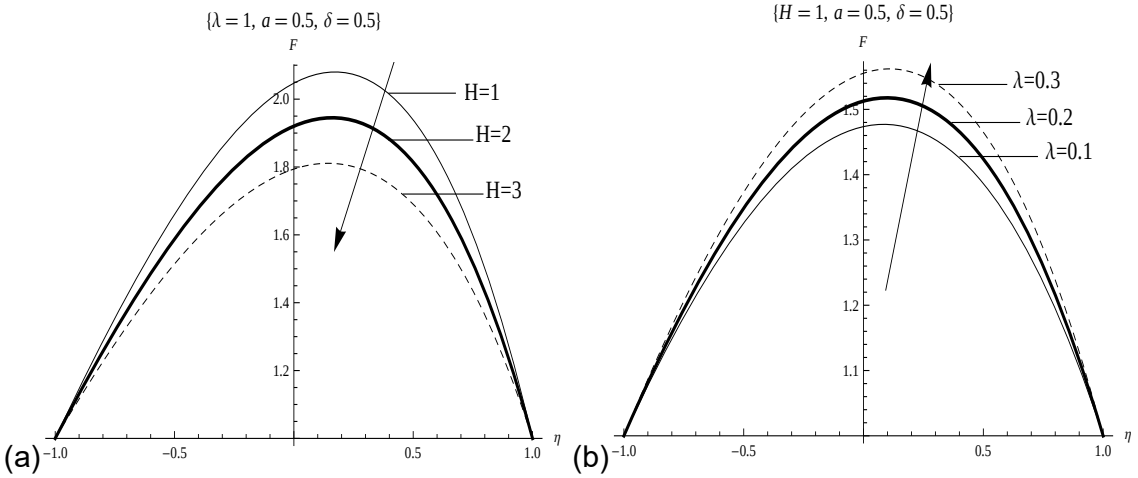

Figure 3.6. Effects of (a) Hartmann number and (b) viscous parameter on steady temperature fields.

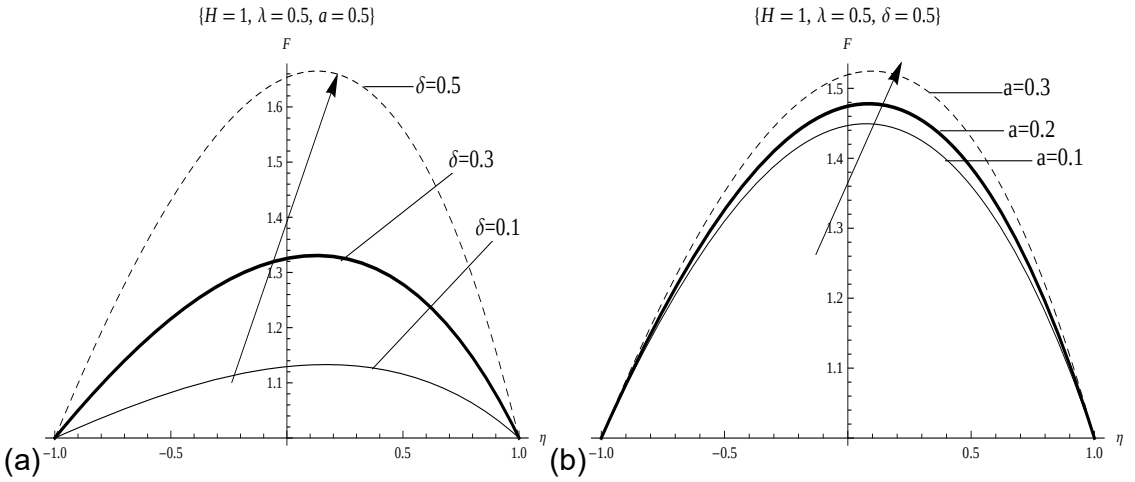

Figure 3.7. Effects of (a) internal heat generation parameter and (b) inverse of couple stress parameter on steady temperature fields.

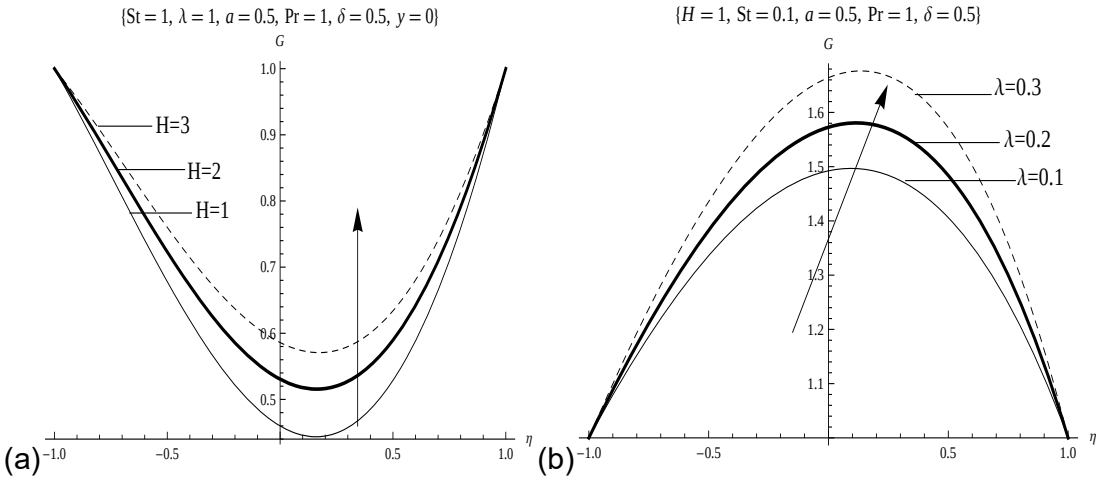

Figure 3.8. Effects of (a) Hartmann number and (b) viscous heating parameter on unsteady temperature fields.

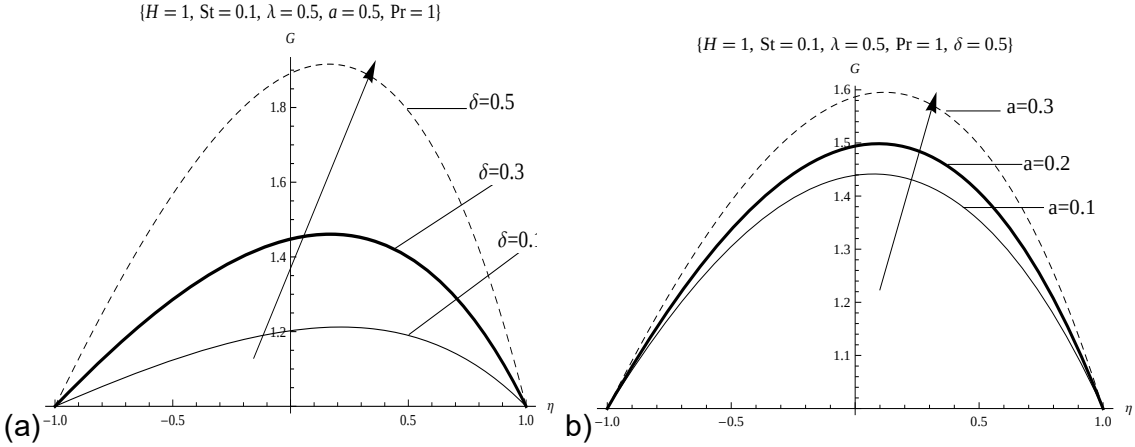

Figure 3.9. Effects of (a) internal heat generation parameter and (b) inverse of couple stress parameter on unsteady temperature fields.

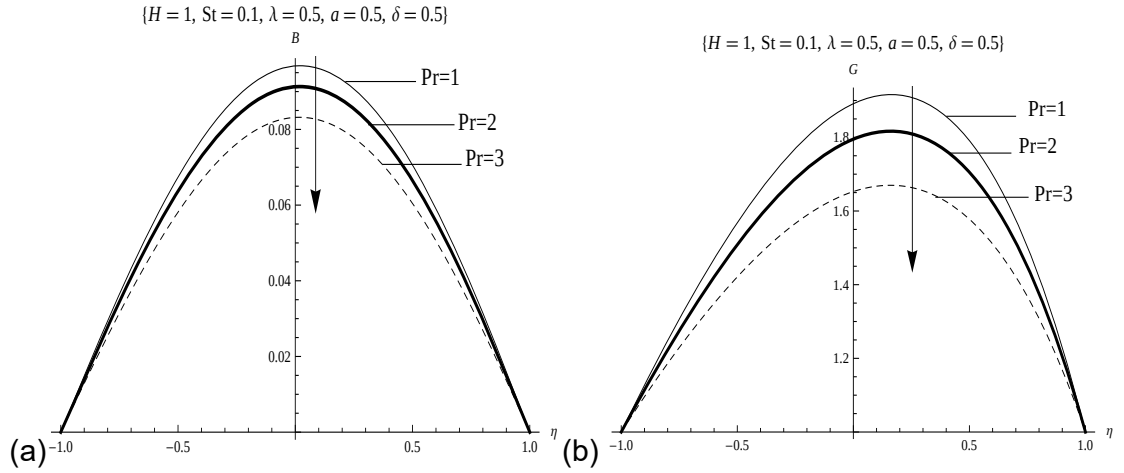

Figure 3.10. Effects of Prandtl number on unsteady (a) velocity fields and (b) temperature fields.

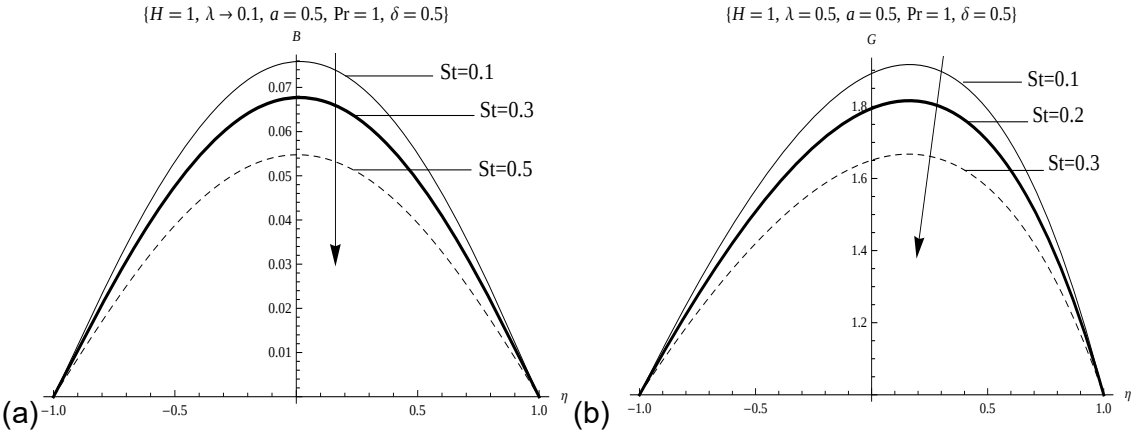

Figure 3.11. Effects of Strouhal number on unsteady (a) velocity fields and (b) temperature fields.

In Figs. 3.12 and 3.13 we fix $\eta = 0$ and plot the periodic regime against time. We investigate the response of fluid velocity and temperature to the variation of identified parameters while others are kept constant as in the earlier analysis. In Fig. 3.12, the periodic velocity is observed to diminish with increasing Hartmann's number, boosted with increasing viscous heating parameter and the couple stress inverse parameter. The retarding effect of the Lorentz forces in the magnetic field has been referred to earlier on and the behaviour due to viscous heating parameter has also been attributed to the buoyancy effects. Figure 3.12 (c) implies that the couple stresses retard the

periodic velocity. Figures 3.13 (a) – (e) captures the behaviour of the periodic fluid temperature in response to variation in the Hartmann's number, viscous heating parameter, internal heat generation parameter, the couple stress inverse parameter, the Prandtl number and the Strouhal number respectively. The Hartmann's number, the viscous heating parameter, the internal heat generation parameter and the inverse of the couple stress parameter increase the periodic temperature, while the Prandtl number and the Strouhal number are seen to diminish it. The physical explanation of these attributes have been pointed out already in the earlier discussion in this article.

We display the observed effects of the couple stresses on the wall shear stress and the rate of heat transfer in the periodic regime in Figs. 3.14 and 3.15. The inverse of the couple stress parameter is observed to decrease the skin friction and enhance the wall heat transfer rate. This means that the couple stresses enhance the skin friction and decrease the wall heat transfer rate.

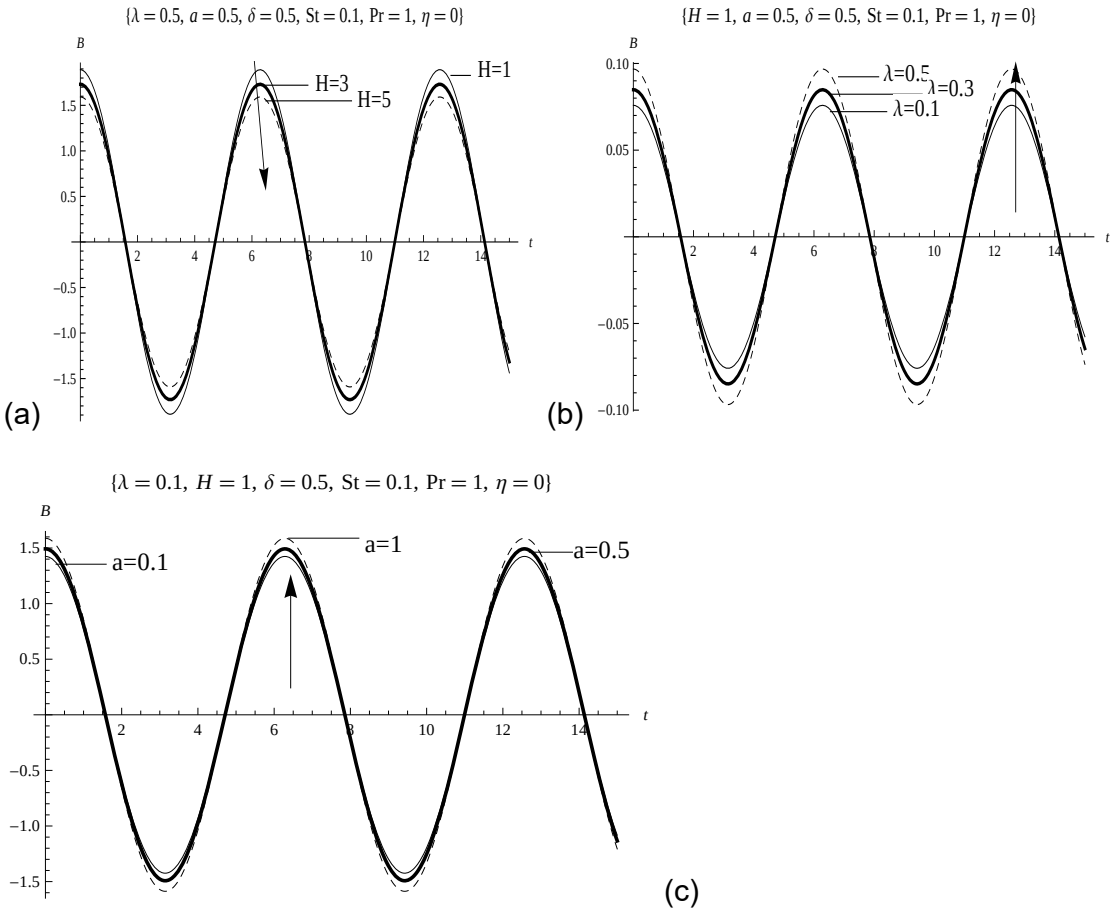

Figure 3.12. Unsteady velocity fields plotted against time varying (a) Hartmann number (b) viscous heating parameter (c) inverse of couple stress parameter.

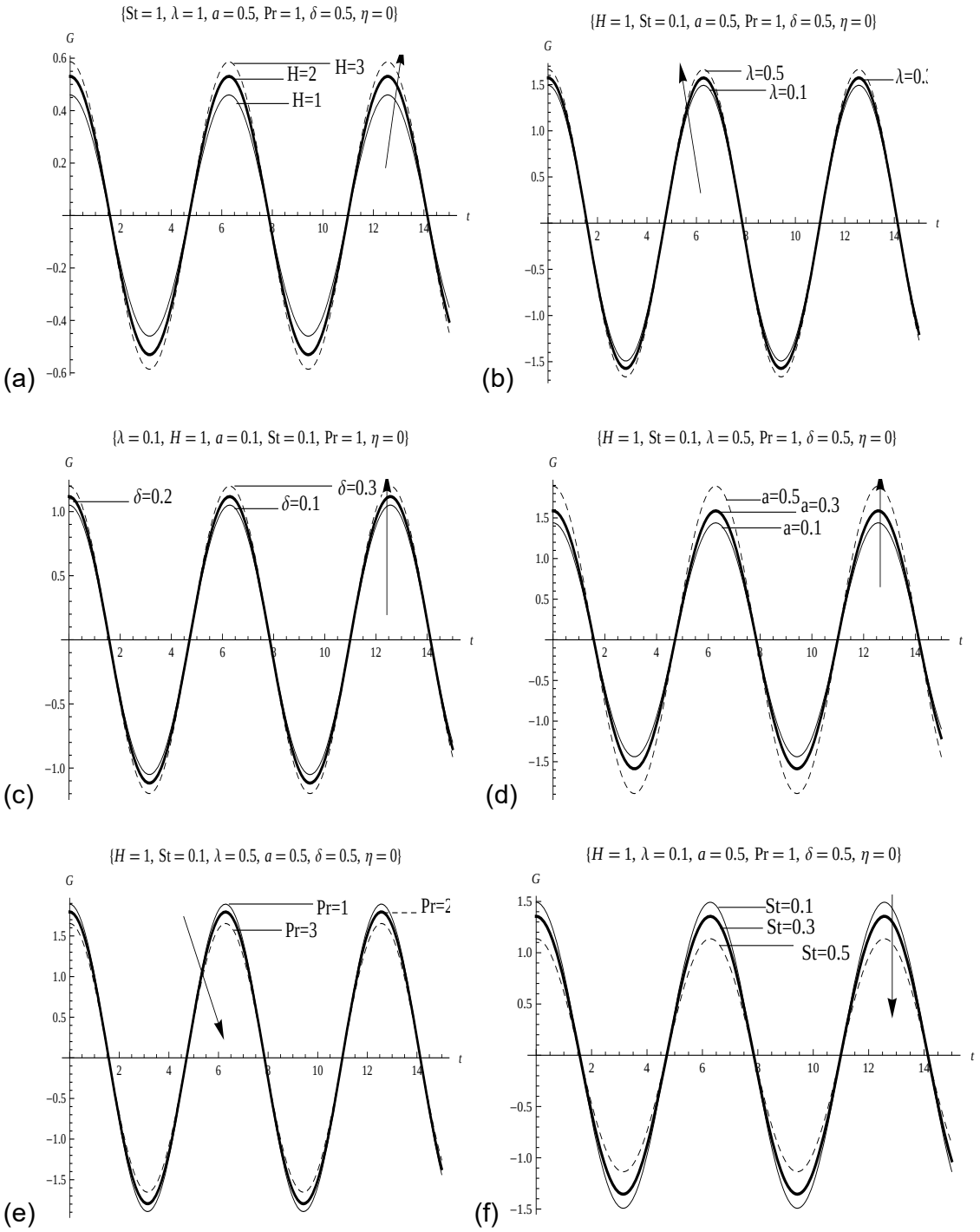

Figure 3.13. Unsteady temperature fields plotted against time varying (a) Hartmann number (b) viscous heating parameter (c) internal heat generating parameter (d) inverse of couple stress parameter (e) Prandtl number and (f) Strouhal number.

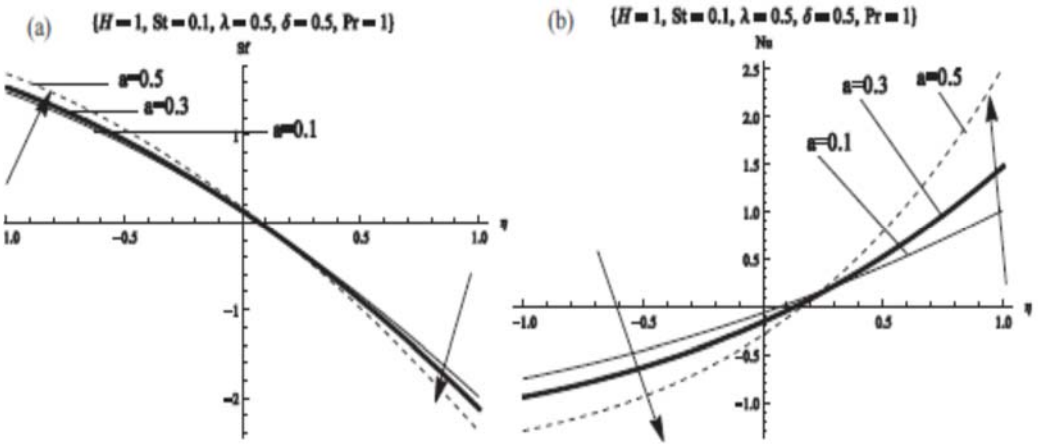

Figure 3.14. (a) Nusselt number plotted against inverse of couple stress parameter. (b) Skin friction plotted against inverse of couple stress parameter.

3.5. Conclusion

MHD natural convection flow of a heat generating couple stress fluid with time-periodic boundary conditions has been investigated. The response of the steady and periodic velocity and temperature fields as well as the skin friction and local Nusselt number to the embedded parameters in the flow system have been outlined with the aid of vivid simulations of the solution. The magnetic field and the couple stresses were observed to have a retarding effect on both the velocity and temperature fields. The viscous heating parameter and the internal heat generation parameter were found to have the opposite influence. A diminishing effect of the Strouhal number on the magnitude of the unsteady velocity and temperature fields suggest a strong dominance of the steady state part of the flow due to strong viscous forces.

CHAPTER FOUR

CONVECTIVE FLOW OF HYDROMAGNETIC COUPLE STRESS FLUID WITH VARYING HEATING THROUGH VERTICAL CHANNEL

Chapter Abstract

This chapter addresses the impact of magnetic field induction on the buoyancy-induced oscillatory flow of couple stress fluid with varying heating. Modelled equations for the incompressible fluid are coupled and nonlinear due to the inclusion of viscous heating and thermal effect on the fluid density. Approximate solutions are constructed and coded on a symbolic package to ease the computational complexity. Graphical representations of the symbolic solutions are presented with detailed explanations. Results of the present computation shows that the effect of induced magnetic field on the oscillatory flow and heat transfer is significant and cannot be neglected.

4.1. Introduction

The convective flow of viscous fluid subjected to periodic heating and cooling plays a vital role in a huge number of home appliances, industry, geology and geophysics, medicine, aerodynamics and much more. In a study by Wang [148], the equations for the buoyancy-induced flow were modeled and separated into steady-periodic regimes. Jha and Ajibade [63-65] popularized the approach by conducting studies under different flow conditions. Following the analysis is a study by Adesanya [3] on micro-channel flow with partial slip and thermal conditions. More recently, Adesanya *et al*. [12] presented results for magnetohydrodynamics convective flows in steady-periodic regimes with constant magnetic fields. Several other related studies on convective flow problems with or without magnetic field can be seen in references [2, 12, 55, 56, 80, 150] and lots more in the literature.

In many cases of engineering interest, induced magnetic field usually act as a flow control mechanism, especially under intense heat. The following studies were conducted by taking induced magnetic field into consideration, Ahmed [15] studied the double diffusivity in a developing flow. Raju *et al.* [99], focused on the convective flow over a stretching surface. Iqbal *et al.* [60] presented a numerical study on a developing nanofluid stagnation point flow. In a similar work, Animasaun and his cohorts [24],

examined the radiative viscoelastic stagnation point flow. Sheikholeslami *et al*. [125] presented an analysis of convective nanofluid problem using Koo-Kleinstrever-Li correlation method. Noreen *et al*. [90] investigated pseudo-plastic peristaltic fluid flow. Kumar and Singh [73] addressed the radial flow through a vertical cylinder with constant heat source. Ghosh *et al*. [48] constructed solution for a convective fluid flow. Raju *et al*. [99] analysed the stagnation point flow. A numerical study of natural convection was discussed extensively by Kumar and Singh [73]. In fact, there are several investigations in various fluid flow problems relating to electrically conducting fluid with induced magnetic fields, some of these can be found in references [18, 20, 25, 49, 59, 70, 81, 87, 91, 93, 107, 128] and references therein.

One major characteristic that distinguishes the couple stress fluid among other non-Newtonian fluids is the inclusion size-dependent microstructure that is of mechanical significance. As explained by Stokes [141] in the couple stress theory, the couple stress constitutive model can easily give explanation for couple stresses, effect of body couples and the non-symmetric stress tensor manifested in several real fluids of technological importance. This important class of fluid has been used extensively in the literature to explain the non-Newtonian behaviour of some real fluid. In view of the huge available references, few of these studies on couple stresses will be described here. Srinivasacharya and Kaladhar [136] applied the model to study the convective flow behaviour in reacting fluids. Srinivas *et al.* [131] applied the model for flow with varying properties. In work by Srinivas *et al*. [130], reported the micropolar fluid flow in a non-Darcian medium. Similar work by Mahabaleshwar *et al.* [76] addressed the hydromagnetic case over a leaky stretching sheet. Kaladhar *et al*. [67] examined the diffusivity problem in a vertical configuration. Ali *et al.* [22] analyzed the MHD oscillatory flow over a stretching surface. Khan *et al.* [86] derived an exact solution of hydromagnetic couple stress fluid using wave transformation approach. Hayat *et al.* [142] examined the developing case in a moving surface subjected to internal heat generation and Newtonian heating. Srinivas and Murthy [133] studied the entropy build-up in immiscible in a channel flow. Adesanya *et al*. [4] reported the effect of couple stresses on hydromagnetic viscoelastic fluid flow. Eldabe and his collaborators [85] discussed the pulsatile flow between solid boundaries. Other interesting results on the application of couple stress theory is not limited to [19, 54, 66, 132, 134] and the cited references.

The above studies on induced magnetic field motivates the present study on the convective couple stress fluid undergoing steady-periodic heating, which has not been done despite the huge number of studies reported on the size-dependent effect. In the following section, the Mathematical analysis for the problem will be presented and the dimensionless coupled boundary-valued-problem would be solved by Adomian decomposition method. Interested readers can see the detailed review, theory and huge applications of the method in [13, 14, 97, 118,119]. Section 4.3 of the paper deals with presentation and discussion of results while the paper is concluded in section 4.4.

4.2. MATHEMATICAL ANALYSIS

Consider the 2-dimensional unsteady couple stress fluid flow with a velocity vector $\bar{q} = (u, v, 0)$ together with the magnetic induction vector $\bar{H} = (b_x, b_y, 0)$. The channel half-width is taken to be *h* and normal to the channel length while the x-axis is normal to the channel length as shown in Figure 4.1 below.

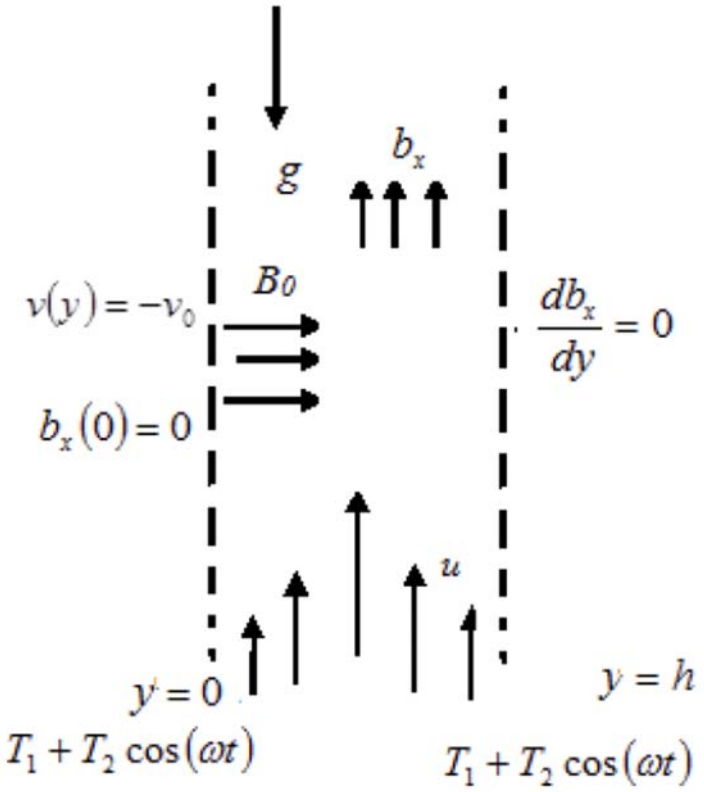

Figure 4.1. Physical model of a problem

The channel length is assumed to be long enough for the flow to be fully developed. In formulating the model, only variations with fluid density and heat source/sink with temperature are considered. The present formulation also catered for dissipations due to fluid friction, couple stresses, and electric charges. With large magnetic suction, the induced magnetic field are also considered, thus, in vector form we have the following, according to [12] and [125]:

Conservation of electric charge: $$\frac{\partial \rho}{\partial t} + \nabla \cdot J = 0 \tag{4.1}$$

Conservation of mass: $$\frac{\partial \rho}{\partial t} + \nabla \cdot \left(\rho \bar{q}\right) = 0 \tag{4.2}$$

Gauss' law of magnetism: $$\nabla \cdot \bar{H} = 0 \tag{4.3}$$

Momentum equation: $$\rho\left(\frac{\partial \bar{q}}{\partial t} + \left(\bar{q} \cdot \nabla\right)\bar{q}\right) = -\nabla P + \mu \nabla^2 \bar{q} + \mu_e \left(\bar{J} \times \bar{H}\right) - \eta \nabla^2 \left(\nabla^2 \bar{q}\right) + \rho \bar{g} \tag{4.4}$$

Energy equation:

$$\rho C_p \left(\frac{\partial T}{\partial t} + \left(\bar{q} \cdot \nabla\right)T\right) = k\nabla^2 T + \mu\left(\nabla \bar{q}\right)^2 + \frac{1}{\sigma}\left(\nabla \bar{H}\right)^2 + \eta\left(\nabla^2 \bar{q}\right)^2 + Q_0\left(T_0 - T\right) \tag{4.5}$$

Conservation of magnetic induction: $$\frac{\partial \bar{H}}{\partial t} + \nabla \times \left(\bar{q} \times \bar{H}\right) = \frac{1}{\sigma \mu_e} \nabla^2 \bar{H} \tag{4.6}$$

Neglecting the variation of fluid density with time and from Equation (4.2), the fully developed case implies that $v(y) = -v_0$ i.e. a constant. In the first approximation, by assuming a small velocity gradient in the momentum equation and eliminating the pressure gradient, we get

$$\frac{\partial u}{\partial t} - v_0 \frac{\partial u}{\partial y} = \nu \frac{\partial^2 u}{\partial y^2} + \frac{\mu_e b_0}{\rho} \frac{\partial b_x}{\partial y} + g\beta\left(T - T_0\right) - \frac{\eta}{\rho} \frac{\partial^4 u}{\partial y^4} \tag{4.7}$$

$$\frac{\partial b_x}{\partial t} - v_0 \frac{\partial b_x}{\partial y} = b_0 \frac{\partial u}{\partial y} + \frac{1}{\mu_e \sigma} \frac{\partial^2 b_x}{\partial y^2} \tag{4.8}$$

$$\rho c_p\left(\frac{\partial T}{\partial t}-v_0\frac{\partial T}{\partial y}\right)=k\frac{\partial^2 T}{\partial y^2}+\mu\left(\frac{\partial u}{\partial y}\right)^2+\frac{1}{\sigma}\left(\frac{\partial b_x}{\partial y}\right)^2+\eta\left(\frac{\partial^2 u}{\partial y^2}\right)^2+Q_0\left(T_0-T\right) \tag{4.9}$$

with

$$\begin{aligned} &u'(0)=u''(0)=0,\quad b_x(0)=0,\quad T(0)=T_1+T_2\cos(\omega t) \qquad y=0\\ &u(h)=u''(h)=0,\ b_x(1)=0,\quad T(h)=T_1+T_2\cos(\omega t) \qquad y=h \end{aligned} \tag{4.10}$$

We introduce the following

$$\left.\begin{aligned} u(t,y)&=\frac{g\beta h^2}{\nu}\left[(T_1-T_0)A(y)+T_2B(y)e^{i\omega t}\right]\\ T(t,y)&=T_0+(T_1-T_0)F(y)+T_2G(y)e^{i\omega t}\\ b_x(t,y)&=\frac{g\beta h^2}{\nu}\left(\frac{\mu_e}{\rho}\right)^{\frac{1}{2}}\left[(T_1-T_0)L(y)+T_2M(y)e^{i\omega t}\right] \end{aligned}\right\} \tag{4.11}$$

along with the dimensionless quantities

$$\left.\begin{aligned} &\eta=\frac{y}{h},\lambda=\frac{\mu}{k}\left(\frac{g\beta h^2}{\nu}\right)^2(T_1-T_0),St=\frac{h^2\omega}{\nu},\mathrm{Pr}=\frac{\mu c_p}{k},\\ &H=\frac{b_0 h}{\nu}\sqrt{\frac{\mu_e}{\rho}},\kappa^2=\frac{h^2\mu}{\eta},\delta=\frac{Q_0h^2}{k},P_m=\sigma\nu\mu_e,s=\frac{v_0h}{\nu} \end{aligned}\right\} \tag{4.12}$$

giving rise to the following orders of perturbations:

$$\left.\begin{aligned} o\left(e^{i\omega t}\right)^0:\ &A^{(4)}(\eta)=\kappa^2\left(A''(\eta)+sA'(\eta)+HL'(\eta)+F(\eta)\right);\\ &\mathrm{A}(0)=0=A''(0)=\mathrm{A}(1)=A''(1)\\ &L''(\eta)=-\left(sP_mL'(\eta)+HP_mA'(\eta)\right);\quad L(0)=0=L(1)\\ &F''(\eta)=\delta F(\eta)-s\,\mathrm{Pr}\,F'(\eta)-\lambda\left(A'(\eta)^2+\frac{A''(\eta)^2}{\kappa^2}+\frac{L'(\eta)^2}{P_m}\right);\\ &F(0)=1=F(1) \end{aligned}\right\} \tag{4.13}$$

$$
\left.
\begin{aligned}
o\left(e^{i\omega t}\right)^1 : B^{(4)}(\eta) &= \kappa^2\left(B''(\eta) + sB'(\eta) - iStB(\eta) + HM'(\eta) + G(\eta)\right); \\
\mathrm{B}(0) &= 0 = B''(0) = B(1) = B''(1) \\
M''(\eta) &= P_m\left(iStB(\eta) - sM'(\eta) + HB'(\eta)\right); \qquad M(0) = 0 = M(1) \\
G''(\eta) &= (\delta + iSt\,\mathrm{Pr})F(\eta) - s\,\mathrm{Pr}\,G'(\eta) - 2\lambda A'(\eta)B'(\eta) - \frac{2\lambda}{\kappa^2}A''(\eta)B''(\eta) \\
&\quad - \frac{2\lambda}{P_m}L'(\eta)M'(\eta) \qquad G(0) = 1 = G(1)
\end{aligned}
\right\} \tag{4.14}
$$

4.2.1. Adomian Method of Solution

As shown in [119], Adomian decomposition method (ADM) is a well-established method for solving all manners of differential equations. In what follows, the coupled differential equations in (4.13)-(4.14) with the boundary conditions gives the equivalent integral equations that is given by:

$$
\begin{aligned}
A(\eta) &= \int_0^\eta \frac{dA(0)}{dY}dY + \int_0^\eta\int_0^\eta\int_0^\eta\left(\frac{d^3A(0)}{dY^3}\right)dYdYdY \\
&\quad + \int_0^\eta\int_0^\eta\int_0^\eta\int_0^\eta \kappa^2\left(A''(Y) + sA'(Y) + HL'(Y) + F(Y)\right)dYdYdYdY
\end{aligned} \tag{4.15}
$$

$$
\begin{aligned}
B(\eta) &= \int_0^\eta \frac{dB(0)}{dY}dY + \int_0^\eta\int_0^\eta\int_0^\eta\left(\frac{d^3B(0)}{dY^3}\right)dYdYdY \\
&\quad + \int_0^\eta\int_0^\eta\int_0^\eta\int_0^\eta \kappa^2\left(B''(Y) + sB'(Y) + HM'(G) - iStB(Y) + G(Y)\right)dYdYdYdY
\end{aligned} \tag{4.16}
$$

$$
\begin{aligned}
F(\eta) &= 1 + \int_0^\eta \frac{dF(0)}{dY}dY + \int_0^\eta\int_0^\eta\left(\delta F(Y) - s\,\mathrm{Pr}\,F'(Y)\right)dYdY \\
&\quad - \lambda\int_0^\eta\int_0^\eta\left(A'(Y)^2 + \frac{A''(Y)^2}{\kappa^2} + \frac{L'(Y)^2}{P_m}\right)dYdY
\end{aligned} \tag{4.17}
$$

$$
\begin{aligned}
G(\eta) &= 1 + \int_0^\eta \frac{dG(0)}{dY}dY + \int_0^\eta\int_0^\eta(\delta + iSt\,\mathrm{Pr})F(Y) - s\,\mathrm{Pr}\,G'(Y)dYdY \\
&\quad - 2\lambda\int_0^\eta\int_0^\eta\left(A'(Y)B'(Y) + \frac{A''(Y)B''(Y)}{\kappa^2} + \frac{L'(Y)M'(Y)}{P_m}\right)dYdY
\end{aligned} \tag{4.18}
$$

$$
L(\eta) = \int_0^y \frac{dL(0)}{dY}dY - \int_0^\eta\int_0^\eta\left(sP_mL'(Y) + HP_mA'(Y)\right)dYdY \tag{4.19}
$$

$$M(\eta)=\int_0^{\eta}\frac{dM(0)}{dY}dY+\int_0^{\eta}\int_0^{\eta}P_m\left(iStB(\eta)-sM'(\eta)+HB'(\eta)\right)dYdY \tag{4.20}$$

The standard assumed series is of the form:

$$\left.\begin{aligned}A(\eta)&=\sum_{n=0}^{\infty}A_n(\eta),\quad B(\eta)=\sum_{n=0}^{\infty}B_n(\eta),\quad F(\eta)=\sum_{n=0}^{\infty}F_n(\eta),\\ G(\eta)&=\sum_{n=0}^{\infty}G_n(\eta),\quad L(\eta)=\sum_{n=0}^{\infty}L_n(\eta),\quad M(\eta)=\sum_{n=0}^{\infty}M_n(\eta)\end{aligned}\right\} \tag{4.21}$$

Substituting (4.21) in (4.15)-(4.20), we get

$$\left.A_0(\eta)=\int_0^{\eta}a_1dY+\int_0^{\eta}\int_0^{\eta}\int_0^{\eta}a_2dYdYdY\;;\;L_0(\eta)=\int_0^{y}l_0dY\;;\;F_0(\eta)=1+\int_0^{y}f_odY\right\} \tag{4.22}$$

with the recurrence relations:

$$\left.\begin{aligned}A_{n+1}(\eta)&=\int_0^{\eta}\int_0^{\eta}\int_0^{\eta}\int_0^{\eta}\kappa^2\left(A_n''(Y)+sA_n'(Y)+HL_n'(Y)+F_n(Y)\right)dYdYdYdY\\ L_{n+1}(\eta)&=-\int_0^{\eta}\int_0^{\eta}\left(sP_mL_n'(Y)+HaP_mA_n'(Y)\right)dYdY\\ F_{n+1}(\eta)&=\int_0^{\eta}\int_0^{\eta}\left(\delta F_n(Y)-s\,\mathrm{Pr}\,F_n'(Y)-\lambda K_n\right)dYdY\end{aligned}\right\} \tag{4.23}$$

Similarly, in the periodic flow regime leads to

$$\left.B_0(\eta)=\int_0^{\eta}b_1dY+\int_0^{\eta}\int_0^{\eta}\int_0^{\eta}b_2dYdYdY\;;M_0(\eta)=\int_0^{y}m_0dY\;;G_0(\eta)=1+\int_0^{y}g_0dY\right\} \tag{4.24}$$

while the rest of the terms are given by

$$\left.\begin{aligned}B_{n+1}(\eta)&=\int_0^{\eta}\int_0^{\eta}\int_0^{\eta}\int_0^{\eta}\kappa^2\left(B_n''(Y)+sB_n'(Y)+HM_n'(G)-iStB_n(Y)+G_n(Y)\right)dYdYdYdY\\ G_{n+1}(\eta)&=\int_0^{\eta}\int_0^{\eta}\left(\left(\delta+iSt\,\mathrm{Pr}\right)F_n(Y)-s\,\mathrm{Pr}\,G_n'(Y)-2\lambda U_n\right)dYdY\\ M_{n+1}(\eta)&=\int_0^{\eta}\int_0^{\eta}P_m\left(iStB_n(\eta)-sM_n'(\eta)+HB_n'(\eta)\right)dYdY\end{aligned}\right\} \tag{4.25}$$

where

$$\left.\begin{aligned} K_n &= \left(\frac{dA_n}{dY}\right)^2 + \frac{1}{\kappa^2}\left(\frac{d^2A_n}{dY^2}\right)^2 + \frac{1}{p_m}\left(\frac{dL_n}{dY}\right)^2 \\ U_n &= \left(\frac{dA_n}{dY}\right)\left(\frac{dB_n}{dY}\right) + \frac{1}{\kappa^2}\left(\frac{d^2A_n}{dY^2}\right)\left(\frac{d^2B_n}{dY^2}\right) + \frac{1}{p_m}\left(\frac{dL_n}{dY}\right)\left(\frac{dM_n}{dY}\right) \end{aligned}\right\} \tag{4.26}$$

the appropriate Adomian Polynomials are:

$$\left.\begin{aligned} K_0 &= \left(\frac{dA_0}{dY}\right)^2 + \frac{1}{\kappa^2}\left(\frac{d^2A_0}{dY^2}\right)^2 + \frac{1}{p_m}\left(\frac{dL_0}{dY}\right)^2 \\ K_1 &= 2\left(\frac{dA_0}{dY}\right)\left(\frac{dA_1}{dY}\right) + \frac{2}{\kappa^2}\left(\frac{d^2A_0}{dY^2}\right)\left(\frac{d^2A_1}{dY^2}\right) + \frac{2}{p_m}\left(\frac{dL_0}{dY}\right)\left(\frac{dL_1}{dY}\right) \\ &\cdots\cdots \\ U_0 &= \left(\frac{dA_0}{dY}\right)\left(\frac{dB_0}{dY}\right) + \frac{1}{\kappa^2}\left(\frac{d^2A_0}{dY^2}\right)\left(\frac{d^2B_0}{dY^2}\right) + \frac{1}{p_m}\left(\frac{dL_0}{dY}\right)\left(\frac{dM_0}{dY}\right) \\ U_1 &= 2\left(\left(\frac{dA_0}{dY}\right)\left(\frac{dB_1}{dY}\right) + \left(\frac{dA_1}{dY}\right)\left(\frac{dB_0}{dY}\right)\right) + \frac{2}{\kappa^2}\left(\left(\frac{d^2A_1}{dY^2}\right)\left(\frac{d^2B_0}{dY^2}\right) + \left(\frac{d^2A_0}{dY^2}\right)\left(\frac{d^2B_1}{dY^2}\right)\right) \\ &\quad + \frac{2}{p_m}\left(\left(\frac{dL_0}{dY}\right)\left(\frac{dM_1}{dY}\right) + \left(\frac{dL_1}{dY}\right)\left(\frac{dM_0}{dY}\right)\right) \\ &\cdots\cdots \end{aligned}\right\} \tag{4.27}$$

The iterative process (4.22)-(4.27) are then coded into MATHEMATICA version 10.0 for easy iteration. Expressions for the unknown constants are also obtained with the aid of the remaining boundary conditions, at the end we obtain the following q^{th} partial sum as the approximate solutions of the coupled differential equations.

$$\begin{aligned} A(\eta) &= \sum_{n=0}^{q} A_n(\eta), \quad B(\eta) = \sum_{n=0}^{q} B_n(\eta), \quad F(\eta) = \sum_{n=0}^{q} F_n(\eta), \\ G(\eta) &= \sum_{n=0}^{q} G_n(\eta), \quad L(\eta) = \sum_{n=0}^{q} L_n(\eta), \quad M(\eta) = \sum_{n=0}^{q} M_n(\eta) \end{aligned} \tag{4.28}$$

Finally, the current density induced are given by

$$J = -\frac{dL}{dy}, K = -\frac{dM}{dy} \tag{4.29}$$

in the steady and periodic flow regimes respectively.

4.3. Results and Discussion

Equations (4.22)–(4.28) are carefully coded in MATHEMATICA version 10.0 for easy iteration of the Adomian decomposition procedure, the following symbolic solutions are obtained graphically due to large output of the computation. Figure 4.2 represents the variation of some important fluid parameters on the steady flow. As shown in Fig. 4.2a, an increase in the magnetic field parameter is seen to decrease the flow velocity because ferrofluid particles agglomerate with increasing induced magnetic field, also the retarding effect of Lorentz forces. The variation of couple stress inverse parameter on the steady flow velocity is also shown in Fig. 4.2b. From the graphical result, an increase in the couple stress inverse parameter is seen to enhance the flow velocity. In other words, an increase in couple stress inverse parameter means a decrease in the non-Newtonian behaviour of the fluid. Hence, an increase in the couple stress parameter is seen to decrease the flow velocity. In Fig. 4.2c, an increase in the viscous heating parameter is observed to enhance the fluid velocity due to increased heat generated in the fluid. Moreover, as presented in Fig. 4.2d, an increase in the magnetic Prandtl number is observed to decrease the steady flow significantly due to increased induced magnetic field. Similarly, Fig. 4.2e shows that an increase in suction Reynolds's number is seen to decrease the flow velocity as much fluid is sucked away from the flow domain. A closer view of Fig. 4.2g revealed the effect of Prandtl number on the fluid flow; it is also observed that the flow velocity decreases with increased Prandtl number since the fluid dynamic viscosity increases. Finally, Fig. 4.2f shows that as the heat sink parameter increases, the fluid temperature distribution within the flow declines accordingly due to heat loss to the ambient.

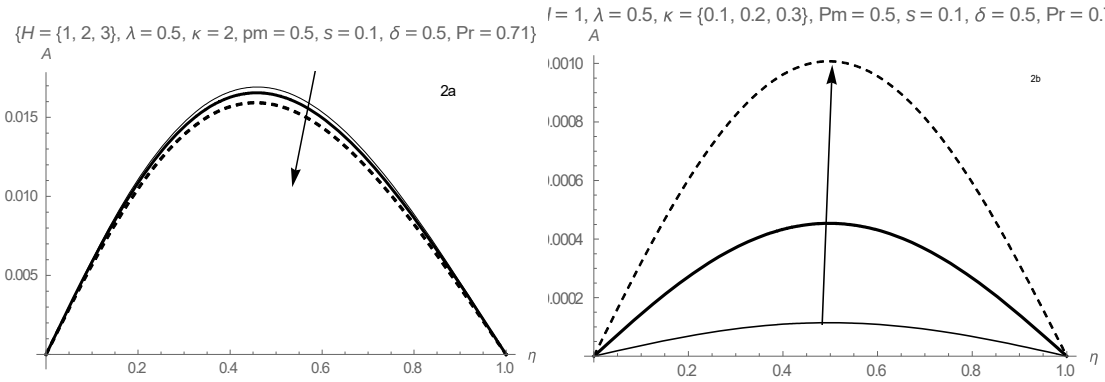

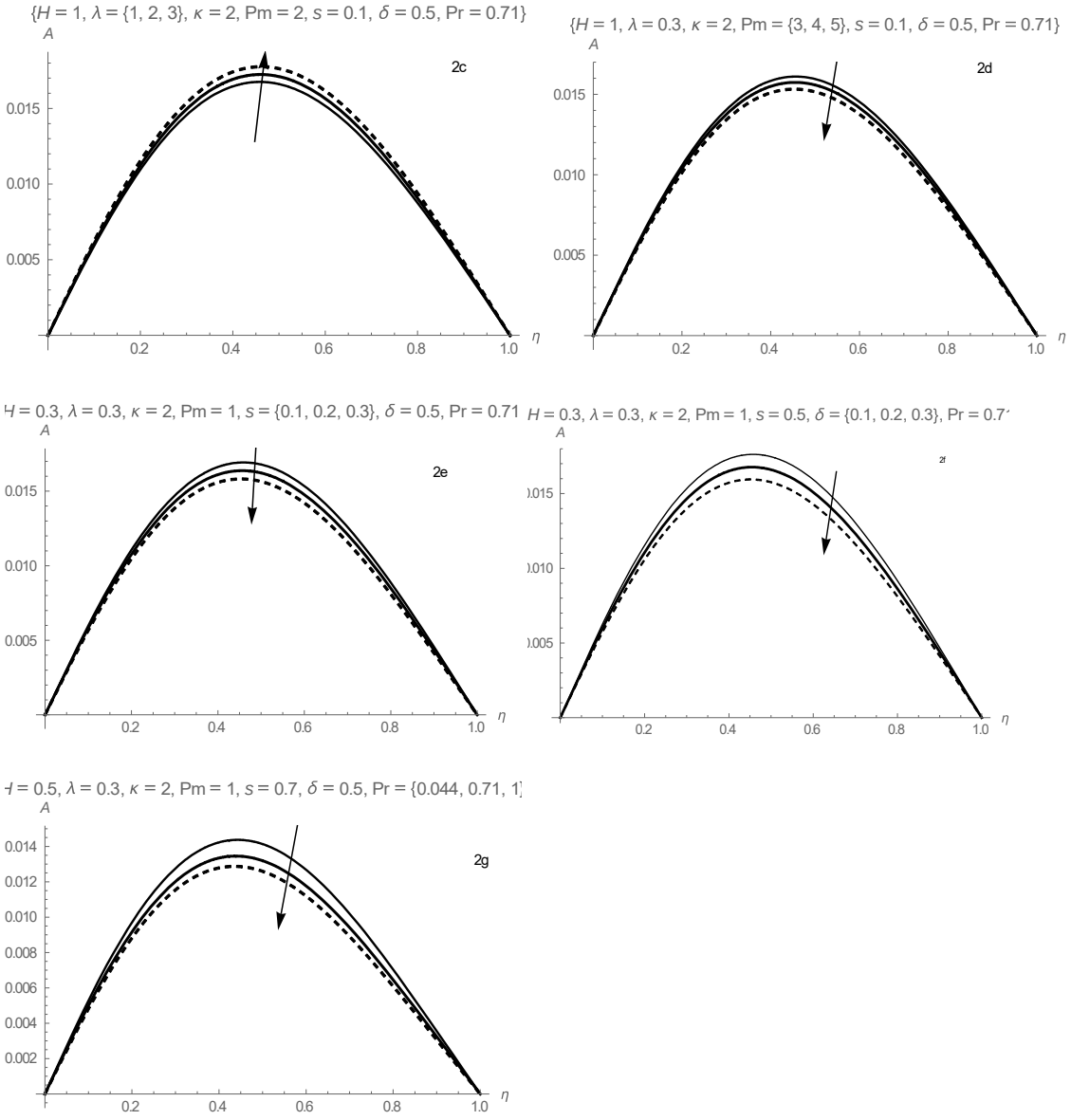

Figure 4.2: Steady velocity profile

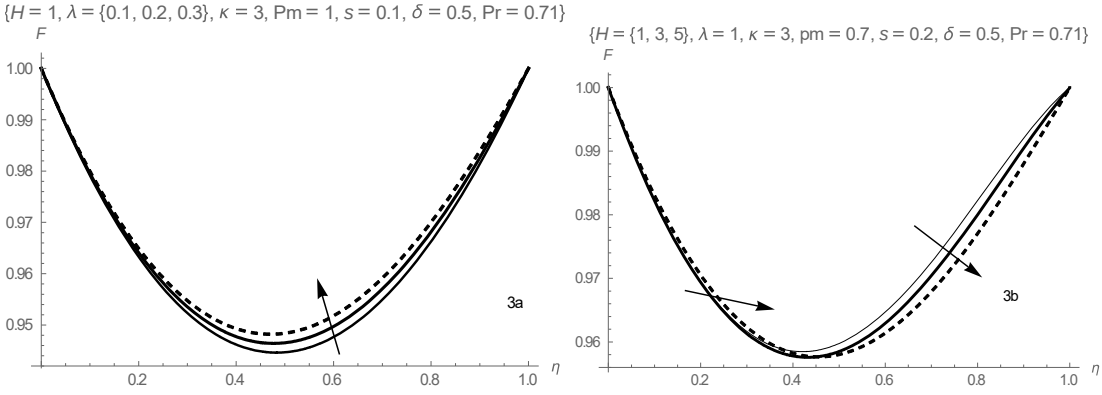

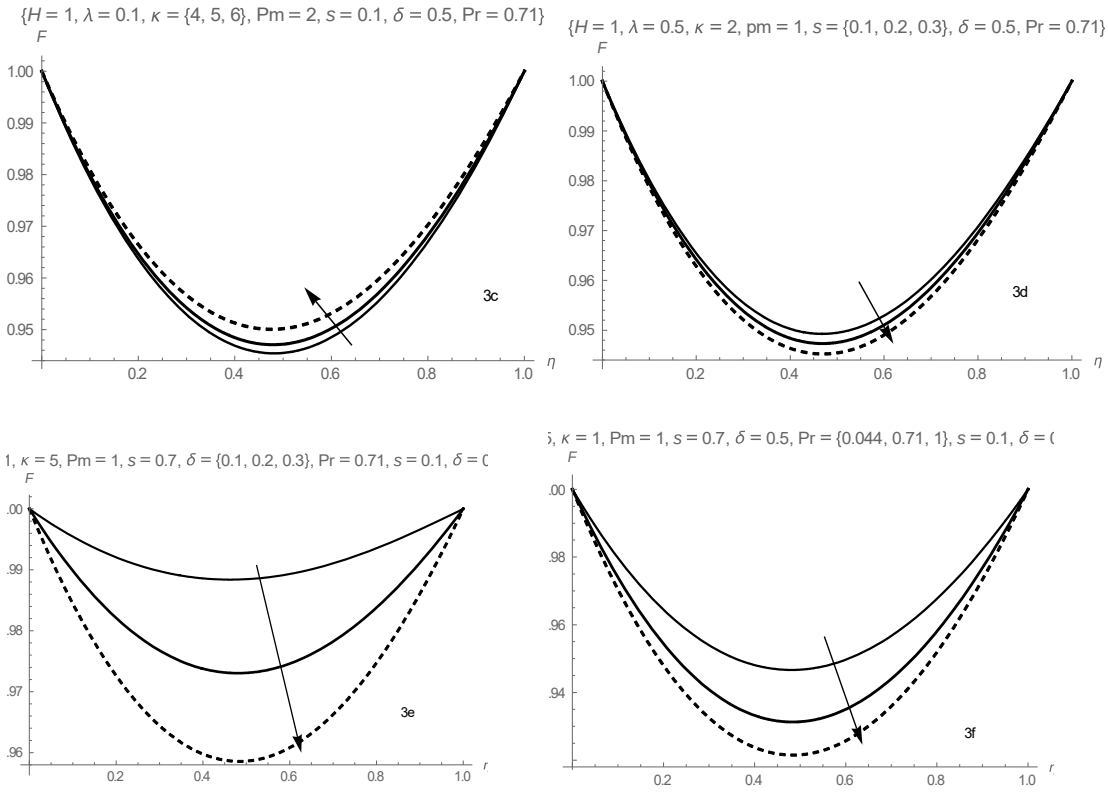

Figure 4.3: Steady temperature profile

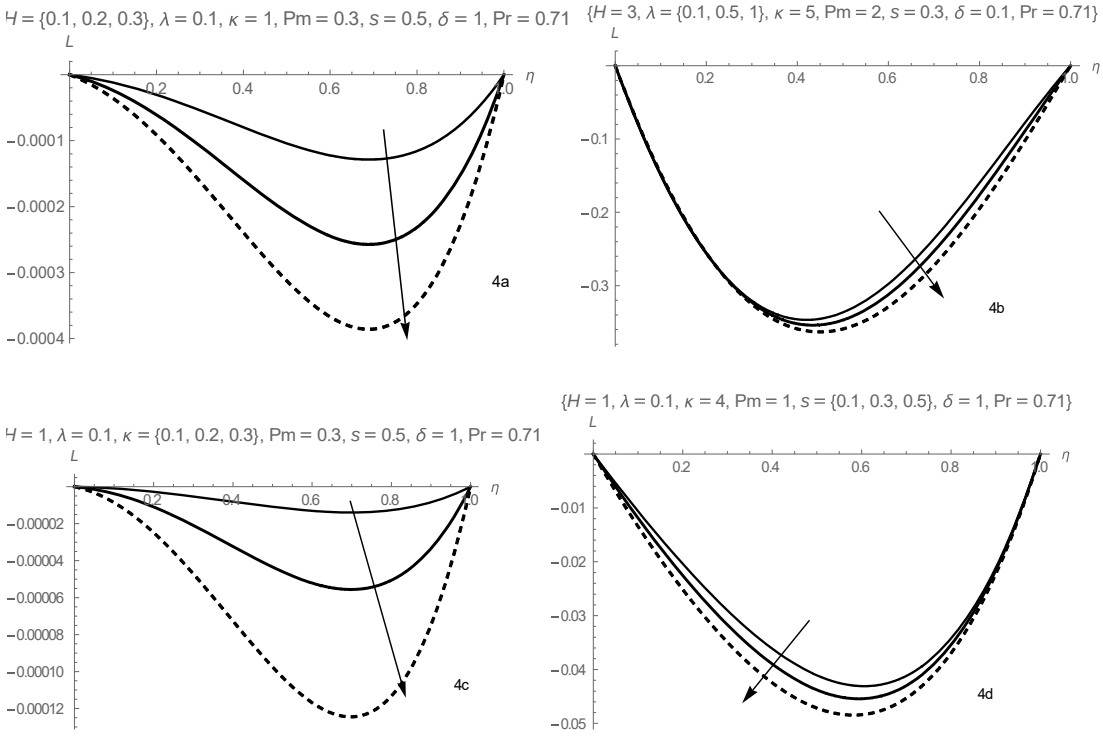

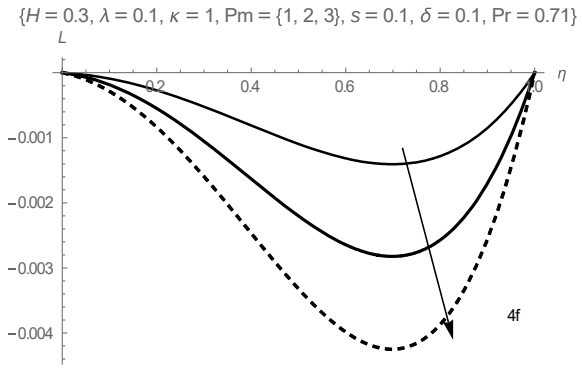

Figure 4.4: Steady induced magnetic field profile

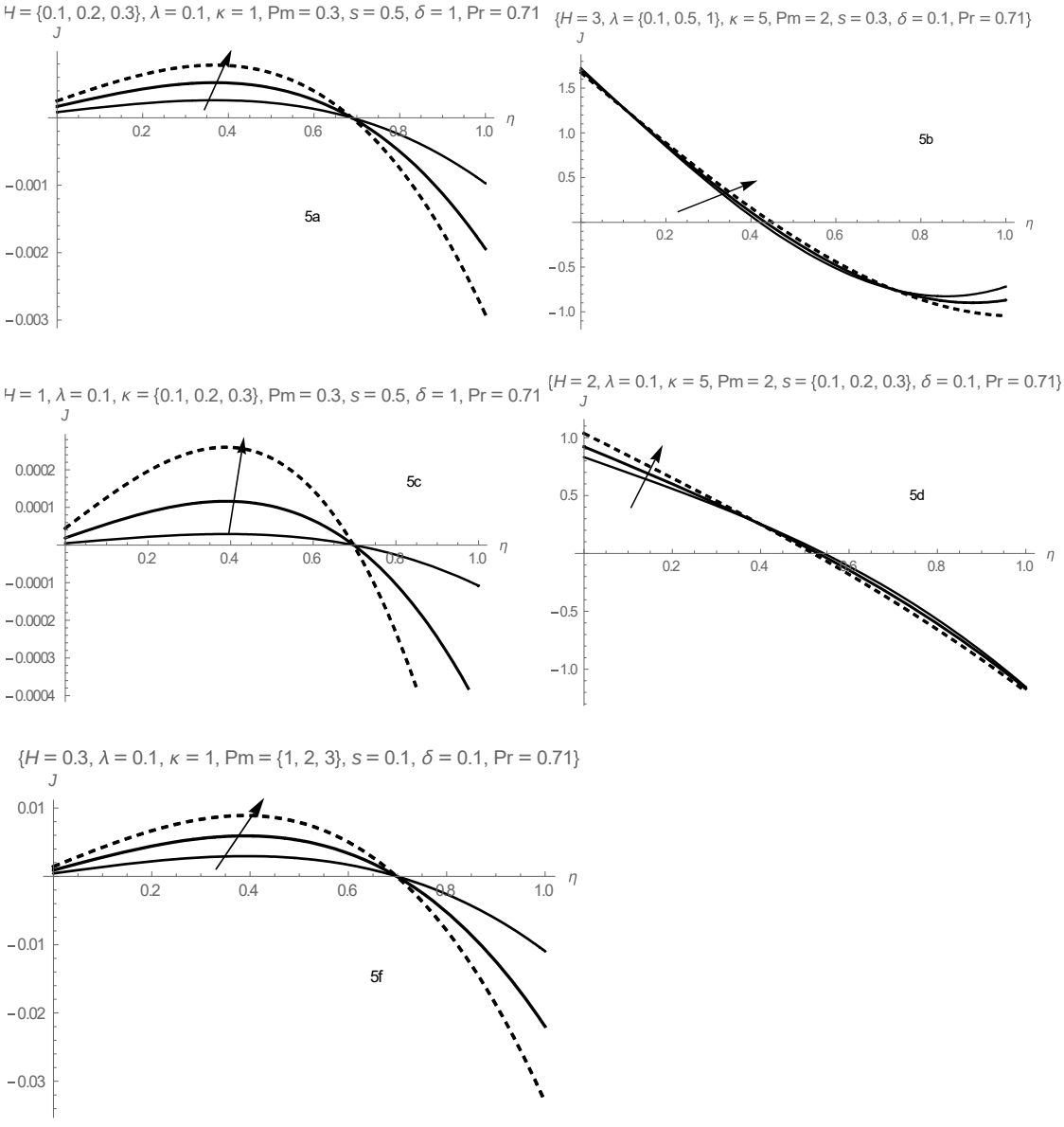

Figure 4.5: Steady induced current density profile

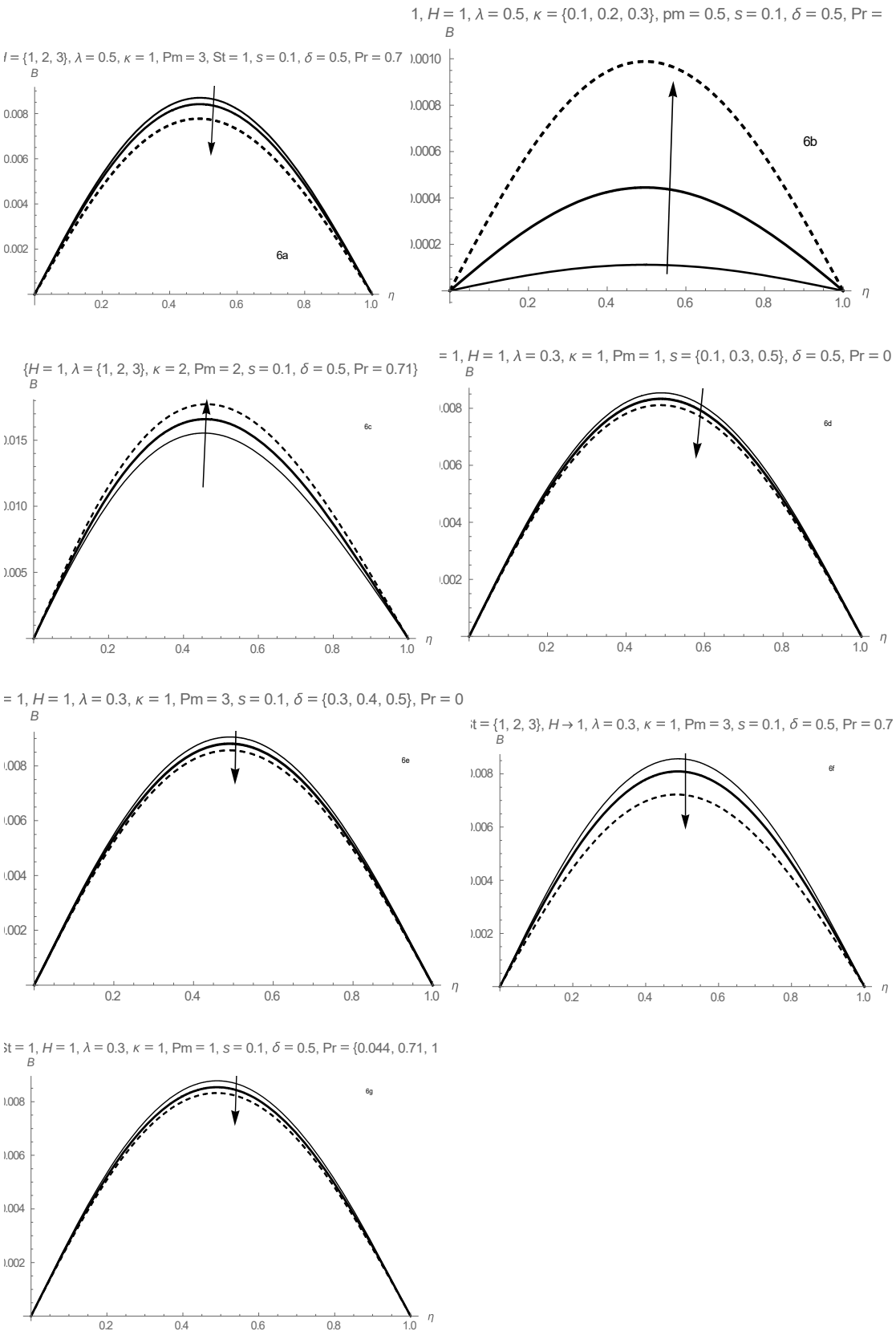

Figure 4.6: Oscillatory velocity profile

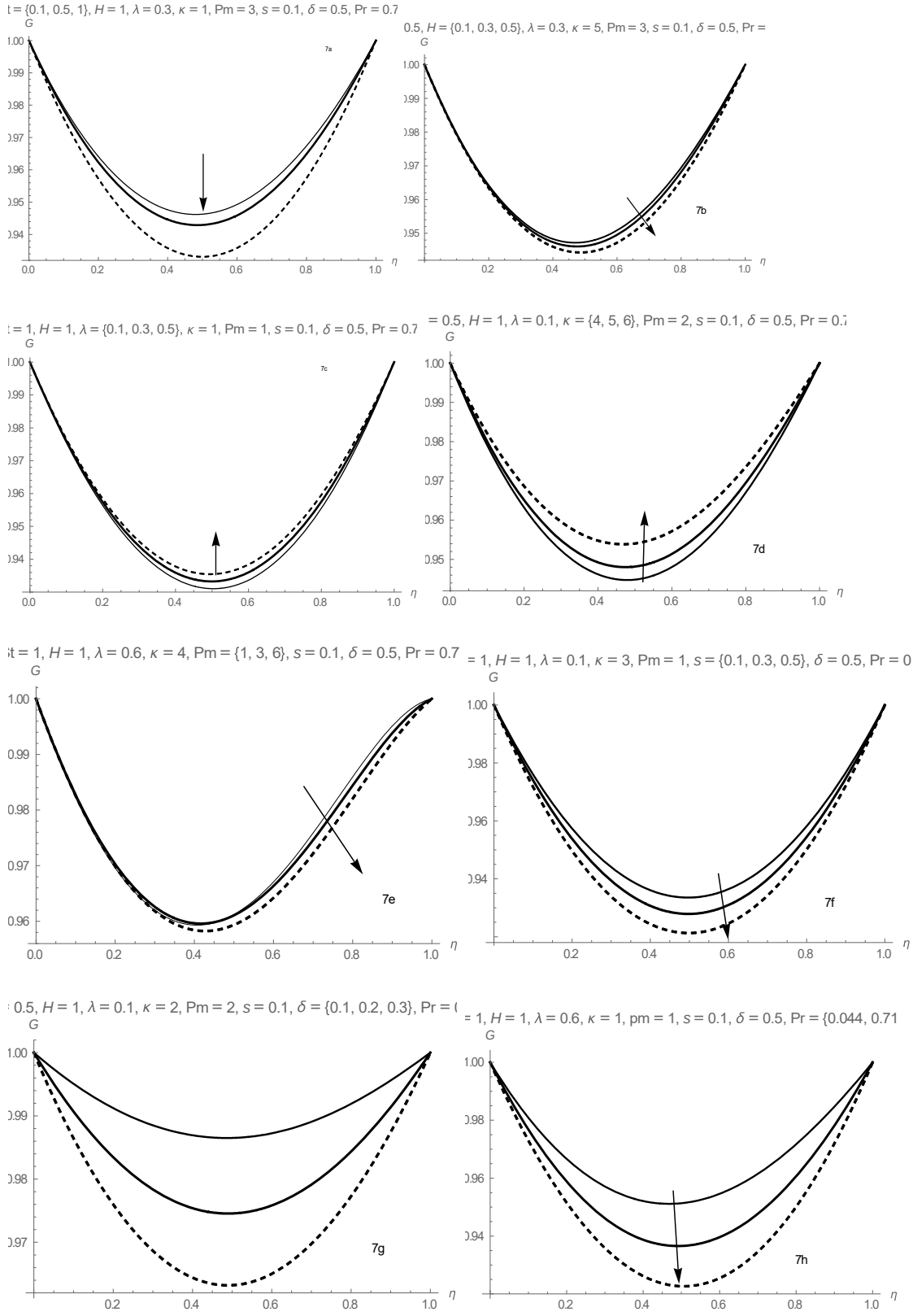

Figure 4.7: Unsteady temperature profile

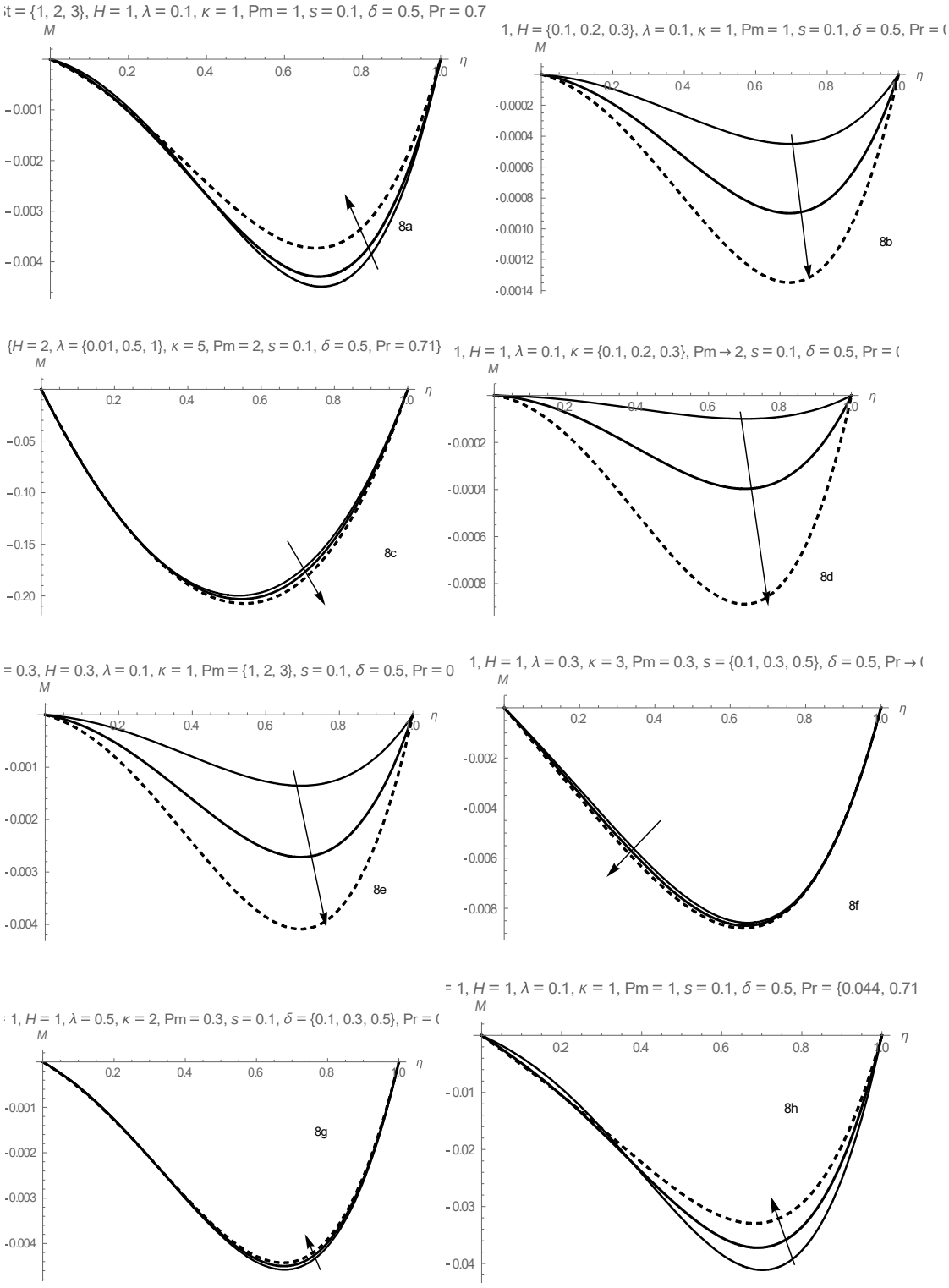

Figure 4.8: Unsteady induced magnetic field

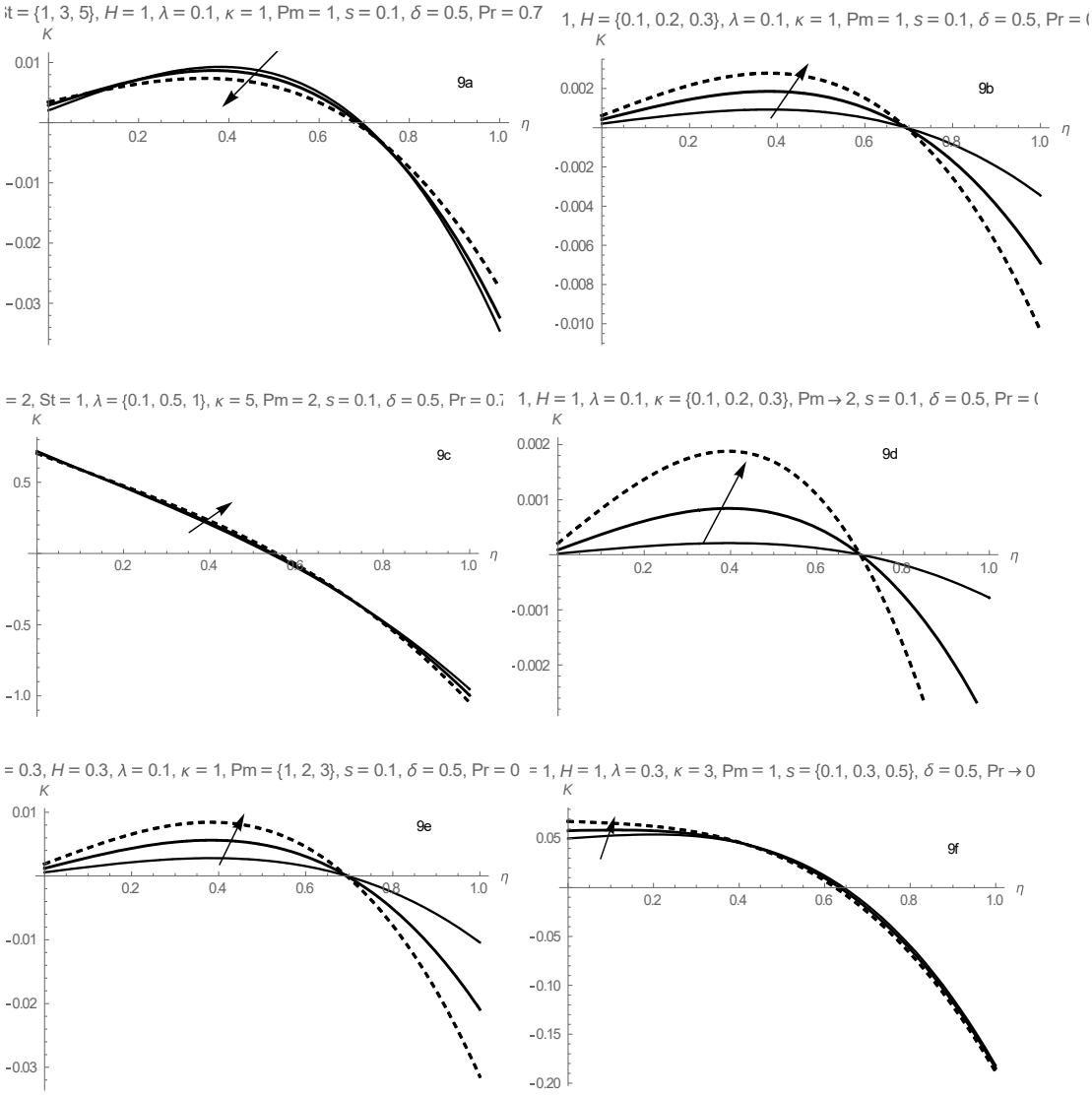

Figure 4.9: Unsteady induced current density profile

Figure 4.3 depicts the variation of steady temperature with pertinent fluid parameters. In Fig. 4.3a, the influence of viscous heating of the fluid on the temperature profile is presented. From the graphical result, an increase in the viscous heating parameter is seen to raise the fluid temperature distribution in the core area of the channel; this is so because the fluid viscosity increases the heat generated due to the frictional interaction of the fluid particles. In Fig. 4.3b, a variation of the fluid temperature with magnetic field is presented. From the plot, the balanced effect of suction and injection on the fluid is clearly seen. However, as seen in Figs. 4.3c and 4.3d, increasing values

of the couple stress parameter is seen to increase the fluid temperature due to thinning of the fluid. Also, note that the couple stress inverse parameter enhances the fluid temperature. Similar conduct to that is seen as the suction parameter increases. In Figs. 4.3e and 4.3f, variation in internal heat loss parameter and Prandtl number are presented, as the heat loss parameter increases, the fluid temperature falls since the heat is dissipated. Lastly, the Prandtl number is seen to decrease the temperature distribution within the domain of flow; this is because as the increased Prandtl number associated with decreased thermal conductivity of the fluid.

Figure 4.4 addresses the response of the induced magnetic field to the variation of fluid parameters. It is important to see that Figs. 4.4(a-f) are all negative due to the flow reversal of the magnetic flux in the channel. On the other hand, the induced current density shown in Figs. 4.5 represents the induced current density which is a direct opposite presentation to the induced magnetic field. Discussion of results in Figs. 4.6-4.9 for the unsteady flow behaviour are seen to conform with the steady case except for reduction in the flow and heat maximum that is associated with increased frequency of heating as highlighted in Figs. 4.5f, 4.6f and 4.7a. As a result, the discussion will not be repeated.

4.4. Conclusion

The convective flow of hydromagnetic couple stress fluid with induced magnetic field has been addressed here in the steady-periodic regimes. The momentum, energy and magnetic induction equations are formulated, made dimensionless and solved by Adomian decomposition method. The main contribution to knowledge from the present study are as follows:

- Increasing values of Hartman number, Strouhal number, couple stress parameter and heat loss parameter decreases the flow velocity while viscous heating of the fluid encourages both steady and oscillatory flow profiles.
- Fluid temperature distribution is seen to improve with increasing values of the viscous heating parameter, Hartman number, couple stress parameter while it decreases with increasing values of the Prandtl number, heat loss parameter, suction parameter and Strouhal number.

- Increasing values of Hartman number, viscous heating, suction and magnetic Prandtl number are seen to enhance the induced current density while an increase in Strouhal number decreases it.

CHAPTER FIVE

MIXED CONVECTIVE FLOW OF UNSTEADY HYDROMAGNETIC COUPLE STRESS FLUID THROUGH A VERTICAL CHANNEL FILLED WITH POROUS MEDIUM

Chapter Abstract

In this chapter, the mixed convective flow of an electrically conducting, viscous incompressible couple stress fluid through a vertical channel filled with a saturated porous medium has been investigated. The fluid is assumed to be driven by both buoyancy force and oscillatory pressure gradient parallel to the channel plates. A uniform magnetic field of strength B_0 is imposed transverse to the channel boundaries. The temperature of the right channel plate is assumed to vary periodically, and the temperature difference between the plates is high enough to induce radiative heat transfer. Under these assumptions, the equations governing the two-dimensional couple stress fluid flow are formulated and exact solutions of the velocity and the temperature fields are obtained. The effects of radiation, Hall current, porous medium permeability and other various flow parameters on the flow and heat transfer are presented graphically and discussed extensively.

5.1. Introduction

Fluid flow and heat transfer in varied mechanical configurations filled with porous media continues to be an area of research interest for both Newtonian and non-Newtonian fluids. Engineers, scientists and technocrats have over time exploited the ubiquitous nature of porous media to develop machinery, equipment and industrial processes that has seen transformation of the world through stages from the first to the fourth industrial revolution. It cannot be an exaggeration to postulate that modernity has to a larger extent depended on exploitation and manipulation of fluid flow systems through porous materials. Khaled and Vafai [71] pointed out that transport theories in porous media have played a defining role in the advancement of a plethora of applications, examples of which are geology, chemical reactors, drying and liquid composite moulding, combustion and biological applications. The Handbook of Porous Media, Vafai [145], provides a succinct overview of the latest theories on flow,

transport, and heat exchange processes in porous media. [94] and [106] are some examples of recent studies on flow and heat transfer in porous media.

Liquid foams, geological materials, emulsions, hydrocarbon oils, polymeric fluids, etc, are examples of fluids belonging to a class broadly described by the generic term non-Newtonian. Industrial applications are dominated by fluids falling into this class and their complex hydrodynamic characteristics necessitated the emergence of a robust and complex non-Newtonian rheology. Models encountered in literature include the Power law model, fluids of the differential type, visco-elastic fluid models like the Johnson-Seagalman model, the Oldroyd model, the Casson fluid model, the couple stress model and many others, see for instance [30,45,141] . The couple stress fluid model is a generalisation of the classical Newtonian constitutive model for viscous fluids that account for the inclusion of couple stresses, body couples and non-symmetric tensors in the fluid medium [34]. Fluids such as lubricants, synthetic oils, paints, and blood, which contain tiny microstructures can be modelled efficiently by the couple stress fluid model. Couple stress fluids find applications as surfactants, coolants, lubricating fluids, toothpaste and gels, pharmaceutical mixtures, ferrofluids used in shock absorbers and many more [6].

Complexities arising from solving various couple stress fluid models and the wide application horizon has motivated many scholars to continue with active research in the couple stress fluid model. Hassan [51] used modified Adomian decomposition method to analyse a reactive hydromagnetic couple stress fluid flow through a channel filled with saturated porous media. Makinde and Eegunjobi [78] investigated the inherent irreversibility in a steady flow of a couple stress fluid through a vertical channel packed with saturated porous substances. Murthy *et al.* [101] studied the entropy generation in a steady flow of two immiscible couple stress fluids in a horizontal channel bounded by two porous beds at the bottom and top. Hassan and Fenuga [52] investigated the effects of thermal radiation on the flow of a reactive hydromagnetic heat generating couple stress fluid through a porous channel. When an external magnetic field is imposed onto a moving electrically conducting fluid, current is induced into the fluid which in turn polarises the fluid and a drag-like force (Lorentz force) is formed. This magnetohydrodynamic (MHD) phenomenon has pertinent applications in thermo-electrical systems like heat exchangers, cooling of electronic devices,

electromagnetic processing of materials, metal purification and astrophysical applications [29].

Meanwhile studies of oscillatory MHD convection fluid flow in porous media have gained increased attention due to wide applications in physiology, physics and engineering. Examples in engineering include MHD generators, food processing industry, chemical process industry, centrifugation and filtration processes and rotating machinery, see [47] and [68]. In physiology, peristaltic motion is the major mechanism through which heat and fluid get transported through biological systems like the human body, and MHD principles are applied to accelerate the flow of blood which is useful in the treatment of some disorders [103]. Nayak and Dash [89] studied transient hydromagnetic flow of an electrically conducting couple stress fluid in a rotating frame of reference through a saturated porous channel under the influence of pulsatile pressure gradient. Sankad and Nagathan [109] examined the effects of MHD couple stress fluid in peristaltic flow with porous medium under the impact of slip, heat transfer and wall properties. MHD effects on peristaltic flow of a couple stress fluid in a channel with permeable walls was studied by Ramachandraiah *et al*. [100]. The novelty of the work of these researchers is that their work provides a guideline for some biomedical instruments like blood pumps in dialysis and heart lung machine. The problem of oscillatory MHD flow of blood in a porous arteriole in the presence of chemical reaction was investigated by Misra and Adhikary [83]. The work provides useful insights to biophysicists, physiologists and clinicians. Adesanya and Makinde [9] investigated the effect of slip on the hydromagnetic pulsatile flow through a channel filled with saturated porous medium with time dependent boundary condition on the heated wall. Other related recent studies are found in [35, 40, 92].

Most of the studies cited above concentrated on one dimensional flow, overlooking the fact that the applied magnetic field induces a secondary flow in the direction parallel to it. Veera Krishna and Chand Basha [146] investigated the effects of radiation and Hall current on MHD oscillatory convection two dimensional flow of a viscous fluid in a vertical channel filled with a porous medium, and Veera Krishna *et al*. [147] investigated the same type of flow but of a second grade fluid. Motivated by these papers and the need to contribute to the ongoing studies, this article studies mixed convective two dimensional flow of unsteady MHD couple stress fluid through a vertical channel filled with a porous medium. All the previous studies on oscillatory

fluid flow neglect the effect of couple stresses and this explains why the current study is worthwhile.

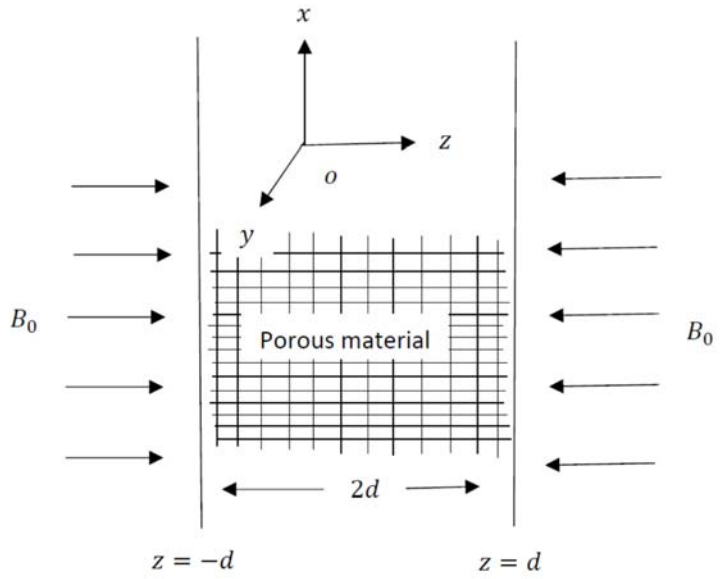

Figure 5.1. Physical model and coordinate system of the problem.

5.2. Mathematical Formulation and Solution of the Problem

The schematic diagram of an unsteady mixed convection flow of electrically conducting, viscous, incompressible couple stress fluid between two infinite vertical plates in the presence of Hall current and thermal radiation is illustrated in Fig. 5.1. The fluid is driven by both buoyancy force and an oscillating pressure gradient parallel to the channel plates. The channel plates are at a distance $2d$ apart and the channel is filled with a homogeneous and isotropic porous medium. A Cartesian coordinate system $0(x, y, z)$ is chosen such that the x-axis lies along the centre of the channel in a vertical upward direction and the z-axis is oriented perpendicular to the planes of the plates. In this way, the boundary plates at $z = -d$ and $z = d$ are parallel to the xy-plane and the magnetic field of strength B_0 is applied in the transverse xz-plane as shown in the figure. The magnetic field induces a secondary flow in the z-direction. Following Veera Krishna *et al*. [147] and Veera Krishna and Chand Basha [146], the equations governing the flow under the influence of the imposed magnetic field are

$$\frac{\partial u}{\partial t} = -\frac{1}{\rho}\frac{\partial p}{\partial x} + \nu\frac{\partial^2 u}{\partial z^2} - \frac{\sigma {B_0}^2}{\rho}u - \frac{\nu}{k}u + g\beta T - \frac{\eta}{\rho}\frac{\partial^4 u}{\partial z^4}, \tag{5.1}$$

$$\frac{\partial w}{\partial t} = \nu \frac{\partial^2 w}{\partial z^2} - \frac{\sigma {B_0}^2}{\rho} w - \frac{\nu}{k} w - \frac{\eta}{\rho} \frac{\partial^4 w}{\partial z^4}\,, \tag{5.2}$$

$$\rho C_p \frac{\partial T}{\partial t} = \mathrm{K} \frac{\partial^2 T}{\partial z^2} - \frac{\partial q_r}{\partial z}. \tag{5.3}$$

The boundary conditions for the problem are given as

$$u'' = u = w = T = 0, \quad z = -d,$$

$$u'' = u = w = 0, T = T_w \cos \omega t\,, \quad z = d, \tag{5.4}$$

where T_w is the mean temperature of the plate $z = d$ and ω is the frequency of the oscillations.

Assuming that the fluid is optically thin with a relatively low density [31], the radiative heat flux $\frac{\partial q_r}{\partial z}$ in Eq. (5.3) is given by

$$\frac{\partial q_r}{\partial z} = 4{\alpha_2}^2 (T - T_0), \tag{5.5}$$

where α_2 is the mean radiation absorption coefficient. Taking the reference temperature at the left channel plate T_0 to be equal to 0 reduces Eq. (5.5) to

$$\frac{\partial q_r}{\partial z} = 4{\alpha_2}^2 T. \tag{5.6}$$

Introducing the dimensionless variables

$$z^* = \frac{z}{d}\,, x^* = \frac{x}{d}\,, u^* = \frac{u}{U}\,, v^* = \frac{v}{U}\,, q^* = \frac{q}{U}\,, t^* = \frac{tU}{d}\,, \omega^* = \frac{\omega d}{U}\,,$$

$$p^* = \frac{p}{\rho U^2}\,, T^* = \frac{T}{T_w}\,, \tag{5.7}$$

transforms the governing Eqs. (5.1) – (5.3) to, after dropping the asterisks, the non-dimensional form

$$\frac{\partial u}{\partial t} = -\frac{\partial p}{\partial x} + \frac{1}{R} \frac{\partial^2 u}{\partial z^2} - \frac{Ha^2}{R} u - \frac{D^{-1}}{R} u + \frac{Gr}{R} T - \frac{1}{\kappa^2 R} \frac{\partial^4 u}{\partial z^4}\,, \tag{5.8}$$

$$\frac{\partial w}{\partial t} = \frac{1}{R} \frac{\partial^2 w}{\partial z^2} - \frac{Ha^2}{R} w - \frac{D^{-1}}{R} w - \frac{1}{\kappa^2 R} \frac{\partial^4 w}{\partial z^4}\,, \tag{5.9}$$

$$\frac{\partial T}{\partial t} = \frac{1}{Pe}\frac{\partial^2 T}{\partial z^2} - \frac{\delta^2}{Pe}T. \tag{5.10}$$

where $R = \frac{Ud}{v}$ is the Reynolds number, $D = \frac{k}{d^2}$ is the Darcy parameter, $Gr = \frac{g\beta d^2 T_w}{vU}$ is the thermal Grashof number, $Pe = \frac{\rho C_p dU}{\mathrm{K}}$ is the Peclet number, $\delta = \frac{2\alpha_2 d}{\sqrt{\mathrm{K}}}$ is the thermal radiation parameter, $Ha^2 = \frac{\sigma B_0^2 d^2}{\rho\nu}$ is the Hartmann number and $\kappa^2 = \frac{d^2\nu}{\eta}$ is the couple stress parameter.

The transformed boundary conditions are

$$u'' = u = w = T = 0, \quad z = -1,$$

$$u'' = u = w = 0, T = \cos\omega t\,, \quad z = 1. \tag{5.11}$$

Assuming a complex solution of the form

$$q = u + iw, \tag{5.12}$$

reduces Eqs. (5.8) and (5.9) to a single equation of the form

$$\frac{\partial q}{\partial t} = -\frac{\partial p}{\partial x} + \frac{1}{R}\frac{\partial^2 q}{\partial z^2} - \left(\frac{Ha^2}{R} + \frac{1}{DR}\right)q - \frac{1}{\kappa^2 R}\frac{\partial^4 q}{\partial z^4} + \frac{Gr}{R}T. \tag{5.13}$$

The system of equations to be solved now reduces to a system of two equations, namely eq. (5.10) and eq. (5.13).

The boundary conditions in complex form are:

$$q = T = 0, \quad z = -1,$$

$$q = 0, T = e^{i\omega t}, \quad z = 1. \tag{5.14}$$

For a purely oscillatory flow, we assume that

$$-\frac{\partial p}{\partial x} = \lambda e^{i\omega t}, q(t,z) = \phi(z)e^{i\omega t} \; and \; T(t,z) = \theta(z)e^{i\omega t} \tag{5.15}$$

where λ is any positive constant and ω is the frequency of oscillation. Substituting Eq. (5.15) into Eq. (5.13) gives

$$i\omega\phi(z)e^{i\omega t} = \lambda e^{i\omega t} + \frac{1}{R}\phi''(z)e^{i\omega t} - \frac{1}{R}(Ha^2 + S^2)\phi(z)e^{i\omega t} -$$

$$\frac{1}{\kappa^2 R}\phi''''(z)e^{i\omega t} + \frac{Gr}{R}\theta(z)e^{i\omega t}\ , \tag{5.16}$$

where $S^2 = \frac{1}{D}$ is the porous medium parameter. Equivalently, since $e^{i\omega t}$ is common, we get

$$i\omega\phi(z) = \lambda + \frac{1}{R}\frac{d^2\phi}{dz^2} - \frac{1}{R}(Ha^2 + S^2)\phi(z) - \frac{1}{\kappa^2 R}\frac{d^4\phi}{dz^4} + \frac{Gr}{R}\theta(z), \tag{5.17}$$

which simplifies to;

$$\frac{d^4\phi}{dz^4} = \kappa^2\left[R\lambda + \frac{d^2\phi}{dz^2} - (Ha^2 + S^2 + Ri\omega)\phi + Gr\theta\right] \tag{5.18}$$

along with boundary conditions

$$\phi(\pm 1) = 0 = \phi''(\pm 1). \tag{5.19}$$

For the temperature field, after substituting Eq. (5.15) into Eq. (5.10), we get

$$\theta Peiwe^{iwt} = \frac{d^2\theta}{dz^2}e^{iwt} - \delta^2\theta e^{iwt}, \tag{5.20}$$

which becomes

$$\frac{d^2\phi}{dz^2} - \gamma^2\theta = 0, \qquad \gamma^2 = \delta^2 + Pei\omega, \tag{5.21}$$

with the boundary conditions:

$$\theta(1) = 1,\ \ \theta(-1) = 0. \tag{5.22}$$

Solving the ordinary differential equation Eq. (5.21) under boundary conditions given by Eq. (5.22) gives

$$\theta(z) = \frac{\sinh\gamma(z+1)}{\sinh 2\gamma}. \tag{5.23}$$

In exponential form, $\theta(z)$ is equivalently written as

$$\theta(z) = \frac{e^{\sqrt{\delta^2+Pei\omega}-z\sqrt{\delta^2+Pei\omega}\left(1+e^{2z\sqrt{\delta^2+Pei\omega}}\right)}}{1+e^{2\sqrt{\delta^2+Pei\omega}}}\ . \tag{5.24}$$

In this way, the exact solution for the temperature field is obtained as

$$T(z,t) = \frac{e^{\sqrt{\delta^2+Pei\omega}-z\sqrt{\delta^2+Pei\omega}\left(1+e^{2z\sqrt{\delta^2+Pei\omega}}\right)}}{1+e^{2\sqrt{\delta^2+Pei\omega}}} e^{i\omega t}. \quad (5.25)$$

Eq. (5.18) becomes, after substituting Eq. (5.24),

$$\frac{d^4\phi}{dz^4} = \kappa^2\left[R\lambda + \frac{d^2\phi}{dz^2} - (Ha^2 + S^2 + Ri\omega)\phi + Gr\frac{e^{\sqrt{\delta^2+Pei\omega}-z\sqrt{\delta^2+Pei\omega}\left(1+e^{2z\sqrt{\delta^2+Pei\omega}}\right)}}{1+e^{2\sqrt{\delta^2+Pei\omega}}}\right], \quad (5.26)$$

along with boundary conditions in Eq. (5.19). Due to the massive output of the symbolic solution for $\phi(z)$ only the graphical solution will be presented in the following section 3.

For the type of flow investigated herein, the two quantities of engineering importance are the rate of heat transfer Nu (Nusselt number) at the channel walls and the wall shear stress C_f (skin friction). From the temperature field, Eq. (5.24), we can obtain the rate of heat transfer at the left channel wall $z = -1$ and is given by

$$Nu = -\left(\frac{\partial\theta}{\partial z}\right)_{z=-1} = -\frac{\sqrt{\delta^2+Pei\omega}\left(1-e^{2\sqrt{\delta^2+Pei\omega}}\right)}{1+e^{2\sqrt{\delta^2+Pei\omega}}} \quad . \quad (5.27)$$

Similarly, from the velocity field we obtain the skin friction at the left channel wall as

$$C_f = \left(\frac{\partial\phi}{\partial z} - \frac{1}{\kappa^2}\frac{\partial^3\phi}{\partial z^3}\right)_{z=-1} \quad (5.28)$$

Table 5.1. Skin friction (C_f) at the left wall plate $z = -1$

κ	δ	Ha	S	R	Pe	ω	Gr	λ	C_f
1	1	1	1	1	1	1	1	1	1.44055
								2	2.28076
								3	3.12096
							1	1	1.44055
							2		2.04090
							3		2.64125
						1	1		1.44055
						2			1.30865
						3			1.16637
					0.71	1			1.46063
					1				1.44055
					2				1.35264
				1	1				1.44055
				2					2.22470
				3					2.94170
			1	1					1.44055
			2						1.20823
			3						0.98416
		1	1						1.44055
		2							1.20823
		3							0.98416
	1	1							1.44055
	2								1.25160
	3								1.13504
0.1	1								1.71249
0.2									1.69894
0.3									1.67749

Table 5.2. Rate of heat transfer (Nu)

Pe	δ	ω	Nu
0.71	0.1	1	0.163580
1			0.293853
2			0.815061
1	0.1		0.293853
	0.2		0.314346
	0.3		0.348063
	1	1	0.875163
		2	1.133940
		3	1.408950

5.3. Results and Discussion

Equations (5.24) and (5.26) are coded into a computer symbolic package, MATHEMATICA, for successful computation of the graphical solutions. A qualitative as well as quantitative analysis of the effects of the underlying parameters on the velocity and fluid temperature profiles is carried out with the aid of simulated graphs. The computational results for the velocity profiles are presented in Figs. 5.2 – 5.9 while results for the fluid temperature profiles are displayed in Figs. 5.10 – 5.12.

In Fig. 5.2, an increase in the couple stress parameter κ is seen to increase the fluid velocity profiles, signifying the thinning of the fluid. A reverse trend is seen with decreasing values of κ that shows the thickening of the fluid together with the decreasing flow velocity. The influence of the magnetic field on the flow field is modelled by the Hartmann number Ha. Increasing the Hartmann number means an increase in the intensity of the magnetic field. In Fig. 5.3, consistent with expectation, the magnitudes of the velocity components are retarded by increasing magnetic field intensity. The transversely applied magnetic field B_0 gives rise to a drag-like force, called the Lorentz force, whose effect on the electrically conducting fluid is to damp the motion. Figure 4 illustrates the variation of the fluid velocity components with the porous medium shape parameter S. The effect of the porous medium shape parameter mirrors that of the Hartmann number. As the parameter S increases, the tortuosity of the porous matrix increases resulting in damping of the flow. The effect of the Reynolds number R on the velocity components is depicted in Fig. 5.5, and the magnitude of

either velocity component is enhanced with increasing Reynolds number. This is consistent with expectation. The influence of the Peclet number Pe on the velocity profiles is shown in Fig. 5.6. The Peclet number is seen to retard the magnitude of the component u and enhance the component w. Similar trends are observed in Fig.5.7 where the effects of the frequency of oscillations on the velocity components are displayed. Figure 5.8 shows the magnitude of both velocity components increasing with increasing Grashof number. Radiative heat transferred from the hot plate at $z = 1$ into the fluid inevitably raises the temperature of the fluid and in the process the viscosity of the fluid is reduced, resulting in increased flow rate. This phenomenon is explained by the fact that when heat is transferred from the heated right plate into the fluid, the increased buoyancy forces enhance the velocity of the bulk of the fluid. The influence of the pressure gradient on the fluid flow is represented by the pressure gradient parameter λ. Figure 5.9 shows both velocity components increasing with an increase in this parameter. This is to be expected since the pressure gradient is one of the driving forces of motion in this study.

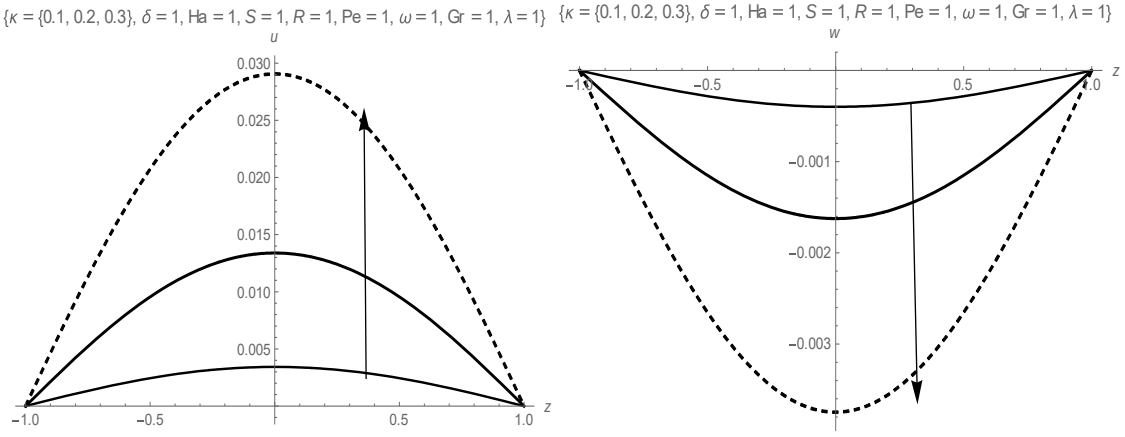

Figure 5.2 Effects of the couple stress parameter κ on fluid velocity profiles u and w.

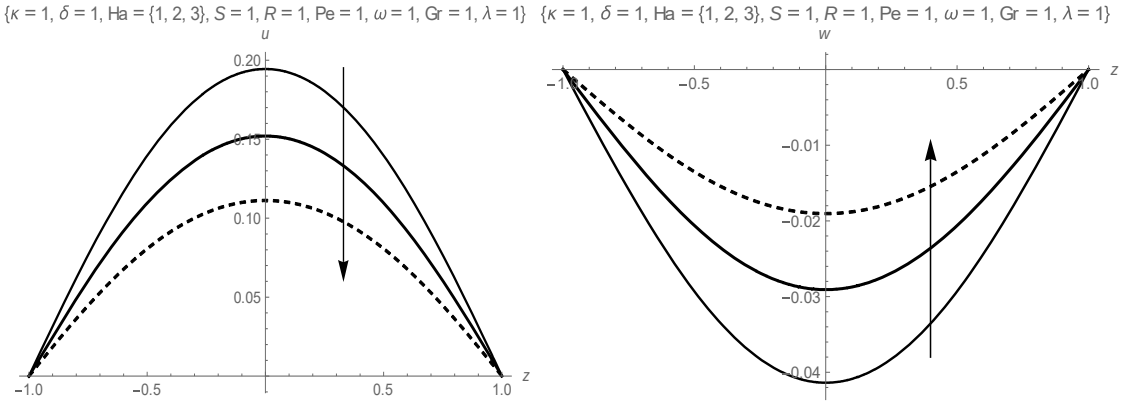

Figure 5.3 Effects of the Hartmann number Ha on fluid velocity profiles u and w.

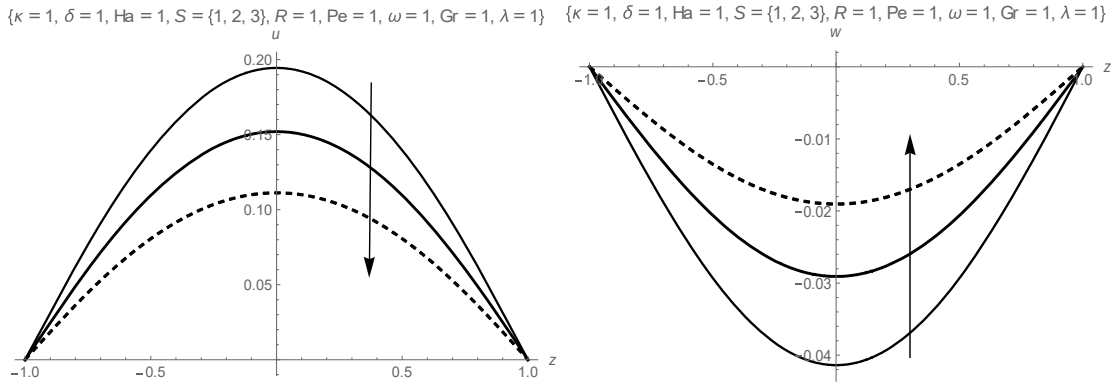

Figure 5.4 Effects of the porous medium parameter S on fluid velocity profiles u and w.

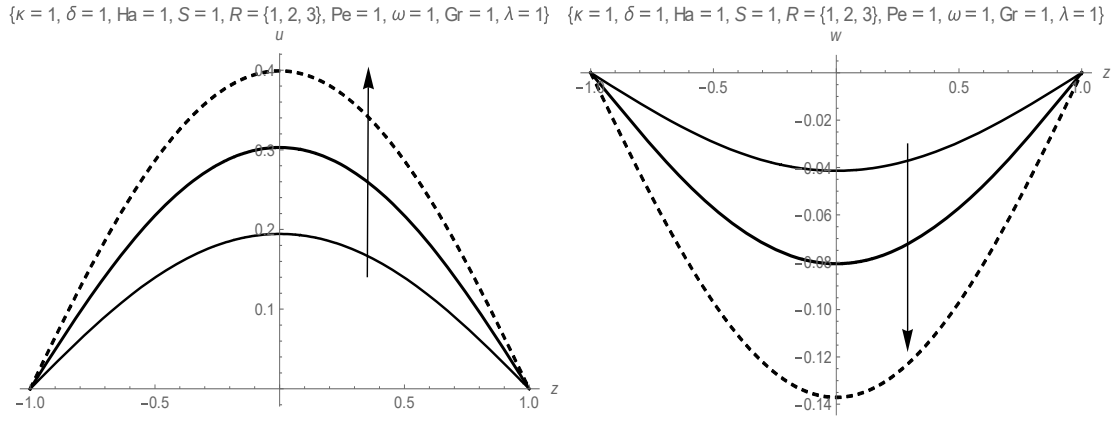

Figure 5.5 Effects of the Reynolds number R on fluid velocity profiles u and w.

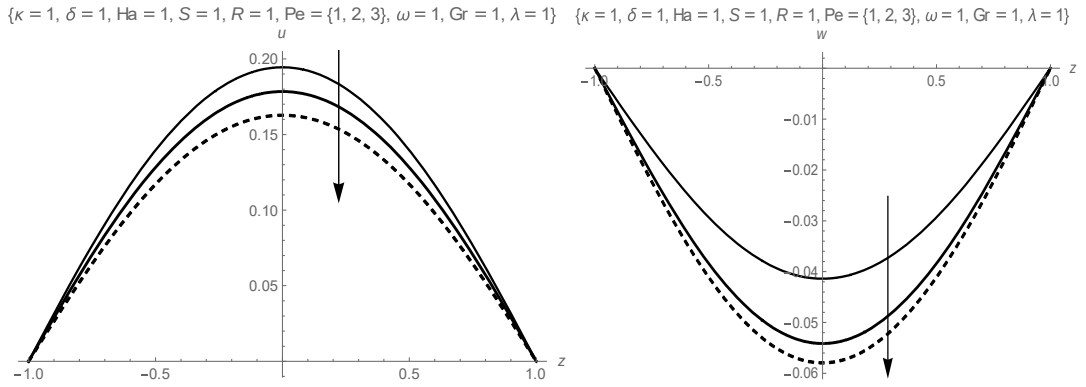

Figure 5.6 Effects of Peclet number Pe on fluid velocity profiles u and w.

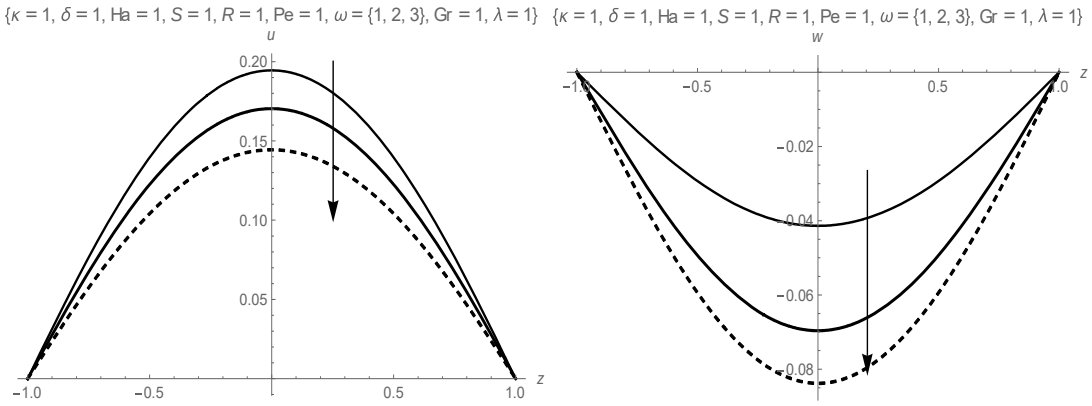

Figure 5.7 Effects of frequency of oscillations ω on fluid velocity profiles u and w.

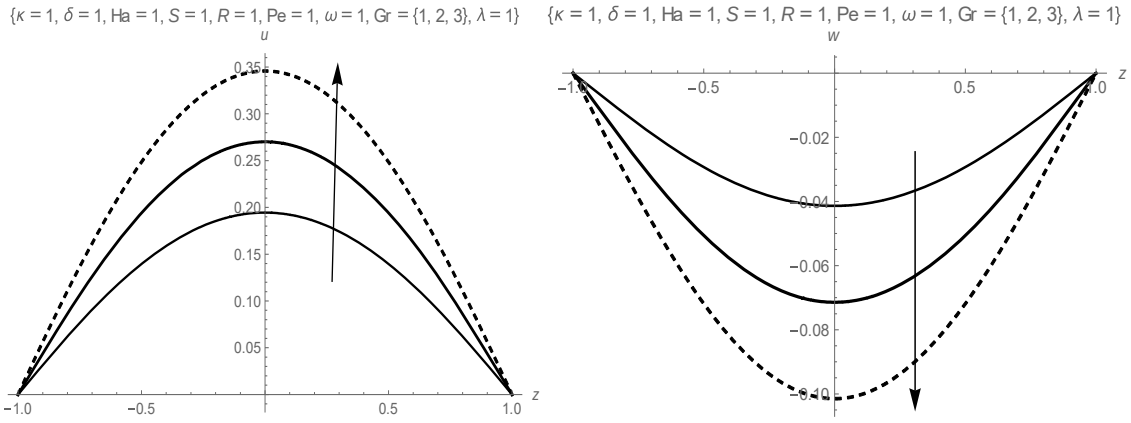

Figure 5.8 Effects of the Grashof number Gr on fluid velocity profiles u and w.

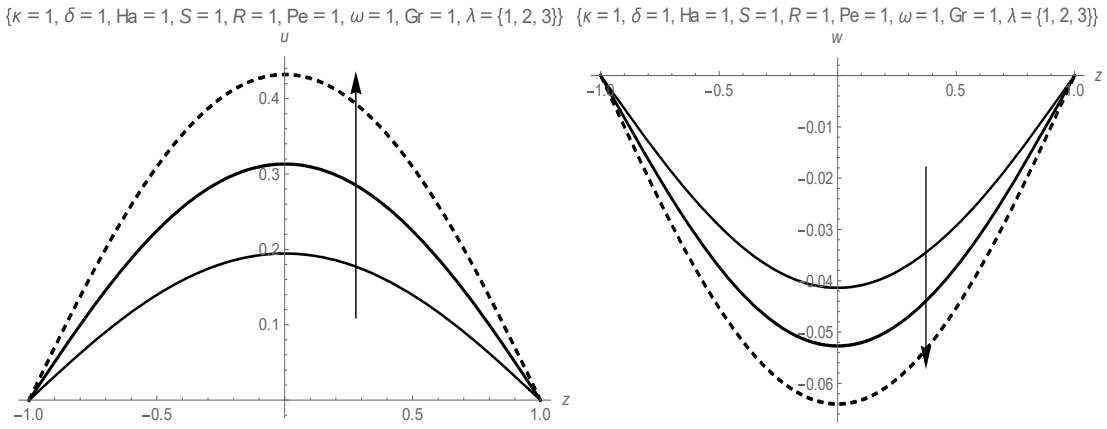

Figure 5.9 Effects of the pressure gradient parameter λ on fluid velocity profiles u and w.

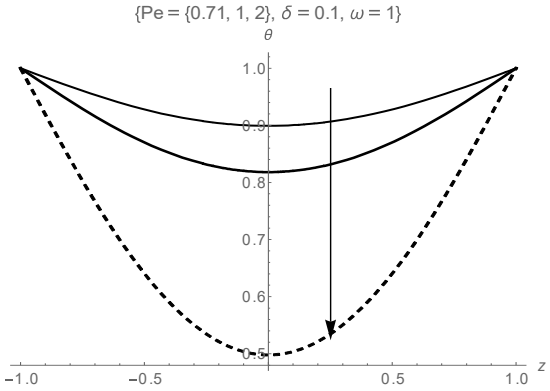

Figure 5.10 Effects of the Peclet number Pe on fluid temperature

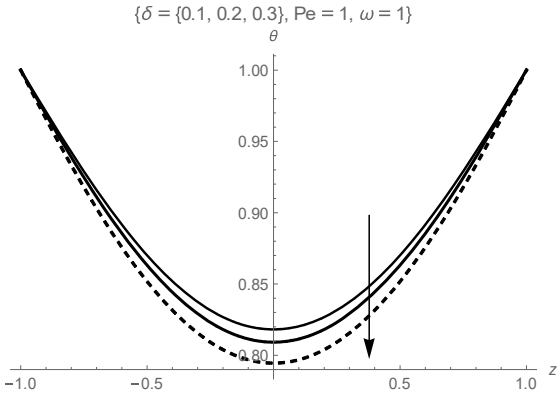

Figure 5.11 Effects of the thermal radiation parameter δ on fluid temperature

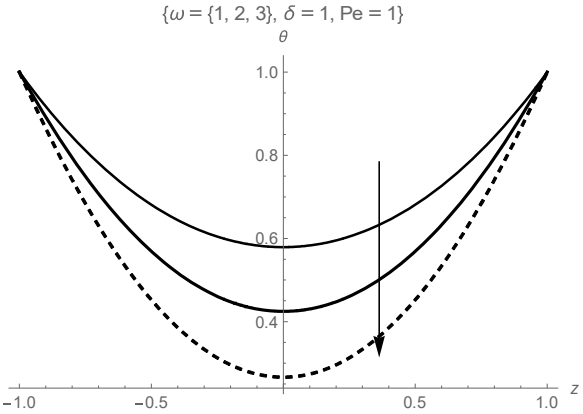

Figure 5.12 Effects of frequency of oscillations ω on fluid temperature

Figure 5.10 shows the fluid temperature diminishing with increasing Peclet number. This phenomenon shows that within the flow, there is dominance of thermal diffusivity over momentum diffusivity. More heat is transferred from the fluid to the cooler channel plate at $z = -1$ resulting in the lowering of the fluid temperature. In Fig.5.11, an increase in the thermal radiation parameter leads to a decrease of the fluid temperature. The same explanation for the phenomenon in Fig. 5.10 also applies in this case. Increasing the radiation parameter results in more radiative heat being transferred from the fluid to the cooler channel plate at $z = 1$ and this, of course, lowers the temperature in the bulk of the fluid. Figure 5.12 shows that an increase in the frequency of oscillations reduces the fluid temperature as well. The increased rate of oscillations inevitably dissipates the heat out of the fluid into the ambient.

Table 5.1 and Table 5.2 show the influence of the thermophysical parameters on the wall shear stress (skin friction) and the heat transfer rate (Nusselt number), respectively. Two interesting trends clearly stand out. Firstly, except for the couple stress parameter, parameters that increase the rate of flow also increase the skin friction and those that decrease the flow rate also decrease the skin friction. The couple stresses increase the flow rate while they marginally decrease the skin friction. Secondly, parameters that decrease the fluid temperature also decrease the heat transfer rate.

5.4. Conclusion

In this chapter, mixed convective flow of an electrically conducting, viscous incompressible couple stress fluid through a vertical channel filled with a saturated porous medium under the influence of an externally applied magnetic field has been investigated. It is observed that the velocity component for the primary flow is enhanced with an increase in the couple stress parameter, the Reynolds number, the Grashof number and the pressure gradient parameter while it is retarded with an increase in the magnetic field, the porous medium parameter, the Peclet number and the frequency of oscillations. The velocity component for the secondary flow is increased with an increase in all the parameters except the magnetic field and the porous medium parameter which retard it. It is further observed that the thermal radiation parameter, the Peclet number and the frequency of oscillations have a retardation effect on the fluid temperature. The investigation also concludes that, except for the couple stresses, parameters that increase (decrease) the fluid velocity also increase (decrease) the wall shear stress and parameters that decrease the fluid temperature also decrease the heat transfer rate. The couple stresses are observed to marginally decrease the skin friction.

CHAPTER SIX
GENERAL DISCUSSION, CONCLUSION AND RECOMMENDATIONS

6.1. General discussion

In this thesis, the modelling of buoyancy-induced hydromagnetic couple stress fluid flow with periodic heat input has been investigated. The governing basic fluid dynamics equations for mass, momentum and energy were derived. The resulting non-linear dimensionless differential equations were solved analytically and numerically using the Adomian decomposition method. A computer symbolic package MATHEMATICA was employed for successful computation of the numerical and graphical solutions. A detailed analysis of the combined effects of the various thermophysical parameters embedded in the flow system on the velocity, temperature, skin friction and Nusselt number profiles was carried out. In flow and heat transfer studies in a channel, the skin friction and the Nusselt number are mostly the two quantities of engineering significance.

6.2. Conclusions

In chapter 3, the MHD natural convection flow of a heat generating couple stress fluid with time-periodic boundary conditions was investigated. The response of steady and periodic velocity and temperature fields as well as the skin friction and local Nusselt number to the embedded parameters in the flow system was outlined with the help of clear simulations of the solution. Some of the important results can be summarised as follows:

- The magnetic field and the couple stresses were observed to have a retarding effect on both the velocity and temperature fields.
- The viscous heating parameter and the internal heat generation parameter were found to have opposing influences.
- A diminishing effect of the Strouhal number on the magnitude of the unsteady velocity and temperature fields suggest a strong dominance of the steady state part of the flow due to strong viscous forces.
- The couple stresses enhanced the skin friction and decreased the wall heat transfer rate

In Chapter 4, the convective flow of hydromagnetic couple stress fluid with induced magnetic field was considered in the steady-periodic regimes with varying heating. Some of the pertinent results can be summarised as follows:

- Increasing values of Hartman number, Strouhal number, couple stress parameter and heat loss parameter decreased the flow velocity while viscous heating of the fluid enhanced both steady and oscillatory flow profiles.
- Fluid temperature distribution was seen to increase with increasing values of the viscous heating parameter, Hartman number and couple stress parameter while it decreased with increasing values of the Prandtl number, heat loss parameter, suction parameter and Strouhal number.
- Increasing values of the Hartman number, viscous heating, suction and magnetic Prandtl number were seen to enhance the induced current density while an increase in the Strouhal number decreased it.

In Chapter 5, mixed convective flow of an electrically conducting, viscous incompressible couple stress fluid through a vertical channel filled with a saturated porous medium was investigated. The following conclusions were drawn:

- The velocity component for the primary flow was enhanced with an increase in the thermal radiation parameter and the Reynolds number and retarded with an increase in the Grashof number, the frequency of oscillations, The Peclet number, the magnetic field intensity and the couple stress parameter.
- The velocity component for the secondary flow was increased with an increase in the thermal radiation parameter, the Grashof number and the Reynolds number and was retarded by increasing the frequency of oscillations, the Peclet number, the magnetic field intensity and the couple stresses.
- The thermal radiation parameter increases the fluid temperature while the Peclet number and the frequency of oscillations reduces it.
- Except for the couple stresses, parameters that increase (decrease) the fluid velocity also increase (decrease) the wall shear stress and parameters that decrease the fluid temperature also decrease the heat transfer rate.
- The couple stresses are observed to marginally decrease the skin friction.

6.3. Recommendations

It has been stated that the distinguishing characteristic features of the couple stress non-Newtonian fluid is the inclusion of the size-dependent microstructure that renders it to be of desirable mechanical significance. Understanding the combined effects of the couple stresses and the other parameters on the flow field variables will inform optimal designs of devices and processes in technological areas where channel flows are applied. In this study, apart from the effect of the other pertinent parameters, the couple stresses were found to have significant effect on the flow velocity, temperature, skin friction and Nusselt number. For instance, the effect of increasing the skin friction informs the strength of the material to be used to avoid bursting of pipes in machinery. Where Nusselt number is increased, it means that heat loss can be avoided by enhanced insulation. Similarly, other recommendations can be made.

6.4. Future research work

Future work maybe:

- To consider the same type of flows studied in this thesis but with a different type of fluid like a Casson fluid, third grade fluid or other non-Newtonian fluids.
- To use other numerical methods like the homotopy analysis method, the spectral methods, etc., to solve exactly the same problems studied and compare the results.

APPENDIX 1

Solution of $\varphi(z)$ in equation (5.26) of chapter 5

$\varphi(z)$ = (-((1.`

2.718281828459045`^(0.7071067811865475` $\sqrt{\kappa^2+\sqrt{\kappa^2\,(-4.`\,\beta+\kappa^2)}}$ -0.7071067811865475` y $\sqrt{\kappa^2+\sqrt{\kappa^2\,(-4.`\,\beta+\kappa^2)}}$) κ2 (-2.`

Gr β κ2+Gr γ2 κ2+Gr γ2 $\sqrt{\kappa^2\,(-4.`\,\beta+\kappa^2)}$ -2.` R γ4 λ-2.` R β κ2 λ+2.` R γ2

κ2 λ))/((1.` +2.718281828459045`^(1.4142135623730951` $\sqrt{\kappa^2+\sqrt{\kappa^2\,(-4.`\,\beta+\kappa^2)}}$) $\sqrt{\kappa^2\,(-4.`\,\beta+\kappa^2)}$ (γ4+β

κ2-1.` γ2 κ2) (κ2+$\sqrt{\kappa^2\,(-4.`\,\beta+\kappa^2)}$)))-(0.5`

2.718281828459045`^(0.7071067811865475` $\sqrt{\kappa^2-1.`\,\sqrt{\kappa^2\,(-4.`\,\beta+\kappa^2)}}$ -0.7071067811865475` y $\sqrt{\kappa^2-1.`\,\sqrt{\kappa^2\,(-4.`\,\beta+\kappa^2)}}$) (-2.`

Gr β γ2 κ2+Gr β κ4+Gr β κ2 $\sqrt{\kappa^2\,(-4.`\,\beta+\kappa^2)}$ +R γ4 κ2 λ+R β κ4 λ-1.` R γ2 κ4

λ+R γ4 $\sqrt{\kappa^2\,(-4.`\,\beta+\kappa^2)}$ λ+R β κ2 $\sqrt{\kappa^2\,(-4.`\,\beta+\kappa^2)}$ λ-1.` R γ2 κ2 $\sqrt{\kappa^2\,(-4.`\,\beta+\kappa^2)}$

λ))/((1.` +2.718281828459045`^(1.4142135623730951` $\sqrt{\kappa^2-1.`\,\sqrt{\kappa^2\,(-4.`\,\beta+\kappa^2)}}$) β $\sqrt{\kappa^2\,(-4.`\,\beta+\kappa^2)}$ (γ4+β

κ2-1.` γ2 κ2))-(0.5`

2.718281828459045`^(0.7071067811865475` $\sqrt{\kappa^2-1.`\,\sqrt{\kappa^2\,(-4.`\,\beta+\kappa^2)}}$ +0.7071067811865475` y $\sqrt{\kappa^2-1.`\,\sqrt{\kappa^2\,(-4.`\,\beta+\kappa^2)}}$) (-2.`

Gr β γ2 κ2+Gr β κ4+Gr β κ2 $\sqrt{\kappa^2\,(-4.`\,\beta+\kappa^2)}$ +R γ4 κ2 λ+R β κ4 λ-1.` R γ2 κ4

λ+R γ4 $\sqrt{\kappa^2\,(-4.`\,\beta+\kappa^2)}$ λ+R β κ2 $\sqrt{\kappa^2\,(-4.`\,\beta+\kappa^2)}$ λ-1.` R γ2 κ2 $\sqrt{\kappa^2\,(-4.`\,\beta+\kappa^2)}$

λ))/((1.` +2.718281828459045`^(1.4142135623730951` $\sqrt{\kappa^2-1.`\,\sqrt{\kappa^2\,(-4.`\,\beta+\kappa^2)}}$) β $\sqrt{\kappa^2\,(-4.`\,\beta+\kappa^2)}$ (γ4+β

κ2-1.` γ2 κ2))-(0.5`

2.718281828459045`^(0.7071067811865475` $\sqrt{\kappa^2+\sqrt{\kappa^2\,(-4.`\,\beta+\kappa^2)}}$ +0.7071067811865475` y $\sqrt{\kappa^2+\sqrt{\kappa^2\,(-4.`\,\beta+\kappa^2)}}$) (2.` Gr β

γ2 κ2-1.` Gr β κ4+Gr β κ2 $\sqrt{\kappa^2\,(-4.`\,\beta+\kappa^2)}$ -1.` R γ4 κ2 λ-1.` R β κ4 λ+R γ2

κ4 λ+R γ4 $\sqrt{\kappa^2\,(-4.`\,\beta+\kappa^2)}$ λ+R β κ2 $\sqrt{\kappa^2\,(-4.`\,\beta+\kappa^2)}$ λ-1.` R γ2 κ2 $\sqrt{\kappa^2\,(-4.`\,\beta+\kappa^2)}$

λ))/((1.` +2.718281828459045`^(1.4142135623730951` $\sqrt{\kappa^2+\sqrt{\kappa^2\,(-4.`\,\beta+\kappa^2)}}$) β $\sqrt{\kappa^2\,(-4.`\,\beta+\kappa^2)}$ (γ4+β

κ2-1.` γ2 κ2))+(2.` 1.4142135623730951`

2.718281828459045`^(-0.7071067811865475` y $\sqrt{\kappa^2-1.`\,\sqrt{\kappa^2\,(-4.`\,\beta+\kappa^2)}}$ -0.7071067811865475` y $\sqrt{\kappa^2+\sqrt{\kappa^2\,(-4.`\,\beta+\kappa^2)}}$) (-4.`

1.4142135623730951`

2.718281828459045`^(γ+1.4142135623730951` y $\sqrt{\kappa^2-1.`\,\sqrt{\kappa^2\,(-4.`\,\beta+\kappa^2)}}$ +0.7071067811865475` y $\sqrt{\kappa^2+\sqrt{\kappa^2\,(-4.`\,\beta+\kappa^2)}}$ +y (-1.` γ-0.7071067811865475` $\sqrt{\kappa^2-1.`\,\sqrt{\kappa^2\,(-4.`\,\beta+\kappa^2)}}$)

Gr β2 κ2-4.` 1.4142135623730951`

2.718281828459045`

$\gamma+2.\grave{}\ y\ \gamma+1.4142135623730951\grave{}\ \ y\sqrt{\kappa^2-1.\grave{}\ \sqrt{\kappa^2\ (-4.\grave{}\ \beta+\kappa^2)}}+0.7071067811865475\grave{}\ \ y\sqrt{\kappa^2+\sqrt{\kappa^2\ (-4.\grave{}\ \beta+\kappa^2)}}+y\ (-1.\grave{}\ \gamma-0.7071067811865475\grave{}\ \ \sqrt{\kappa^2-1.\grave{}\ \sqrt{\kappa^2\ (-4.\grave{}\ \ldots$

Gr β2 κ2-4.` 1.4142135623730951`

2.718281828459045`

$\gamma+0.7071067811865475\grave{}\ \ y\sqrt{\kappa^2+\sqrt{\kappa^2\ (-4.\grave{}\ \beta+\kappa^2)}}+y\left(-1.\grave{}\ \gamma+0.7071067811865475\grave{}\ \ \sqrt{\kappa^2-1.\grave{}\ \sqrt{\kappa^2\ (-4.\grave{}\ \beta+\kappa^2)}}\right)$ Gr β2 κ2-4.`

1.4142135623730951`

2.718281828459045`

$\gamma+2.\grave{}\ y\ \gamma+0.7071067811865475\grave{}\ \ y\sqrt{\kappa^2+\sqrt{\kappa^2\ (-4.\grave{}\ \beta+\kappa^2)}}+y\left(-1.\grave{}\ \gamma+0.7071067811865475\grave{}\ \ \sqrt{\kappa^2-1.\grave{}\ \sqrt{\kappa^2\ (-4.\grave{}\ \beta+\kappa^2)}}\right)$ Gr β2

κ2-4.` 1.4142135623730951`

2.718281828459045`

$\gamma+0.7071067811865475\grave{}\ \ y\sqrt{\kappa^2-1.\grave{}\ \sqrt{\kappa^2\ (-4.\grave{}\ \beta+\kappa^2)}}+1.4142135623730951\grave{}\ \ y\sqrt{\kappa^2+\sqrt{\kappa^2\ (-4.\grave{}\ \beta+\kappa^2)}}+y\left(-1.\grave{}\ \gamma-0.7071067811865475\grave{}\ \ \sqrt{\kappa^2+\sqrt{\kappa^2\ (-4.\grave{}\ \beta+\kappa^2)}}\right)$

Gr β2 κ2-4.` 1.4142135623730951`

2.718281828459045`

$\gamma+2.\grave{}\ y\ \gamma+0.7071067811865475\grave{}\ \ y\sqrt{\kappa^2-1.\grave{}\ \sqrt{\kappa^2\ (-4.\grave{}\ \beta+\kappa^2)}}+1.4142135623730951\grave{}\ \ y\sqrt{\kappa^2+\sqrt{\kappa^2\ (-4.\grave{}\ \beta+\kappa^2)}}+y\ (-1.\grave{}\ \gamma-0.7071067811865475\grave{}\ \ \sqrt{\kappa^2+\sqrt{\kappa^2\ (-4.\grave{}\ \beta+\kappa^2 \ldots$

Gr β2 κ2-4.` 1.4142135623730951`

2.718281828459045`

$\gamma+0.7071067811865475\grave{}\ \ y\sqrt{\kappa^2-1.\grave{}\ \sqrt{\kappa^2\ (-4.\grave{}\ \beta+\kappa^2)}}+y\left(-1.\grave{}\ \gamma+0.7071067811865475\grave{}\ \ \sqrt{\kappa^2+\sqrt{\kappa^2\ (-4.\grave{}\ \beta+\kappa^2)}}\right)$ Gr β2 κ2-4.`

1.4142135623730951`

2.718281828459045`

$\gamma+2.\grave{}\ y\ \gamma+0.7071067811865475\grave{}\ \ y\sqrt{\kappa^2-1.\grave{}\ \sqrt{\kappa^2\ (-4.\grave{}\ \beta+\kappa^2)}}+y\left(-1.\grave{}\ \gamma+0.7071067811865475\grave{}\ \ \sqrt{\kappa^2+\sqrt{\kappa^2\ (-4.\grave{}\ \beta+\kappa^2)}}\right)$ Gr β2

κ2+1.4142135623730951`

2.718281828459045`

$\gamma+1.4142135623730951\grave{}\ \ y\sqrt{\kappa^2-1.\grave{}\ \sqrt{\kappa^2\ (-4.\grave{}\ \beta+\kappa^2)}}+0.7071067811865475\grave{}\ \ y\sqrt{\kappa^2+\sqrt{\kappa^2\ (-4.\grave{}\ \beta+\kappa^2)}}+y\left(-1.\grave{}\ \gamma-0.7071067811865475\grave{}\ \ \sqrt{\kappa^2-1.\grave{}\ \sqrt{\kappa^2\ (-4.\grave{}\ \beta+\kappa^2)}}\right)$

Gr β κ4+1.4142135623730951`

2.718281828459045`

$\gamma+2.\grave{}\ y\ \gamma+1.4142135623730951\grave{}\ \ y\sqrt{\kappa^2-1.\grave{}\ \sqrt{\kappa^2\ (-4.\grave{}\ \beta+\kappa^2)}}+0.7071067811865475\grave{}\ \ y\sqrt{\kappa^2+\sqrt{\kappa^2\ (-4.\grave{}\ \beta+\kappa^2)}}+y\ (-1.\grave{}\ \gamma-0.7071067811865475\grave{}\ \ \sqrt{\kappa^2-1.\grave{}\ \sqrt{\kappa^2\ (-4.\grave{}\ \ldots$

Gr β κ4+1.4142135623730951`

2.718281828459045`

$\gamma+0.7071067811865475\grave{}\ \ y\sqrt{\kappa^2+\sqrt{\kappa^2\ (-4.\grave{}\ \beta+\kappa^2)}}+y\left(-1.\grave{}\ \gamma+0.7071067811865475\grave{}\ \ \sqrt{\kappa^2-1.\grave{}\ \sqrt{\kappa^2\ (-4.\grave{}\ \beta+\kappa^2)}}\right)$ Gr β

κ4+1.4142135623730951`

2.718281828459045:

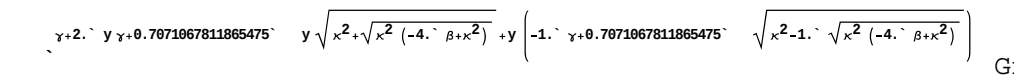

Gr β

K4+1.4142135623730951`

2.718281828459045:

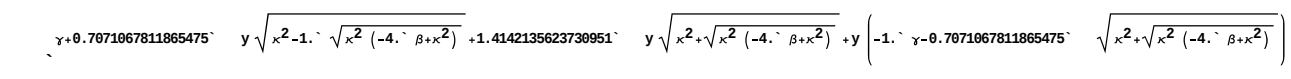

Gr β K4+1.4142135623730951`

2.718281828459045:

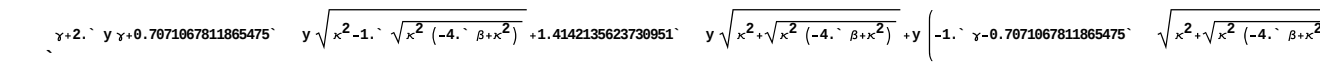

Gr β K4+1.4142135623730951`

2.718281828459045:

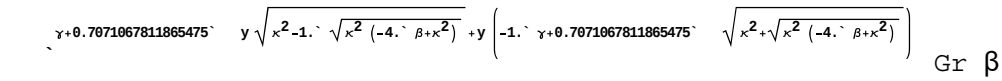

Gr β

K4+1.4142135623730951`

2.718281828459045:

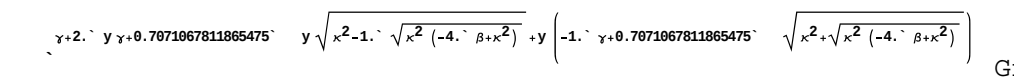

Gr β K4-

2.` 1.4142135623730951`

2.718281828459045:

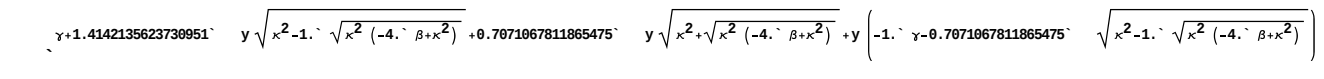

Gr β γ2 $\sqrt{\kappa^2 (-4.` \beta + \kappa^2)}$ -2.` 1.4142135623730951`

2.718281828459045:

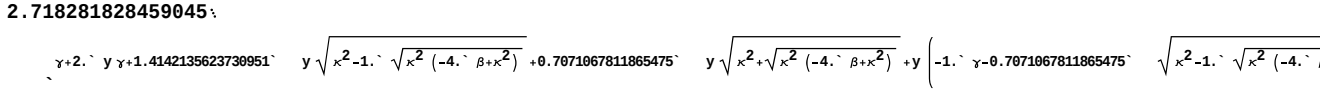

Gr β γ2 $\sqrt{\kappa^2 (-4.` \beta + \kappa^2)}$ -2.` 1.4142135623730951`

2.718281828459045:

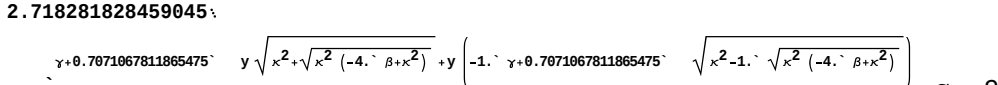

Gr β γ2

$\sqrt{\kappa^2 (-4.` \beta + \kappa^2)}$ -2.` 1.4142135623730951`

2.718281828459045:

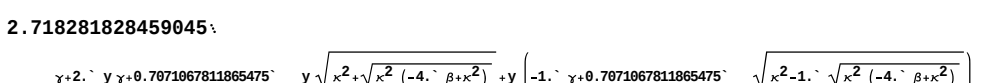

Gr β γ2

$\sqrt{\kappa^2 (-4.` \beta + \kappa^2)}$ +2.` 1.4142135623730951`

2.718281828459045:

Gr β γ2 $\sqrt{\kappa^2 (-4.` \beta + \kappa^2)}$ +2.` 1.4142135623730951`

2.718281828459045`

$$\gamma+2.`\ y\,\gamma+0.7071067811865475`\ y\sqrt{\kappa^2-1.`\sqrt{\kappa^2(-4.`\beta+\kappa^2)}}+1.4142135623730951`\ y\sqrt{\kappa^2+\sqrt{\kappa^2(-4.`\beta+\kappa^2)}}+y\left(-1.`\gamma-0.7071067811865475`\sqrt{\kappa^2+\sqrt{\kappa^2(-4.`\beta+\kappa^2}}\right.$$

$$\mathrm{Gr}\ \beta\ \gamma 2\ \sqrt{\kappa^2(-4.`\beta+\kappa^2)}+2.`\ 1.4142135623730951`$$

2.718281828459045`

$$\gamma+0.7071067811865475`\ y\sqrt{\kappa^2-1.`\sqrt{\kappa^2(-4.`\beta+\kappa^2)}}+y\left(-1.`\gamma+0.7071067811865475`\sqrt{\kappa^2+\sqrt{\kappa^2(-4.`\beta+\kappa^2)}}\right)\ \mathrm{Gr}\ \beta\ \gamma 2$$

$$\sqrt{\kappa^2(-4.`\beta+\kappa^2)}+2.`\ 1.4142135623730951`$$

2.718281828459045`

$$\gamma+2.`\ y\,\gamma+0.7071067811865475`\ y\sqrt{\kappa^2-1.`\sqrt{\kappa^2(-4.`\beta+\kappa^2)}}+y\left(-1.`\gamma+0.7071067811865475`\sqrt{\kappa^2+\sqrt{\kappa^2(-4.`\beta+\kappa^2)}}\right)\ \mathrm{Gr}\ \beta\ \gamma 2$$

$$\sqrt{\kappa^2(-4.`\beta+\kappa^2)}+1.4142135623730951`$$

2.718281828459045`

$$\gamma+1.4142135623730951`\ y\sqrt{\kappa^2-1.`\sqrt{\kappa^2(-4.`\beta+\kappa^2)}}+0.7071067811865475`\ y\sqrt{\kappa^2+\sqrt{\kappa^2(-4.`\beta+\kappa^2)}}+y\left(-1.`\gamma-0.7071067811865475`\sqrt{\kappa^2-1.`\sqrt{\kappa^2(-4.`\beta+\kappa^2)}}\right)$$

$$\mathrm{Gr}\ \beta\ \kappa 2\ \sqrt{\kappa^2(-4.`\beta+\kappa^2)}+1.4142135623730951`$$

2.718281828459045`

$$\gamma+2.`\ y\,\gamma+1.4142135623730951`\ y\sqrt{\kappa^2-1.`\sqrt{\kappa^2(-4.`\beta+\kappa^2)}}+0.7071067811865475`\ y\sqrt{\kappa^2+\sqrt{\kappa^2(-4.`\beta+\kappa^2)}}+y\left(-1.`\gamma-0.7071067811865475`\sqrt{\kappa^2-1.`\sqrt{\kappa^2(-4.`}}\right.$$

$$\mathrm{Gr}\ \beta\ \kappa 2\ \sqrt{\kappa^2(-4.`\beta+\kappa^2)}+1.4142135623730951`$$

2.718281828459045`

$$\gamma+0.7071067811865475`\ y\sqrt{\kappa^2+\sqrt{\kappa^2(-4.`\beta+\kappa^2)}}+y\left(-1.`\gamma+0.7071067811865475`\sqrt{\kappa^2-1.`\sqrt{\kappa^2(-4.`\beta+\kappa^2)}}\right)\ \mathrm{Gr}\ \beta\ \kappa 2$$

$$\sqrt{\kappa^2(-4.`\beta+\kappa^2)}+1.4142135623730951`$$

2.718281828459045`

$$\gamma+2.`\ y\,\gamma+0.7071067811865475`\ y\sqrt{\kappa^2+\sqrt{\kappa^2(-4.`\beta+\kappa^2)}}+y\left(-1.`\gamma+0.7071067811865475`\sqrt{\kappa^2-1.`\sqrt{\kappa^2(-4.`\beta+\kappa^2)}}\right)\ \mathrm{Gr}\ \beta\ \kappa 2$$

$$\sqrt{\kappa^2(-4.`\beta+\kappa^2)}-1.`\ 1.4142135623730951`$$

2.718281828459045`

$$\gamma+0.7071067811865475`\ y\sqrt{\kappa^2-1.`\sqrt{\kappa^2(-4.`\beta+\kappa^2)}}+1.4142135623730951`\ y\sqrt{\kappa^2+\sqrt{\kappa^2(-4.`\beta+\kappa^2)}}+y\left(-1.`\gamma-0.7071067811865475`\sqrt{\kappa^2+\sqrt{\kappa^2(-4.`\beta+\kappa^2)}}\right)$$

$$\mathrm{Gr}\ \beta\ \kappa 2\ \sqrt{\kappa^2(-4.`\beta+\kappa^2)}-1.`\ 1.4142135623730951`$$

2.718281828459045`

$$\gamma+2.`\ y\,\gamma+0.7071067811865475`\ y\sqrt{\kappa^2-1.`\sqrt{\kappa^2(-4.`\beta+\kappa^2)}}+1.4142135623730951`\ y\sqrt{\kappa^2+\sqrt{\kappa^2(-4.`\beta+\kappa^2)}}+y\left(-1.`\gamma-0.7071067811865475`\sqrt{\kappa^2+\sqrt{\kappa^2(-4.`\beta+\kappa^2}}\right.$$

$$\mathrm{Gr}\ \beta\ \kappa 2\ \sqrt{\kappa^2(-4.`\beta+\kappa^2)}-1.`\ 1.4142135623730951`$$

2.718281828459045`

$$\gamma+0.7071067811865475`\ y\sqrt{\kappa^2-1.`\sqrt{\kappa^2(-4.`\beta+\kappa^2)}}+y\left(-1.`\gamma+0.7071067811865475`\sqrt{\kappa^2+\sqrt{\kappa^2(-4.`\beta+\kappa^2)}}\right)\ \mathrm{Gr}\ \beta\ \kappa 2$$

$\sqrt{\kappa^2\,(-4.`\,\beta+\kappa^2)}$ -1.` 1.4142135623730951`

2.718281828459045$^{\gamma}$

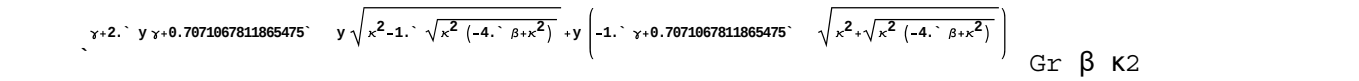

Gr β κ2 $\sqrt{\kappa^2\,(-4.`\,\beta+\kappa^2)}$ -4.`

2.718281828459045$^{\gamma}$

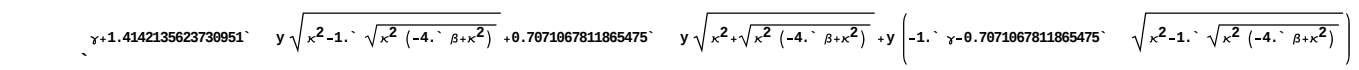

Gr β γ3 $\sqrt{\kappa^2-1.`\,\sqrt{\kappa^2\,(-4.`\,\beta+\kappa^2)}}$ +4.`

2.718281828459045$^{\gamma}$

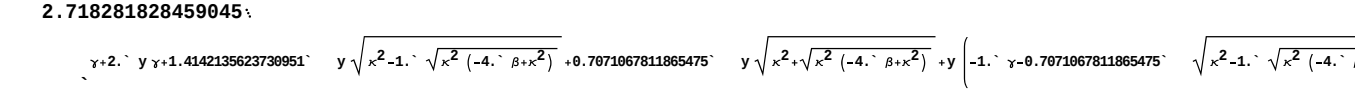

Gr β γ3 $\sqrt{\kappa^2-1.`\,\sqrt{\kappa^2\,(-4.`\,\beta+\kappa^2)}}$ +4.`

2.718281828459045$^{\gamma}$

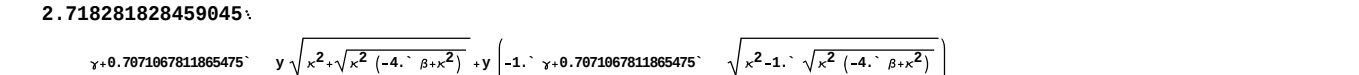

Gr β γ3 $\sqrt{\kappa^2-1.`\,\sqrt{\kappa^2\,(-4.`\,\beta+\kappa^2)}}$ -4.`

2.718281828459045$^{\gamma}$

Gr β γ3 $\sqrt{\kappa^2-1.`\,\sqrt{\kappa^2\,(-4.`\,\beta+\kappa^2)}}$ +4.`

2.718281828459045$^{\gamma}$

Gr β γ κ2 $\sqrt{\kappa^2-1.`\,\sqrt{\kappa^2\,(-4.`\,\beta+\kappa^2)}}$ -4.`

2.718281828459045$^{\gamma}$

Gr β γ κ2 $\sqrt{\kappa^2-1.`\,\sqrt{\kappa^2\,(-4.`\,\beta+\kappa^2)}}$ -4.`

2.718281828459045$^{\gamma}$

Gr β γ κ2 $\sqrt{\kappa^2-1.`\,\sqrt{\kappa^2\,(-4.`\,\beta+\kappa^2)}}$ +4.`

2.718281828459045^

$$\gamma+2.\grave{}\, y\, \gamma+0.7071067811865475\grave{}\quad y\sqrt{\kappa^2+\sqrt{\kappa^2\,(-4.\grave{}\,\beta+\kappa^2)}}+y\left(-1.\grave{}\,\gamma+0.7071067811865475\grave{}\quad\sqrt{\kappa^2-1.\grave{}\,\sqrt{\kappa^2\,(-4.\grave{}\,\beta+\kappa^2)}}\right)\ \text{Gr}\ \beta\ \gamma\ \text{K2}\ \sqrt{\kappa^2-1.\grave{}\,\sqrt{\kappa^2\,(-4.\grave{}\,\beta+\kappa^2)}}+$$

2.718281828459045^

$$\gamma+1.4142135623730951\grave{}\quad y\sqrt{\kappa^2-1.\grave{}\,\sqrt{\kappa^2\,(-4.\grave{}\,\beta+\kappa^2)}}+0.7071067811865475\grave{}\quad y\sqrt{\kappa^2+\sqrt{\kappa^2\,(-4.\grave{}\,\beta+\kappa^2)}}+y\left(-1.\grave{}\,\gamma-0.7071067811865475\grave{}\quad\sqrt{\kappa^2-1.\grave{}\,\sqrt{\kappa^2\,(-4.\grave{}\,\beta+\kappa^2)}}\right)\ \text{Gr}\ \gamma3\ \text{K2}\ \sqrt{\kappa^2-1.\grave{}\,\sqrt{\kappa^2\,(-4.\grave{}\,\beta+\kappa^2)}}-1.\grave{}$$

2.718281828459045^

$$\gamma+2.\grave{}\, y\, \gamma+1.4142135623730951\grave{}\quad y\sqrt{\kappa^2-1.\grave{}\,\sqrt{\kappa^2\,(-4.\grave{}\,\beta+\kappa^2)}}+0.7071067811865475\grave{}\quad y\sqrt{\kappa^2+\sqrt{\kappa^2\,(-4.\grave{}\,\beta+\kappa^2)}}+y\left(-1.\grave{}\,\gamma-0.7071067811865475\grave{}\quad\sqrt{\kappa^2-1.\grave{}\,\sqrt{\kappa^2\,(-4.\grave{}\,\beta+\kappa^2)}}\right)\ \text{Gr}\ \gamma3\ \text{K2}\ \sqrt{\kappa^2-1.\grave{}\,\sqrt{\kappa^2\,(-4.\grave{}\,\beta+\kappa^2)}}-1.\grave{}$$

2.718281828459045^

$$\gamma+0.7071067811865475\grave{}\quad y\sqrt{\kappa^2+\sqrt{\kappa^2\,(-4.\grave{}\,\beta+\kappa^2)}}+y\left(-1.\grave{}\,\gamma+0.7071067811865475\grave{}\quad\sqrt{\kappa^2-1.\grave{}\,\sqrt{\kappa^2\,(-4.\grave{}\,\beta+\kappa^2)}}\right)\ \text{Gr}\ \gamma3\ \text{K2}\ \sqrt{\kappa^2-1.\grave{}\,\sqrt{\kappa^2\,(-4.\grave{}\,\beta+\kappa^2)}}+$$

2.718281828459045^

$$\gamma+2.\grave{}\, y\, \gamma+0.7071067811865475\grave{}\quad y\sqrt{\kappa^2+\sqrt{\kappa^2\,(-4.\grave{}\,\beta+\kappa^2)}}+y\left(-1.\grave{}\,\gamma+0.7071067811865475\grave{}\quad\sqrt{\kappa^2-1.\grave{}\,\sqrt{\kappa^2\,(-4.\grave{}\,\beta+\kappa^2)}}\right)\ \text{Gr}\ \gamma3\ \text{K2}\ \sqrt{\kappa^2-1.\grave{}\,\sqrt{\kappa^2\,(-4.\grave{}\,\beta+\kappa^2)}}-1.\grave{}$$

2.718281828459045^

$$\gamma+1.4142135623730951\grave{}\quad y\sqrt{\kappa^2-1.\grave{}\,\sqrt{\kappa^2\,(-4.\grave{}\,\beta+\kappa^2)}}+0.7071067811865475\grave{}\quad y\sqrt{\kappa^2+\sqrt{\kappa^2\,(-4.\grave{}\,\beta+\kappa^2)}}+y\left(-1.\grave{}\,\gamma-0.7071067811865475\grave{}\quad\sqrt{\kappa^2-1.\grave{}\,\sqrt{\kappa^2\,(-4.\grave{}\,\beta+\kappa^2)}}\right)\ \text{Gr}\ \gamma\ \text{K4}\ \sqrt{\kappa^2-1.\grave{}\,\sqrt{\kappa^2\,(-4.\grave{}\,\beta+\kappa^2)}}+$$

2.718281828459045^

$$\gamma+2.\grave{}\, y\, \gamma+1.4142135623730951\grave{}\quad y\sqrt{\kappa^2-1.\grave{}\,\sqrt{\kappa^2\,(-4.\grave{}\,\beta+\kappa^2)}}+0.7071067811865475\grave{}\quad y\sqrt{\kappa^2+\sqrt{\kappa^2\,(-4.\grave{}\,\beta+\kappa^2)}}+y\left(-1.\grave{}\,\gamma-0.7071067811865475\grave{}\quad\sqrt{\kappa^2-1.\grave{}\,\sqrt{\kappa^2\,(-4.\grave{}\,\beta+\kappa^2)}}\right)\ \text{Gr}\ \gamma\ \text{K4}\ \sqrt{\kappa^2-1.\grave{}\,\sqrt{\kappa^2\,(-4.\grave{}\,\beta+\kappa^2)}}+$$

2.718281828459045^

$$\gamma+0.7071067811865475\grave{}\quad y\sqrt{\kappa^2+\sqrt{\kappa^2\,(-4.\grave{}\,\beta+\kappa^2)}}+y\left(-1.\grave{}\,\gamma+0.7071067811865475\grave{}\quad\sqrt{\kappa^2-1.\grave{}\,\sqrt{\kappa^2\,(-4.\grave{}\,\beta+\kappa^2)}}\right)\ \text{Gr}\ \gamma\ \text{K4}\ \sqrt{\kappa^2-1.\grave{}\,\sqrt{\kappa^2\,(-4.\grave{}\,\beta+\kappa^2)}}-1.\grave{}$$

2.718281828459045^

$$\gamma+2.\grave{}\, y\, \gamma+0.7071067811865475\grave{}\quad y\sqrt{\kappa^2+\sqrt{\kappa^2\,(-4.\grave{}\,\beta+\kappa^2)}}+y\left(-1.\grave{}\,\gamma+0.7071067811865475\grave{}\quad\sqrt{\kappa^2-1.\grave{}\,\sqrt{\kappa^2\,(-4.\grave{}\,\beta+\kappa^2)}}\right)\ \text{Gr}\ \gamma\ \text{K4}$$

$$\sqrt{\kappa^2 - 1.` \sqrt{\kappa^2 \left(-4.` \beta + \kappa^2\right)}} + 2.`$$

2.718281828459045

$$`\gamma + 1.4142135623730951` \; y \sqrt{\kappa^2 - 1.` \sqrt{\kappa^2 \left(-4.` \beta + \kappa^2\right)}} + 0.7071067811865475` \; y \sqrt{\kappa^2 + \sqrt{\kappa^2 \left(-4.` \beta + \kappa^2\right)}} + y \left(-1.` \gamma - 0.7071067811865475` \; \sqrt{\kappa^2 - 1.` \sqrt{\kappa^2 \left(-4.` \beta + \kappa^2\right)}}\right)$$

$$\text{Gr } \beta \; \gamma \; \sqrt{\kappa^2 \left(-4.` \beta + \kappa^2\right)} \; \sqrt{\kappa^2 - 1.` \sqrt{\kappa^2 \left(-4.` \beta + \kappa^2\right)}} - 2.`$$

2.718281828459045

$$`\gamma + 2.` \; y \gamma + 1.4142135623730951` \; y \sqrt{\kappa^2 - 1.` \sqrt{\kappa^2 \left(-4.` \beta + \kappa^2\right)}} + 0.7071067811865475` \; y \sqrt{\kappa^2 + \sqrt{\kappa^2 \left(-4.` \beta + \kappa^2\right)}} + y \left(-1.` \gamma - 0.7071067811865475` \; \sqrt{\kappa^2 - 1.` \sqrt{\kappa^2 \left(-4.` \beta + \kappa^2\right)}}\right)$$

$$\text{Gr } \beta \; \gamma \; \sqrt{\kappa^2 \left(-4.` \beta + \kappa^2\right)} \; \sqrt{\kappa^2 - 1.` \sqrt{\kappa^2 \left(-4.` \beta + \kappa^2\right)}} - 2.`$$

2.718281828459045

$$`\gamma + 0.7071067811865475` \; y \sqrt{\kappa^2 + \sqrt{\kappa^2 \left(-4.` \beta + \kappa^2\right)}} + y \left(-1.` \gamma + 0.7071067811865475` \; \sqrt{\kappa^2 - 1.` \sqrt{\kappa^2 \left(-4.` \beta + \kappa^2\right)}}\right) \text{Gr } \beta \; \gamma$$

$$\sqrt{\kappa^2 \left(-4.` \beta + \kappa^2\right)} \; \sqrt{\kappa^2 - 1.` \sqrt{\kappa^2 \left(-4.` \beta + \kappa^2\right)}} + 2.`$$

2.718281828459045

$$`\gamma + 2.` \; y \gamma + 0.7071067811865475` \; y \sqrt{\kappa^2 + \sqrt{\kappa^2 \left(-4.` \beta + \kappa^2\right)}} + y \left(-1.` \gamma + 0.7071067811865475` \; \sqrt{\kappa^2 - 1.` \sqrt{\kappa^2 \left(-4.` \beta + \kappa^2\right)}}\right) \text{Gr } \beta \; \gamma$$

$$\sqrt{\kappa^2 \left(-4.` \beta + \kappa^2\right)} \; \sqrt{\kappa^2 - 1.` \sqrt{\kappa^2 \left(-4.` \beta + \kappa^2\right)}} +$$

2.718281828459045

$$`\gamma + 1.4142135623730951` \; y \sqrt{\kappa^2 - 1.` \sqrt{\kappa^2 \left(-4.` \beta + \kappa^2\right)}} + 0.7071067811865475` \; y \sqrt{\kappa^2 + \sqrt{\kappa^2 \left(-4.` \beta + \kappa^2\right)}} + y \left(-1.` \gamma - 0.7071067811865475` \; \sqrt{\kappa^2 - 1.` \sqrt{\kappa^2 \left(-4.` \beta + \kappa^2\right)}}\right)$$

$$\text{Gr } \gamma 3 \; \sqrt{\kappa^2 \left(-4.` \beta + \kappa^2\right)} \; \sqrt{\kappa^2 - 1.` \sqrt{\kappa^2 \left(-4.` \beta + \kappa^2\right)}} - 1.`$$

2.718281828459045

$$`\gamma + 2.` \; y \gamma + 1.4142135623730951` \; y \sqrt{\kappa^2 - 1.` \sqrt{\kappa^2 \left(-4.` \beta + \kappa^2\right)}} + 0.7071067811865475` \; y \sqrt{\kappa^2 + \sqrt{\kappa^2 \left(-4.` \beta + \kappa^2\right)}} + y \left(-1.` \gamma - 0.7071067811865475` \; \sqrt{\kappa^2 - 1.` \sqrt{\kappa^2 \left(-4.` \beta + \kappa^2\right)}}\right)$$

$$\text{Gr } \gamma 3 \; \sqrt{\kappa^2 \left(-4.` \beta + \kappa^2\right)} \; \sqrt{\kappa^2 - 1.` \sqrt{\kappa^2 \left(-4.` \beta + \kappa^2\right)}} - 1.`$$

2.718281828459045

$$`\gamma + 0.7071067811865475` \; y \sqrt{\kappa^2 + \sqrt{\kappa^2 \left(-4.` \beta + \kappa^2\right)}} + y \left(-1.` \gamma + 0.7071067811865475` \; \sqrt{\kappa^2 - 1.` \sqrt{\kappa^2 \left(-4.` \beta + \kappa^2\right)}}\right) \text{Gr } \gamma 3$$

$$\sqrt{\kappa^2 \left(-4.` \beta + \kappa^2\right)} \; \sqrt{\kappa^2 - 1.` \sqrt{\kappa^2 \left(-4.` \beta + \kappa^2\right)}} +$$

2.718281828459045

$$`\gamma + 2.` \; y \gamma + 0.7071067811865475` \; y \sqrt{\kappa^2 + \sqrt{\kappa^2 \left(-4.` \beta + \kappa^2\right)}} + y \left(-1.` \gamma + 0.7071067811865475` \; \sqrt{\kappa^2 - 1.` \sqrt{\kappa^2 \left(-4.` \beta + \kappa^2\right)}}\right) \text{Gr } \gamma 3$$

$$\sqrt{\kappa^2 \left(-4.` \beta + \kappa^2\right)} \; \sqrt{\kappa^2 - 1.` \sqrt{\kappa^2 \left(-4.` \beta + \kappa^2\right)}} - 1.`$$

2.718281828459045⁵

$$\gamma+1.4142135623730951\ y\sqrt{\kappa^2-1.\sqrt{\kappa^2(-4.\beta+\kappa^2)}}+0.7071067811865475\ y\sqrt{\kappa^2+\sqrt{\kappa^2(-4.\beta+\kappa^2)}}+y\left(-1.\gamma-0.7071067811865475\ \sqrt{\kappa^2-1.\sqrt{\kappa^2(-4.\beta+\kappa^2)}}\right)$$

$$\text{Gr}\ \gamma\ \text{K2}\ \sqrt{\kappa^2(-4.\beta+\kappa^2)}\ \sqrt{\kappa^2-1.\sqrt{\kappa^2(-4.\beta+\kappa^2)}}+$$

2.718281828459045⁵

$$2.\gamma+1.4142135623730951\ y\sqrt{\kappa^2-1.\sqrt{\kappa^2(-4.\beta+\kappa^2)}}+0.7071067811865475\ y\sqrt{\kappa^2+\sqrt{\kappa^2(-4.\beta+\kappa^2)}}+y\left(-1.\gamma-0.7071067811865475\ \sqrt{\kappa^2-1.\sqrt{\kappa^2(-4.\beta+\kappa^2)}}\right.$$

$$\text{Gr}\ \gamma\ \text{K2}\ \sqrt{\kappa^2(-4.\beta+\kappa^2)}\ \sqrt{\kappa^2-1.\sqrt{\kappa^2(-4.\beta+\kappa^2)}}+$$

2.718281828459045⁵

$$\gamma+0.7071067811865475\ y\sqrt{\kappa^2+\sqrt{\kappa^2(-4.\beta+\kappa^2)}}+y\left(-1.\gamma+0.7071067811865475\ \sqrt{\kappa^2-1.\sqrt{\kappa^2(-4.\beta+\kappa^2)}}\right)\ \text{Gr}\ \gamma\ \text{K2}$$

$$\sqrt{\kappa^2(-4.\beta+\kappa^2)}\ \sqrt{\kappa^2-1.\sqrt{\kappa^2(-4.\beta+\kappa^2)}}-1.$$

2.718281828459045⁵

$$2.\gamma+0.7071067811865475\ y\sqrt{\kappa^2+\sqrt{\kappa^2(-4.\beta+\kappa^2)}}+y\left(-1.\gamma+0.7071067811865475\ \sqrt{\kappa^2-1.\sqrt{\kappa^2(-4.\beta+\kappa^2)}}\right)\ \text{Gr}\ \gamma\ \text{K2}$$

$$\sqrt{\kappa^2(-4.\beta+\kappa^2)}\ \sqrt{\kappa^2-1.\sqrt{\kappa^2(-4.\beta+\kappa^2)}}-4.$$

2.718281828459045⁵

$$\gamma+0.7071067811865475\ y\sqrt{\kappa^2-1.\sqrt{\kappa^2(-4.\beta+\kappa^2)}}+1.4142135623730951\ y\sqrt{\kappa^2+\sqrt{\kappa^2(-4.\beta+\kappa^2)}}+y\left(-1.\gamma-0.7071067811865475\ \sqrt{\kappa^2+\sqrt{\kappa^2(-4.\beta+\kappa^2)}}\right)$$

$$\text{Gr}\ \beta\ \gamma3\ \sqrt{\kappa^2+\sqrt{\kappa^2(-4.\beta+\kappa^2)}}+4.$$

2.718281828459045⁵

$$2.\gamma+0.7071067811865475\ y\sqrt{\kappa^2-1.\sqrt{\kappa^2(-4.\beta+\kappa^2)}}+1.4142135623730951\ y\sqrt{\kappa^2+\sqrt{\kappa^2(-4.\beta+\kappa^2)}}+y\left(-1.\gamma-0.7071067811865475\ \sqrt{\kappa^2+\sqrt{\kappa^2(-4.\beta+\kappa^2)}}\right.$$

$$\text{Gr}\ \beta\ \gamma3\ \sqrt{\kappa^2+\sqrt{\kappa^2(-4.\beta+\kappa^2)}}+4.$$

2.718281828459045⁵

$$\gamma+0.7071067811865475\ y\sqrt{\kappa^2-1.\sqrt{\kappa^2(-4.\beta+\kappa^2)}}+y\left(-1.\gamma+0.7071067811865475\ \sqrt{\kappa^2+\sqrt{\kappa^2(-4.\beta+\kappa^2)}}\right)\ \text{Gr}\ \beta\ \gamma3$$

$$\sqrt{\kappa^2+\sqrt{\kappa^2(-4.\beta+\kappa^2)}}-4.$$

2.718281828459045⁵

$$2.\gamma+0.7071067811865475\ y\sqrt{\kappa^2-1.\sqrt{\kappa^2(-4.\beta+\kappa^2)}}+y\left(-1.\gamma+0.7071067811865475\ \sqrt{\kappa^2+\sqrt{\kappa^2(-4.\beta+\kappa^2)}}\right)\ \text{Gr}\ \beta\ \gamma3$$

$$\sqrt{\kappa^2+\sqrt{\kappa^2(-4.\beta+\kappa^2)}}+4.$$

2.718281828459045⁵

$$\gamma+0.7071067811865475\ y\sqrt{\kappa^2-1.\sqrt{\kappa^2(-4.\beta+\kappa^2)}}+1.4142135623730951\ y\sqrt{\kappa^2+\sqrt{\kappa^2(-4.\beta+\kappa^2)}}+y\left(-1.\gamma-0.7071067811865475\ \sqrt{\kappa^2+\sqrt{\kappa^2(-4.\beta+\kappa^2)}}\right)$$

$$\mathrm{Gr}\ \beta\ \gamma\ \kappa 2\ \sqrt{\kappa^2+\sqrt{\kappa^2\left(-4.`\beta+\kappa^2\right)}}\ -4.`$$

2.718281828459045$\wedge$

$$`\gamma+2.`\ y\ \gamma+0.7071067811865475`\ \ y\sqrt{\kappa^2-1.`\sqrt{\kappa^2\left(-4.`\beta+\kappa^2\right)}}+1.4142135623730951`\ \ y\sqrt{\kappa^2+\sqrt{\kappa^2\left(-4.`\beta+\kappa^2\right)}}+y\left(-1.`\gamma-0.7071067811865475`\ \sqrt{\kappa^2+\sqrt{\kappa^2\left(-4.`\beta+\kappa^2\right.}}\right.$$

$$\mathrm{Gr}\ \beta\ \gamma\ \kappa 2\ \sqrt{\kappa^2+\sqrt{\kappa^2\left(-4.`\beta+\kappa^2\right)}}\ -4.`$$

2.718281828459045$\wedge$

$$`\gamma+0.7071067811865475`\ \ y\sqrt{\kappa^2-1.`\sqrt{\kappa^2\left(-4.`\beta+\kappa^2\right)}}+y\left(-1.`\gamma+0.7071067811865475`\ \sqrt{\kappa^2+\sqrt{\kappa^2\left(-4.`\beta+\kappa^2\right)}}\right)\ \mathrm{Gr}\ \beta\ \gamma\ \kappa 2$$

$$\sqrt{\kappa^2+\sqrt{\kappa^2\left(-4.`\beta+\kappa^2\right)}}\ +4.`$$

2.718281828459045$\wedge$

$$`\gamma+2.`\ y\ \gamma+0.7071067811865475`\ \ y\sqrt{\kappa^2-1.`\sqrt{\kappa^2\left(-4.`\beta+\kappa^2\right)}}+y\left(-1.`\gamma+0.7071067811865475`\ \sqrt{\kappa^2+\sqrt{\kappa^2\left(-4.`\beta+\kappa^2\right)}}\right)\ \mathrm{Gr}\ \beta\ \gamma\ \kappa 2$$

$$\sqrt{\kappa^2+\sqrt{\kappa^2\left(-4.`\beta+\kappa^2\right)}}\ +$$

2.718281828459045$\wedge$

$$`\gamma+0.7071067811865475`\ \ y\sqrt{\kappa^2-1.`\sqrt{\kappa^2\left(-4.`\beta+\kappa^2\right)}}+1.4142135623730951`\ \ y\sqrt{\kappa^2+\sqrt{\kappa^2\left(-4.`\beta+\kappa^2\right)}}+y\left(-1.`\gamma-0.7071067811865475`\ \sqrt{\kappa^2+\sqrt{\kappa^2\left(-4.`\beta+\kappa^2\right.}}\right.$$

$$\mathrm{Gr}\ \gamma 3\ \kappa 2\ \sqrt{\kappa^2+\sqrt{\kappa^2\left(-4.`\beta+\kappa^2\right)}}\ -1.`$$

2.718281828459045$\wedge$

$$`\gamma+2.`\ y\ \gamma+0.7071067811865475`\ \ y\sqrt{\kappa^2-1.`\sqrt{\kappa^2\left(-4.`\beta+\kappa^2\right)}}+1.4142135623730951`\ \ y\sqrt{\kappa^2+\sqrt{\kappa^2\left(-4.`\beta+\kappa^2\right)}}+y\left(-1.`\gamma-0.7071067811865475`\ \sqrt{\kappa^2+\sqrt{\kappa^2\left(-4.`\beta+\kappa^2\right.}}\right.$$

$$\mathrm{Gr}\ \gamma 3\ \kappa 2\ \sqrt{\kappa^2+\sqrt{\kappa^2\left(-4.`\beta+\kappa^2\right)}}\ -1.`$$

2.718281828459045$\wedge$

$$`\gamma+0.7071067811865475`\ \ y\sqrt{\kappa^2-1.`\sqrt{\kappa^2\left(-4.`\beta+\kappa^2\right)}}+y\left(-1.`\gamma+0.7071067811865475`\ \sqrt{\kappa^2+\sqrt{\kappa^2\left(-4.`\beta+\kappa^2\right)}}\right)\ \mathrm{Gr}\ \gamma 3\ \kappa 2$$

$$\sqrt{\kappa^2+\sqrt{\kappa^2\left(-4.`\beta+\kappa^2\right)}}\ +$$

2.718281828459045$\wedge$

$$`\gamma+2.`\ y\ \gamma+0.7071067811865475`\ \ y\sqrt{\kappa^2-1.`\sqrt{\kappa^2\left(-4.`\beta+\kappa^2\right)}}+y\left(-1.`\gamma+0.7071067811865475`\ \sqrt{\kappa^2+\sqrt{\kappa^2\left(-4.`\beta+\kappa^2\right)}}\right)\ \mathrm{Gr}\ \gamma 3\ \kappa 2$$

$$\sqrt{\kappa^2+\sqrt{\kappa^2\left(-4.`\beta+\kappa^2\right)}}\ -1.`$$

2.718281828459045$\wedge$

$$`\gamma+0.7071067811865475`\ \ y\sqrt{\kappa^2-1.`\sqrt{\kappa^2\left(-4.`\beta+\kappa^2\right)}}+1.4142135623730951`\ \ y\sqrt{\kappa^2+\sqrt{\kappa^2\left(-4.`\beta+\kappa^2\right)}}+y\left(-1.`\gamma-0.7071067811865475`\ \sqrt{\kappa^2+\sqrt{\kappa^2\left(-4.`\beta+\kappa^2\right)}}\right)$$

$$\mathrm{Gr}\ \gamma\ \kappa 4\ \sqrt{\kappa^2+\sqrt{\kappa^2\left(-4.`\beta+\kappa^2\right)}}\ +$$

2.718281828459045`

`γ+2.` y γ+0.7071067811865475` y $\sqrt{\kappa^2-1.` \sqrt{\kappa^2 (-4.` \beta+\kappa^2)}}$ +1.4142135623730951` y $\sqrt{\kappa^2+\sqrt{\kappa^2 (-4.` \beta+\kappa^2)}}$ +y $\left(-1.` \gamma-0.7071067811865475` \sqrt{\kappa^2+\sqrt{\kappa^2 (-4.` \beta+\kappa^2}}\right.$

Gr γ K4 $\sqrt{\kappa^2+\sqrt{\kappa^2 (-4.` \beta+\kappa^2)}}$ +

2.718281828459045`

`γ+0.7071067811865475` y $\sqrt{\kappa^2-1.` \sqrt{\kappa^2 (-4.` \beta+\kappa^2)}}$ +y $\left(-1.` \gamma+0.7071067811865475` \sqrt{\kappa^2+\sqrt{\kappa^2 (-4.` \beta+\kappa^2)}}\right)$ Gr γ K4

$\sqrt{\kappa^2+\sqrt{\kappa^2 (-4.` \beta+\kappa^2)}}$ -1.`

2.718281828459045`

`γ+2.` y γ+0.7071067811865475` y $\sqrt{\kappa^2-1.` \sqrt{\kappa^2 (-4.` \beta+\kappa^2)}}$ +y $\left(-1.` \gamma+0.7071067811865475` \sqrt{\kappa^2+\sqrt{\kappa^2 (-4.` \beta+\kappa^2)}}\right)$ Gr γ K4

$\sqrt{\kappa^2+\sqrt{\kappa^2 (-4.` \beta+\kappa^2)}}$ -2.`

2.718281828459045`

`γ+0.7071067811865475` y $\sqrt{\kappa^2-1.` \sqrt{\kappa^2 (-4.` \beta+\kappa^2)}}$ +1.4142135623730951` y $\sqrt{\kappa^2+\sqrt{\kappa^2 (-4.` \beta+\kappa^2)}}$ +y $\left(-1.` \gamma-0.7071067811865475` \sqrt{\kappa^2+\sqrt{\kappa^2 (-4.` \beta+\kappa^2)}}\right)$

Gr β γ $\sqrt{\kappa^2 (-4.` \beta+\kappa^2)}$ $\sqrt{\kappa^2+\sqrt{\kappa^2 (-4.` \beta+\kappa^2)}}$ +2.`

2.718281828459045`

`γ+2.` y γ+0.7071067811865475` y $\sqrt{\kappa^2-1.` \sqrt{\kappa^2 (-4.` \beta+\kappa^2)}}$ +1.4142135623730951` y $\sqrt{\kappa^2+\sqrt{\kappa^2 (-4.` \beta+\kappa^2)}}$ +y $\left(-1.` \gamma-0.7071067811865475` \sqrt{\kappa^2+\sqrt{\kappa^2 (-4.` \beta+\kappa^2}}\right.$

Gr β γ $\sqrt{\kappa^2 (-4.` \beta+\kappa^2)}$ $\sqrt{\kappa^2+\sqrt{\kappa^2 (-4.` \beta+\kappa^2)}}$ +2.`

2.718281828459045`

`γ+0.7071067811865475` y $\sqrt{\kappa^2-1.` \sqrt{\kappa^2 (-4.` \beta+\kappa^2)}}$ +y $\left(-1.` \gamma+0.7071067811865475` \sqrt{\kappa^2+\sqrt{\kappa^2 (-4.` \beta+\kappa^2)}}\right)$ Gr β γ

$\sqrt{\kappa^2 (-4.` \beta+\kappa^2)}$ $\sqrt{\kappa^2+\sqrt{\kappa^2 (-4.` \beta+\kappa^2)}}$ -2.`

2.718281828459045`

`γ+2.` y γ+0.7071067811865475` y $\sqrt{\kappa^2-1.` \sqrt{\kappa^2 (-4.` \beta+\kappa^2)}}$ +y $\left(-1.` \gamma+0.7071067811865475` \sqrt{\kappa^2+\sqrt{\kappa^2 (-4.` \beta+\kappa^2)}}\right)$ Gr β γ

$\sqrt{\kappa^2 (-4.` \beta+\kappa^2)}$ $\sqrt{\kappa^2+\sqrt{\kappa^2 (-4.` \beta+\kappa^2)}}$ -1.`

2.718281828459045`

`γ+0.7071067811865475` y $\sqrt{\kappa^2-1.` \sqrt{\kappa^2 (-4.` \beta+\kappa^2)}}$ +1.4142135623730951` y $\sqrt{\kappa^2+\sqrt{\kappa^2 (-4.` \beta+\kappa^2)}}$ +y $\left(-1.` \gamma-0.7071067811865475` \sqrt{\kappa^2+\sqrt{\kappa^2 (-4.` \beta+\kappa^2)}}\right)$

Gr γ3 $\sqrt{\kappa^2 (-4.` \beta+\kappa^2)}$ $\sqrt{\kappa^2+\sqrt{\kappa^2 (-4.` \beta+\kappa^2)}}$ +

2.718281828459045`

`γ+2.` y γ+0.7071067811865475` y $\sqrt{\kappa^2-1.` \sqrt{\kappa^2 (-4.` \beta+\kappa^2)}}$ +1.4142135623730951` y $\sqrt{\kappa^2+\sqrt{\kappa^2 (-4.` \beta+\kappa^2)}}$ +y $\left(-1.` \gamma-0.7071067811865475` \sqrt{\kappa^2+\sqrt{\kappa^2 (-4.` \beta+\kappa^2}}\right.$

Gr γ3 $\sqrt{\kappa^2 \left(-4.` \beta + \kappa^2\right)}$ $\sqrt{\kappa^2 + \sqrt{\kappa^2 \left(-4.` \beta + \kappa^2\right)}}$ +

2.718281828459045$^{\gamma + 0.7071067811865475` \, y \sqrt{\kappa^2 - 1.` \sqrt{\kappa^2 \left(-4.` \beta + \kappa^2\right)}} + y \left(-1.` \gamma + 0.7071067811865475` \, \sqrt{\kappa^2 + \sqrt{\kappa^2 \left(-4.` \beta + \kappa^2\right)}}\right)}$ Gr γ3

$\sqrt{\kappa^2 \left(-4.` \beta + \kappa^2\right)}$ $\sqrt{\kappa^2 + \sqrt{\kappa^2 \left(-4.` \beta + \kappa^2\right)}}$ -1.`

2.718281828459045$^{\gamma + 2.` \, y \, \gamma + 0.7071067811865475` \, y \sqrt{\kappa^2 - 1.` \sqrt{\kappa^2 \left(-4.` \beta + \kappa^2\right)}} + y \left(-1.` \gamma + 0.7071067811865475` \, \sqrt{\kappa^2 + \sqrt{\kappa^2 \left(-4.` \beta + \kappa^2\right)}}\right)}$ Gr γ3

$\sqrt{\kappa^2 \left(-4.` \beta + \kappa^2\right)}$ $\sqrt{\kappa^2 + \sqrt{\kappa^2 \left(-4.` \beta + \kappa^2\right)}}$ +

2.718281828459045$^{\gamma + 0.7071067811865475` \, y \sqrt{\kappa^2 - 1.` \sqrt{\kappa^2 \left(-4.` \beta + \kappa^2\right)}} + 1.4142135623730951` \, y \sqrt{\kappa^2 + \sqrt{\kappa^2 \left(-4.` \beta + \kappa^2\right)}} + y \left(-1.` \gamma - 0.7071067811865475` \, \sqrt{\kappa^2 + \sqrt{\kappa^2 \left(-4.` \beta + \kappa^2\right)}}\right)}$

Gr γ κ2 $\sqrt{\kappa^2 \left(-4.` \beta + \kappa^2\right)}$ $\sqrt{\kappa^2 + \sqrt{\kappa^2 \left(-4.` \beta + \kappa^2\right)}}$ -1.`

2.718281828459045$^{\gamma + 2.` \, y \, \gamma + 0.7071067811865475` \, y \sqrt{\kappa^2 - 1.` \sqrt{\kappa^2 \left(-4.` \beta + \kappa^2\right)}} + 1.4142135623730951` \, y \sqrt{\kappa^2 + \sqrt{\kappa^2 \left(-4.` \beta + \kappa^2\right)}} + y \left(-1.` \gamma - 0.7071067811865475` \, \sqrt{\kappa^2 + \sqrt{\kappa^2 \left(-4.` \beta + \kappa^2\right)}}\right)}$

Gr γ κ2 $\sqrt{\kappa^2 \left(-4.` \beta + \kappa^2\right)}$ $\sqrt{\kappa^2 + \sqrt{\kappa^2 \left(-4.` \beta + \kappa^2\right)}}$ -1.`

2.718281828459045$^{\gamma + 0.7071067811865475` \, y \sqrt{\kappa^2 - 1.` \sqrt{\kappa^2 \left(-4.` \beta + \kappa^2\right)}} + y \left(-1.` \gamma + 0.7071067811865475` \, \sqrt{\kappa^2 + \sqrt{\kappa^2 \left(-4.` \beta + \kappa^2\right)}}\right)}$ Gr γ κ2

$\sqrt{\kappa^2 \left(-4.` \beta + \kappa^2\right)}$ $\sqrt{\kappa^2 + \sqrt{\kappa^2 \left(-4.` \beta + \kappa^2\right)}}$ +

2.718281828459045$^{\gamma + 2.` \, y \, \gamma + 0.7071067811865475` \, y \sqrt{\kappa^2 - 1.` \sqrt{\kappa^2 \left(-4.` \beta + \kappa^2\right)}} + y \left(-1.` \gamma + 0.7071067811865475` \, \sqrt{\kappa^2 + \sqrt{\kappa^2 \left(-4.` \beta + \kappa^2\right)}}\right)}$ Gr γ κ2

$\sqrt{\kappa^2 \left(-4.` \beta + \kappa^2\right)}$ $\sqrt{\kappa^2 + \sqrt{\kappa^2 \left(-4.` \beta + \kappa^2\right)}}$ -4.` 1.4142135623730951`

2.718281828459045$^{y \, \gamma + 1.4142135623730951` \, y \sqrt{\kappa^2 - 1.` \sqrt{\kappa^2 \left(-4.` \beta + \kappa^2\right)}} + 0.7071067811865475` \, y \sqrt{\kappa^2 + \sqrt{\kappa^2 \left(-4.` \beta + \kappa^2\right)}} + y \left(-1.` \gamma - 0.7071067811865475` \, \sqrt{\kappa^2 - 1.` \sqrt{\kappa^2 \left(-4.` \beta + \kappa^2\right)}}\right.$

R β γ4 λ-4.` 1.4142135623730951`

2.718281828459045$^{2.` \, \gamma + y \, \gamma + 1.4142135623730951` \, y \sqrt{\kappa^2 - 1.` \sqrt{\kappa^2 \left(-4.` \beta + \kappa^2\right)}} + 0.7071067811865475` \, y \sqrt{\kappa^2 + \sqrt{\kappa^2 \left(-4.` \beta + \kappa^2\right)}} + y \left(-1.` \gamma - 0.7071067811865475` \, \sqrt{\kappa^2 - 1.` \sqrt{\kappa^2 \left(-4.` \right.\right.}}$

R β γ4 λ-4.` 1.4142135623730951`

2.718281828459045`

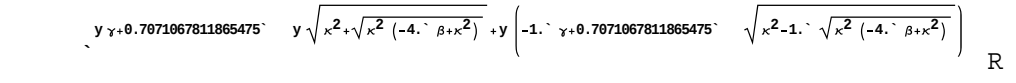

R β γ4 λ-4.` 1.4142135623730951`

2.718281828459045`

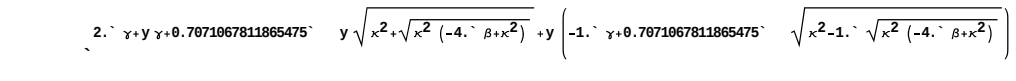

R β γ4 λ-4.` 1.4142135623730951`

2.718281828459045`

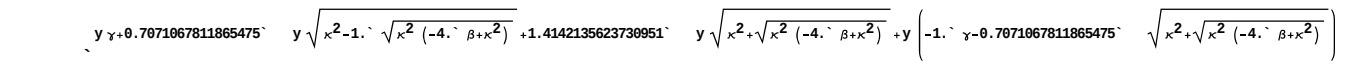

R β γ4 λ-4.` 1.4142135623730951`

2.718281828459045`

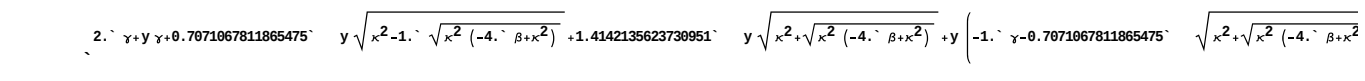

R β γ4 λ-4.` 1.4142135623730951`

2.718281828459045`

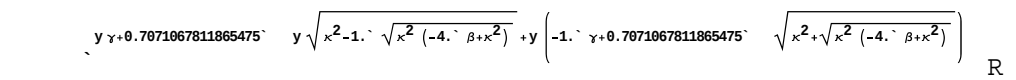

R β γ4 λ-4.` 1.4142135623730951`

2.718281828459045`

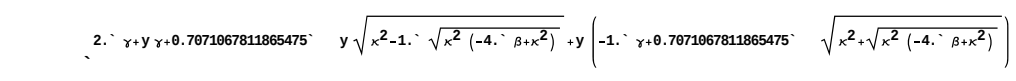

R β2 κ2 λ-4.` 1.4142135623730951`

2.718281828459045`

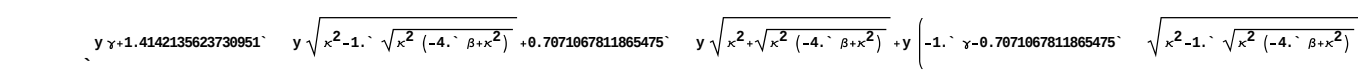

R β2 κ2 λ-4.` 1.4142135623730951`

2.718281828459045`

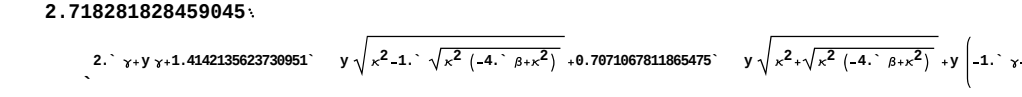

R β2 κ2 λ-4.` 1.4142135623730951`

2.718281828459045`

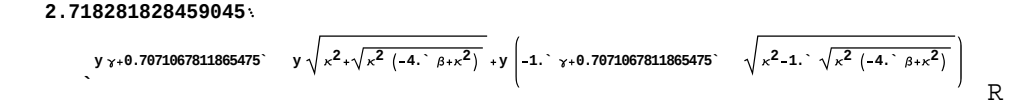

R β2 κ2 λ-4.` 1.4142135623730951`

2.718281828459045`

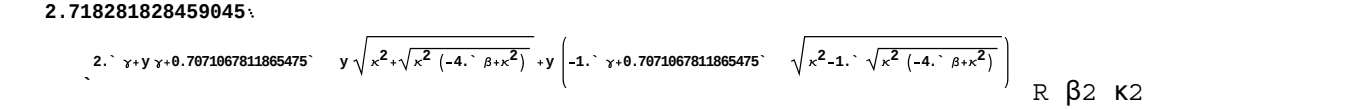

R β2 κ2 λ-4.` 1.4142135623730951`

2.718281828459045`

$2.` \gamma+y\,\gamma+0.7071067811865475` \; y\sqrt{\kappa^{2}-1.` \sqrt{\kappa^{2}\,(-4.` \beta+\kappa^{2})}}+1.4142135623730951` \; y\sqrt{\kappa^{2}+\sqrt{\kappa^{2}\,(-4.` \beta+\kappa^{2})}}+y\left(-1.` \gamma-0.7071067811865475` \; \sqrt{\kappa^{2}+\sqrt{\kappa^{2}\,(-4.` \beta+\kappa^{2}}}\right.$ `

R β2 κ2 λ-4.` 1.4142135623730951`

2.718281828459045`

$y\,\gamma+0.7071067811865475` \; y\sqrt{\kappa^{2}-1.` \sqrt{\kappa^{2}\,(-4.` \beta+\kappa^{2})}}+y\left(-1.` \gamma+0.7071067811865475` \; \sqrt{\kappa^{2}+\sqrt{\kappa^{2}\,(-4.` \beta+\kappa^{2})}}\right)$ ` R β2 κ2 λ-

4.` 1.4142135623730951`

2.718281828459045`

$2.` \gamma+y\,\gamma+0.7071067811865475` \; y\sqrt{\kappa^{2}-1.` \sqrt{\kappa^{2}\,(-4.` \beta+\kappa^{2})}}+y\left(-1.` \gamma+0.7071067811865475` \; \sqrt{\kappa^{2}+\sqrt{\kappa^{2}\,(-4.` \beta+\kappa^{2})}}\right)$ ` R β2 κ2

λ+4.` 1.4142135623730951`

2.718281828459045`

$y\,\gamma+1.4142135623730951` \; y\sqrt{\kappa^{2}-1.` \sqrt{\kappa^{2}\,(-4.` \beta+\kappa^{2})}}+0.7071067811865475` \; y\sqrt{\kappa^{2}+\sqrt{\kappa^{2}\,(-4.` \beta+\kappa^{2})}}+y\left(-1.` \gamma-0.7071067811865475` \; \sqrt{\kappa^{2}-1.` \sqrt{\kappa^{2}\,(-4.` \beta+\kappa^{2})}}\right.$ `

R β γ2 κ2 λ+4.` 1.4142135623730951`

2.718281828459045`

$2.` \gamma+y\,\gamma+1.4142135623730951` \; y\sqrt{\kappa^{2}-1.` \sqrt{\kappa^{2}\,(-4.` \beta+\kappa^{2})}}+0.7071067811865475` \; y\sqrt{\kappa^{2}+\sqrt{\kappa^{2}\,(-4.` \beta+\kappa^{2})}}+y\left(-1.` \gamma-0.7071067811865475` \; \sqrt{\kappa^{2}-1.` \sqrt{\kappa^{2}\,(-4.`}}\right.$ `

R β γ2 κ2 λ+4.` 1.4142135623730951`

2.718281828459045`

$y\,\gamma+0.7071067811865475` \; y\sqrt{\kappa^{2}+\sqrt{\kappa^{2}\,(-4.` \beta+\kappa^{2})}}+y\left(-1.` \gamma+0.7071067811865475` \; \sqrt{\kappa^{2}-1.` \sqrt{\kappa^{2}\,(-4.` \beta+\kappa^{2})}}\right)$ ` R β γ2 κ2

λ+4.` 1.4142135623730951`

2.718281828459045`

$2.` \gamma+y\,\gamma+0.7071067811865475` \; y\sqrt{\kappa^{2}+\sqrt{\kappa^{2}\,(-4.` \beta+\kappa^{2})}}+y\left(-1.` \gamma+0.7071067811865475` \; \sqrt{\kappa^{2}-1.` \sqrt{\kappa^{2}\,(-4.` \beta+\kappa^{2})}}\right)$ ` R β γ2 κ2

λ+4.` 1.4142135623730951`

2.718281828459045`

$y\,\gamma+0.7071067811865475` \; y\sqrt{\kappa^{2}-1.` \sqrt{\kappa^{2}\,(-4.` \beta+\kappa^{2})}}+1.4142135623730951` \; y\sqrt{\kappa^{2}+\sqrt{\kappa^{2}\,(-4.` \beta+\kappa^{2})}}+y\left(-1.` \gamma-0.7071067811865475` \; \sqrt{\kappa^{2}+\sqrt{\kappa^{2}\,(-4.` \beta+\kappa^{2})}}\right)$ `

R β γ2 κ2 λ+4.` 1.4142135623730951`

2.718281828459045`

$2.` \gamma+y\,\gamma+0.7071067811865475` \; y\sqrt{\kappa^{2}-1.` \sqrt{\kappa^{2}\,(-4.` \beta+\kappa^{2})}}+1.4142135623730951` \; y\sqrt{\kappa^{2}+\sqrt{\kappa^{2}\,(-4.` \beta+\kappa^{2})}}+y\left(-1.` \gamma-0.7071067811865475` \; \sqrt{\kappa^{2}+\sqrt{\kappa^{2}\,(-4.` \beta+\kappa^{2}}}\right.$ `

R β γ2 κ2 λ+4.` 1.4142135623730951`

2.718281828459045`

$y\,\gamma+0.7071067811865475` \; y\sqrt{\kappa^{2}-1.` \sqrt{\kappa^{2}\,(-4.` \beta+\kappa^{2})}}+y\left(-1.` \gamma+0.7071067811865475` \; \sqrt{\kappa^{2}+\sqrt{\kappa^{2}\,(-4.` \beta+\kappa^{2})}}\right)$ ` R β γ2 κ2

λ+4.` 1.4142135623730951`

2.718281828459045`

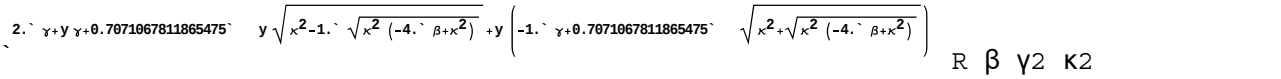

R β γ2 κ2 λ+1.4142135623730951`

2.718281828459045`

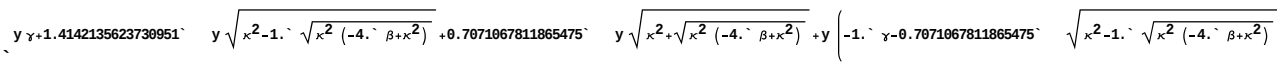

R γ4 κ2 λ+1.4142135623730951`

2.718281828459045`

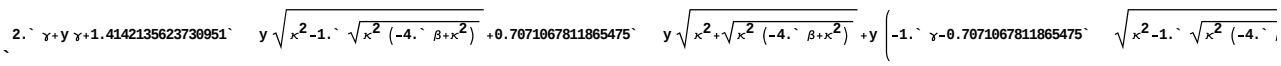

R γ4 κ2 λ+1.4142135623730951`

2.718281828459045`

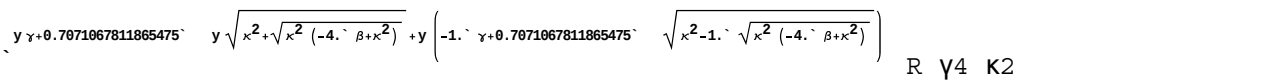

R γ4 κ2 λ+1.4142135623730951`

2.718281828459045`

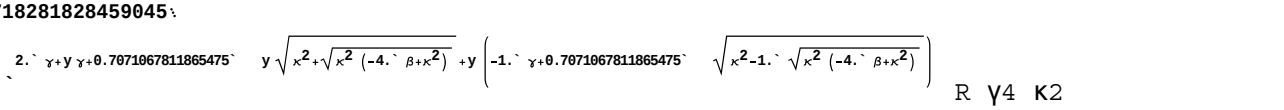

R γ4 κ2 λ+1.4142135623730951`

2.718281828459045`

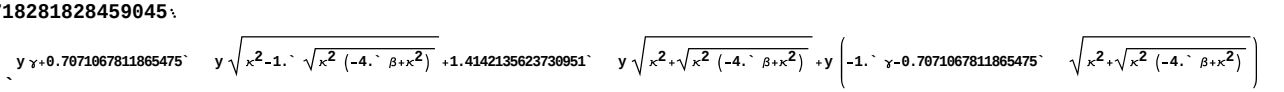

R γ4 κ2 λ+1.4142135623730951`

2.718281828459045`

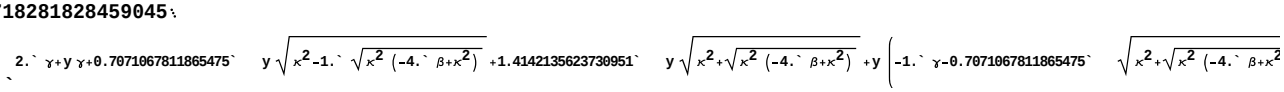

R β κ4 λ+1.4142135623730951`

2.718281828459045`

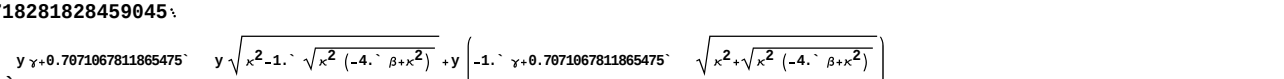

R β κ4 λ+1.4142135623730951`

2.718281828459045`

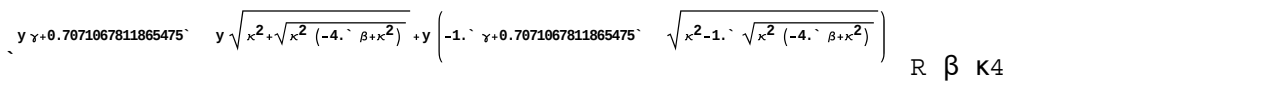

R β κ4 λ+1.4142135623730951`

2.718281828459045`

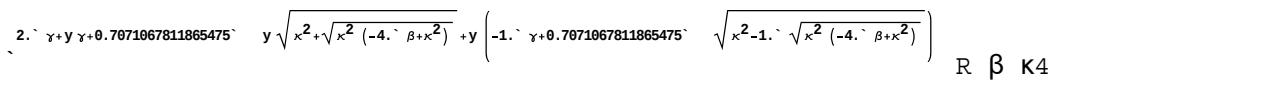

R β κ4 λ+1.4142135623730951`

2.718281828459045`

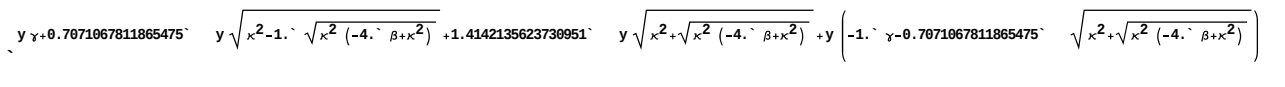

R β κ4 λ+1.4142135623730951`

2.718281828459045`

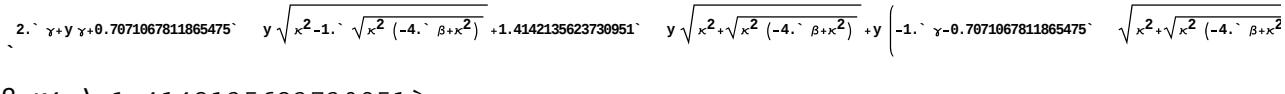

R β κ4 λ+1.4142135623730951`

2.718281828459045`

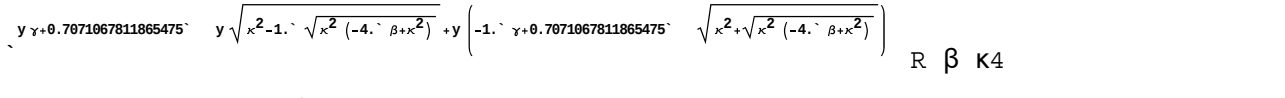

R β κ4 λ+1.4142135623730951`

2.718281828459045`

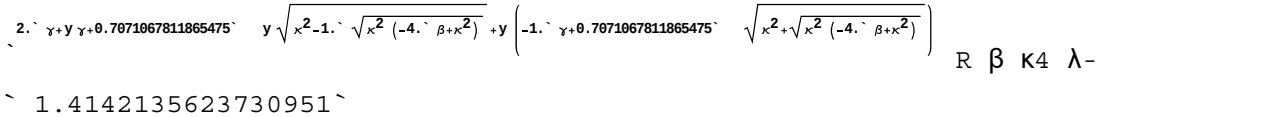

R β κ4 λ-1.` 1.4142135623730951`

2.718281828459045`

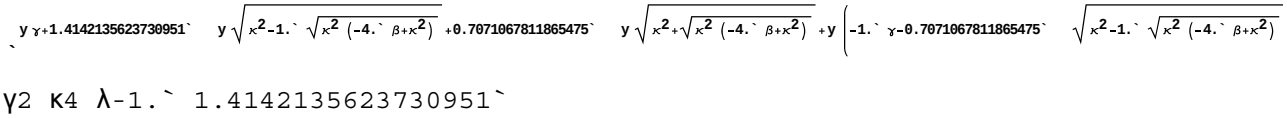

R γ2 κ4 λ-1.` 1.4142135623730951`

2.718281828459045`

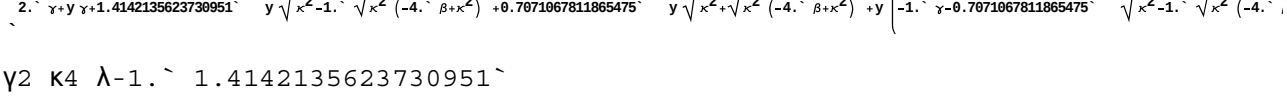

R γ2 κ4 λ-1.` 1.4142135623730951`

2.718281828459045`

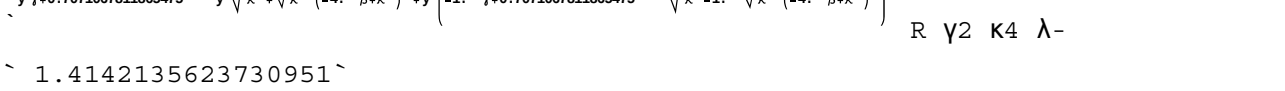

R γ2 κ4 λ-1.` 1.4142135623730951`

2.718281828459045:

```
y γ+0.7071067811865475` y √(κ^2-1.` √(κ^2 (-4.` β+κ^2))) +1.4142135623730951` y √(κ^2+√(κ^2 (-4.` β+κ^2))) +y (-1.` γ-0.7071067811865475` √(κ^2+√(κ^2 (-4.` β+κ^2))))
```

R γ2 κ4 λ-1.` 1.4142135623730951`

2.718281828459045:

```
2.` γ+y γ+0.7071067811865475` y √(κ^2-1.` √(κ^2 (-4.` β+κ^2))) +1.4142135623730951` y √(κ^2+√(κ^2 (-4.` β+κ^2))) +y (-1.` γ-0.7071067811865475` √(κ^2+√(κ^2 (-4.` β+κ^2
```

R γ2 κ4 λ-1.` 1.4142135623730951`

2.718281828459045:

```
y γ+0.7071067811865475` y √(κ^2-1.` √(κ^2 (-4.` β+κ^2))) +y (-1.` γ+0.7071067811865475` √(κ^2+√(κ^2 (-4.` β+κ^2))))
```

R γ2 κ4 λ-1.` 1.4142135623730951`

2.718281828459045:

```
2.` γ+y γ+0.7071067811865475` y √(κ^2-1.` √(κ^2 (-4.` β+κ^2))) +y (-1.` γ+0.7071067811865475` √(κ^2+√(κ^2 (-4.` β+κ^2))))
```

R γ2 κ4 λ+1.4142135623730951`

2.718281828459045:

```
y γ+1.4142135623730951` y √(κ^2-1.` √(κ^2 (-4.` β+κ^2))) +0.7071067811865475` y √(κ^2+√(κ^2 (-4.` β+κ^2))) +y (-1.` γ-0.7071067811865475` √(κ^2-1.` √(κ^2 (-4.` β+κ^2)
```

R γ4 √(κ^2 (-4.` β+κ^2)) λ+1.4142135623730951`

2.718281828459045:

```
2.` γ+y γ+1.4142135623730951` y √(κ^2-1.` √(κ^2 (-4.` β+κ^2))) +0.7071067811865475` y √(κ^2+√(κ^2 (-4.` β+κ^2))) +y (-1.` γ-0.7071067811865475` √(κ^2-1.` √(κ^2 (-4.`
```

R γ4 √(κ^2 (-4.` β+κ^2)) λ+1.4142135623730951`

2.718281828459045:

```
y γ+0.7071067811865475` y √(κ^2+√(κ^2 (-4.` β+κ^2))) +y (-1.` γ+0.7071067811865475` √(κ^2-1.` √(κ^2 (-4.` β+κ^2))))
```

R γ4 √(κ^2 (-4.` β+κ^2)) λ+1.4142135623730951`

2.718281828459045:

```
2.` γ+y γ+0.7071067811865475` y √(κ^2+√(κ^2 (-4.` β+κ^2))) +y (-1.` γ+0.7071067811865475` √(κ^2-1.` √(κ^2 (-4.` β+κ^2))))
```

R γ4 √(κ^2 (-4.` β+κ^2)) λ-1.` 1.4142135623730951`

2.718281828459045:

```
y γ+0.7071067811865475` y √(κ^2-1.` √(κ^2 (-4.` β+κ^2))) +1.4142135623730951` y √(κ^2+√(κ^2 (-4.` β+κ^2))) +y (-1.` γ-0.7071067811865475` √(κ^2+√(κ^2 (-4.` β+κ^2))))
```

R γ4 √(κ^2 (-4.` β+κ^2)) λ-1.` 1.4142135623730951`

2.718281828459045:

```
2.` γ+y γ+0.7071067811865475` y √(κ^2-1.` √(κ^2 (-4.` β+κ^2))) +1.4142135623730951` y √(κ^2+√(κ^2 (-4.` β+κ^2))) +y (-1.` γ-0.7071067811865475` √(κ^2+√(κ^2 (-4.` β+κ^2
```

R γ4 √(κ^2 (-4.` β+κ^2)) λ-1.` 1.4142135623730951`

2.718281828459045`

$$\gamma + 0.7071067811865475 \quad \gamma \sqrt{\kappa^2 - 1.} \sqrt{\kappa^2 (-4. \beta + \kappa^2)} + \gamma \left(-1. \gamma + 0.7071067811865475 \sqrt{\kappa^2 + \sqrt{\kappa^2 (-4. \beta + \kappa^2)}} \right) R\ \gamma 4$$

$$\sqrt{\kappa^2 (-4. \beta + \kappa^2)}\ \lambda - 1.\ 1.4142135623730951$$

2.718281828459045`

$$2. \gamma + \gamma \gamma + 0.7071067811865475 \quad \gamma \sqrt{\kappa^2 - 1.} \sqrt{\kappa^2 (-4. \beta + \kappa^2)} + \gamma \left(-1. \gamma + 0.7071067811865475 \sqrt{\kappa^2 + \sqrt{\kappa^2 (-4. \beta + \kappa^2)}} \right) R\ \gamma 4$$

$$\sqrt{\kappa^2 (-4. \beta + \kappa^2)}\ \lambda + 1.4142135623730951$$

2.718281828459045`

$$\gamma + 1.4142135623730951 \quad \gamma \sqrt{\kappa^2 - 1.} \sqrt{\kappa^2 (-4. \beta + \kappa^2)} + 0.7071067811865475 \quad \gamma \sqrt{\kappa^2 + \sqrt{\kappa^2 (-4. \beta + \kappa^2)}} + \gamma \left(-1. \gamma - 0.7071067811865475 \sqrt{\kappa^2 - 1.} \sqrt{\kappa^2 (-4. \beta + \kappa^2)} \right.$$

$$R\ \beta\ \kappa 2\ \sqrt{\kappa^2 (-4. \beta + \kappa^2)}\ \lambda + 1.4142135623730951$$

2.718281828459045`

$$2. \gamma + \gamma \gamma + 1.4142135623730951 \quad \gamma \sqrt{\kappa^2 - 1.} \sqrt{\kappa^2 (-4. \beta + \kappa^2)} + 0.7071067811865475 \quad \gamma \sqrt{\kappa^2 + \sqrt{\kappa^2 (-4. \beta + \kappa^2)}} + \gamma \left(-1. \gamma - 0.7071067811865475 \sqrt{\kappa^2 - 1.} \sqrt{\kappa^2 (-4.} \right.$$

$$R\ \beta\ \kappa 2\ \sqrt{\kappa^2 (-4. \beta + \kappa^2)}\ \lambda + 1.4142135623730951$$

2.718281828459045`

$$\gamma + 0.7071067811865475 \quad \gamma \sqrt{\kappa^2 + \sqrt{\kappa^2 (-4. \beta + \kappa^2)}} + \gamma \left(-1. \gamma + 0.7071067811865475 \sqrt{\kappa^2 - 1.} \sqrt{\kappa^2 (-4. \beta + \kappa^2)} \right) R\ \beta\ \kappa 2$$

$$\sqrt{\kappa^2 (-4. \beta + \kappa^2)}\ \lambda + 1.4142135623730951$$

2.718281828459045`

$$2. \gamma + \gamma \gamma + 0.7071067811865475 \quad \gamma \sqrt{\kappa^2 + \sqrt{\kappa^2 (-4. \beta + \kappa^2)}} + \gamma \left(-1. \gamma + 0.7071067811865475 \sqrt{\kappa^2 - 1.} \sqrt{\kappa^2 (-4. \beta + \kappa^2)} \right) R\ \beta\ \kappa 2$$

$$\sqrt{\kappa^2 (-4. \beta + \kappa^2)}\ \lambda - 1.\ 1.4142135623730951$$

2.718281828459045`

$$\gamma + 0.7071067811865475 \quad \gamma \sqrt{\kappa^2 - 1.} \sqrt{\kappa^2 (-4. \beta + \kappa^2)} + 1.4142135623730951 \quad \gamma \sqrt{\kappa^2 + \sqrt{\kappa^2 (-4. \beta + \kappa^2)}} + \gamma \left(-1. \gamma - 0.7071067811865475 \sqrt{\kappa^2 + \sqrt{\kappa^2 (-4. \beta + \kappa^2)}} \right)$$

$$R\ \beta\ \kappa 2\ \sqrt{\kappa^2 (-4. \beta + \kappa^2)}\ \lambda - 1.\ 1.4142135623730951$$

2.718281828459045`

$$2. \gamma + \gamma \gamma + 0.7071067811865475 \quad \gamma \sqrt{\kappa^2 - 1.} \sqrt{\kappa^2 (-4. \beta + \kappa^2)} + 1.4142135623730951 \quad \gamma \sqrt{\kappa^2 + \sqrt{\kappa^2 (-4. \beta + \kappa^2)}} + \gamma \left(-1. \gamma - 0.7071067811865475 \sqrt{\kappa^2 + \sqrt{\kappa^2 (-4. \beta + \kappa^2} \right.$$

$$R\ \beta\ \kappa 2\ \sqrt{\kappa^2 (-4. \beta + \kappa^2)}\ \lambda - 1.\ 1.4142135623730951$$

2.718281828459045`

$$\gamma + 0.7071067811865475 \quad \gamma \sqrt{\kappa^2 - 1.} \sqrt{\kappa^2 (-4. \beta + \kappa^2)} + \gamma \left(-1. \gamma + 0.7071067811865475 \sqrt{\kappa^2 + \sqrt{\kappa^2 (-4. \beta + \kappa^2)}} \right) R\ \beta\ \kappa 2$$

$$\sqrt{\kappa^2 (-4. \beta + \kappa^2)}\ \lambda - 1.\ 1.4142135623730951$$

2.718281828459045`

$$2. \gamma + \gamma \gamma + 0.7071067811865475 \quad \gamma \sqrt{\kappa^2 - 1.} \sqrt{\kappa^2 (-4. \beta + \kappa^2)} + \gamma \left(-1. \gamma + 0.7071067811865475 \sqrt{\kappa^2 + \sqrt{\kappa^2 (-4. \beta + \kappa^2)}} \right) R\ \beta\ \kappa 2$$

$\sqrt{\kappa^2\,(-4.`\,\beta+\kappa^2)}$ λ-1.` 1.4142135623730951`

2.718281828459045^

```
y γ+1.4142135623730951`  y √(κ^2-1.` √(κ^2 (-4.` β+κ^2))) +0.7071067811865475`  y √(κ^2+√(κ^2 (-4.` β+κ^2))) +y (-1.` γ-0.7071067811865475`  √(κ^2-1.` √(κ^2 (-4.` β+κ^2)
```

R γ2 κ2 $\sqrt{\kappa^2\,(-4.`\,\beta+\kappa^2)}$ λ-1.` 1.4142135623730951`

2.718281828459045^

```
2.` γ+y γ+1.4142135623730951`  y √(κ^2-1.` √(κ^2 (-4.` β+κ^2))) +0.7071067811865475`  y √(κ^2+√(κ^2 (-4.` β+κ^2))) +y (-1.` γ-0.7071067811865475`  √(κ^2-1.` √(κ^2 (-4.`
```

R γ2 κ2 $\sqrt{\kappa^2\,(-4.`\,\beta+\kappa^2)}$ λ-1.` 1.4142135623730951`

2.718281828459045^

```
y γ+0.7071067811865475`  y √(κ^2+√(κ^2 (-4.` β+κ^2))) +y (-1.` γ+0.7071067811865475`  √(κ^2-1.` √(κ^2 (-4.` β+κ^2))))
```

R γ2 κ2 $\sqrt{\kappa^2\,(-4.`\,\beta+\kappa^2)}$ λ-1.` 1.4142135623730951`

2.718281828459045^

```
2.` γ+y γ+0.7071067811865475`  y √(κ^2+√(κ^2 (-4.` β+κ^2))) +y (-1.` γ+0.7071067811865475`  √(κ^2-1.` √(κ^2 (-4.` β+κ^2))))
```

R γ2 κ2 $\sqrt{\kappa^2\,(-4.`\,\beta+\kappa^2)}$ λ+1.4142135623730951`

2.718281828459045^

```
y γ+0.7071067811865475`  y √(κ^2-1.` √(κ^2 (-4.` β+κ^2))) +1.4142135623730951`  y √(κ^2+√(κ^2 (-4.` β+κ^2))) +y (-1.` γ-0.7071067811865475`  √(κ^2+√(κ^2 (-4.` β+κ^2))))
```

R γ2 κ2 $\sqrt{\kappa^2\,(-4.`\,\beta+\kappa^2)}$ λ+1.4142135623730951`

2.718281828459045^

```
2.` γ+y γ+0.7071067811865475`  y √(κ^2-1.` √(κ^2 (-4.` β+κ^2))) +1.4142135623730951`  y √(κ^2+√(κ^2 (-4.` β+κ^2))) +y (-1.` γ-0.7071067811865475`  √(κ^2+√(κ^2 (-4.` β+κ^2
```

R γ2 κ2 $\sqrt{\kappa^2\,(-4.`\,\beta+\kappa^2)}$ λ+1.4142135623730951`

2.718281828459045^

```
y γ+0.7071067811865475`  y √(κ^2-1.` √(κ^2 (-4.` β+κ^2))) +y (-1.` γ+0.7071067811865475`  √(κ^2+√(κ^2 (-4.` β+κ^2))))
```

R γ2 κ2 $\sqrt{\kappa^2\,(-4.`\,\beta+\kappa^2)}$ λ+1.4142135623730951`

2.718281828459045^

```
2.` γ+y γ+0.7071067811865475`  y √(κ^2-1.` √(κ^2 (-4.` β+κ^2))) +y (-1.` γ+0.7071067811865475`  √(κ^2+√(κ^2 (-4.` β+κ^2))))
```

R γ2 κ2 $\sqrt{\kappa^2\,(-4.`\,\beta+\kappa^2)}$ λ))/((1.` +2.718281828459045`^(2.` γ) β (-4.` β+κ2)) (-2.` γ+1.4142135623730951` $\sqrt{\kappa^2-1.`\,\sqrt{\kappa^2\,(-4.`\,\beta+\kappa^2)}}$ ) (2.` γ+1.4142135623730951` $\sqrt{\kappa^2-1.`\,\sqrt{\kappa^2\,(-4.`\,\beta+\kappa^2)}}$ ) (-2.` γ+1.4142135623730951` $\sqrt{\kappa^2+\sqrt{\kappa^2\,(-4.`\,\beta+\kappa^2)}}$)

$$(2.` \gamma+1.4142135623730951` \sqrt{\kappa^2+\sqrt{\kappa^2\left(-4.` \beta+\kappa^2\right)}}))) /. \beta->(Ha^2+S^2+I*\omega*R) /. \gamma 2->(\delta 2+I*\omega*Pe) /. y->z$$

APPENDIX 2

Articles already published, accepted or submitted for publication

[1] Adesanya, S.O., Makhalemele, C.R., Rundora, L. 2018. *Natural convection flow of heat generating hydromagnetic couple stress fluid with time periodic boundary conditions*, Alexandria Engineering Journal 57, 1977 – 1989.

[2] Makhalemele, C.R., Adesanya, S.O., Rundora L. *Convective flow of hydromagnetic couple stress fluid with varying heating through vertical channel*, Design and Application of Engineering. Submitted in March 2020

[3] Makhalemele, C.R., Rundora, L., Adesanya, S.O. *Mixed convective flow of unsteady hydromagnetic couple stress fluid through a vertical channel filled with porous medium.* Accepted in July 2020

APPENDIX 3

Acceptance letters

Ms. Ref. No.: IJAME-2002
Title: MIXED CONVECTIVE FLOW OF UNSTEADY HYDROMAGNETIC COUPLE STRESS FLUID THROUGH A VERTICAL CHANNEL FILLED WITH POROUS MEDIUM
International Journal of Applied Mechanics and Engineering
Research Paper

Dear Sir,

I am pleased to inform you that your paper entitled
" MIXED CONVECTIVE FLOW OF UNSTEADY HYDROMAGNETIC COUPLE STRESS FLUID THROUGH A VERTICAL CHANNEL FILLED WITH POROUS MEDIUM "
has been accepted for publication in International Journal of Applied Mechanics and Engineering by reviewers.
Paper selected for publication in IJAME are subject to a mandatory charge of $200 before publication (The confirmation of payment is required).

There are all information to pay:
Account name: University of Zielona Góra
Bank Name and Branch: Bank Millennium S.A. O/Zielona Góra
Account numbe and IBAN: PL 88 1160 2202 0000 0000 6021 8954
SWIFT CODE: (BIGBPLPW)
for “IJAME-2002”

After that the paper will be waiting for the language editor comments.
Thank you for submitting your work to International Journal of Applied Mechanics and Engineering.

Yours faithfully
Paweł Jurczak
--
Editor-in-Chief
International Journal of Applied Mechanics and Engineering
Szafrana Street 4, 65-246 Zielona Góra

REFERENCES

[1] Abbas, Z., Hasnain, J., Sajid, M. 2014. *Hydromagnetic mixed convective two-phase flow of couple stress and viscous fluids in an inclined channel*, Z. Naturforsch, 69a, 553-561.

[2] Abbas, Z., Wang, Y., Hayat, T., Oberlack, M. 2008. *Hydromagnetic flow in a viscoelastic fluid due to the oscillatory stretching surface*, International Journal of Non-Linear Mechanics 43 (8), 783 - 793.

[3] Adesanya, S.O. 2015. *Free convective flow of heat generating fluid through a porous vertical channel with velocity slip and temperature jump*, Ain Shams Engineering Journal 6, 1045–1052

[4] Adesanya, S.O., Falade, A.J., Rach, R. 2015. *Effect of Couple Stresses on Hydromagnetic Eyring–Powell Fluid Flow Through A Porous Channel,* Theoretical and Applied Mechanics 42 (2), 135–150.

[5] Adesanya, S.O., Kareem, S.O., Falade, A.J., Arekete, S.A. 2015. *Entropy generation analysis for a reactive couple stress fluid flow through a channel saturated with porous material*, Energy 93, 1239 – 1245.

[6] Adesanya, S.O., Makhalemele, C.R., Rundora, L. 2018. *Natural convection flow of heat generating hydromagnetic couple stress fluid with time periodic boundary conditions*, Alexandria Engineering Journal 57, 1977 – 1989.

[7] Adesanya, S.O., Makinde, O.D. 2012. *Heat transfer to magnetohydrodynamic non-Newtonian couple stress pulsatile flow between two parallel porous plates*, Z.Naturforsch 67a, 647- 656.

[8] Adesanya, S.O., Makinde, O.D. 2014. *Entropy generation in a couple stress fluid flow through porous channel with fluid slippage*, International Journal of Energy 15 (3), 344-362.

[9] Adesanya, S.O., Makinde, O.D. 2014. *MHD oscillatory slip flow and heat transfer in a channel filled with porous media,* U.P.B.Sci.Bull., Series A. 76 (1), 197 – 204.

[10] Adesanya, S.O., Makinde, O.D. 2015. *Effects of couple stresses on entropy generation rate in a porous channel with convective heating.* Comp Appl Math 34,293-307.

[11] Adesanya, S.O., Makinde, O.D. 2015. *Irreversibility analysis in a couple stress film flow along an inclined heated plate with adiabatic free surface*. Phys A 432, 222-229.

[12] Adesanya, S.O., Oluwadare, E.O., Falade, J.A., Makinde, O.D. 2015. *Hydromagnetic natural convection flow between vertical parallel plates with time-periodic boundary conditions*, Journal of Magnetism and Magnetic Materials 396, 295-303.

[13] Adomian, G., Rach, R. 1993. *Inversion of nonlinear stochastic operators*, J. Math. Anal. Appl. 91(1), 39–46.

[14] Adomian, G., Rach, R. 1996. *Modified Adomian polynomials*, Math. Comput. Modelling 24(11), 39–46.

[15] Ahmed, S. 2010. *Induced magnetic field with radiating fluid over a porous vertical plate*: analytical study, Journal of Naval Architecture and Marine Engineering 7, 83-94.

[16] Ahmed, S., Anwar Bég, O., Ghosh, S.K. 2014. *A couple stress fluid modeling on free convection oscillatory hydromagnetic flow in an inclined rotating channel*, Ain Shams Engineering Journal, 5(4), 1249-1265.

[17] Ahmed, M.S., Mohammed, A.E. 2008. *Effect of hall currents and chemical reaction on hydromagnetic flow of a stretching vertical surface with internal heat generation/absorption*, Appl. Math. Model 32,1236-1254 .

[18] Ahmed, S., Zueco, J., López-González, L.M. 2017. *Effects of chemical reaction, heat and mass transfer and viscous dissipation over a MHD flow in a vertical porous wall using perturbation method*, International Journal of Heat and Mass Transfer 104, 409–418.

[19] Akhtar, S., Ali Shah, N. 2016. *Exact solutions for some unsteady flows of a couple stress fluid between parallel plates,* http://dx.doi.org/10.1016/j.asej.2016.05.008.

[20] Akrama, S., Nadeem, S. 2013. *Influence of induced magnetic field and heat transfer on the peristaltic motion of a Jeffrey fluid in an asymmetric channel: Closed form solutions*, Journal of Magnetism and Magnetic Materials 328, 11–20.

[21] Aksoy, Y. 2016. *Effects of couple stresses on the heat transfer and entropy generation rates for a flow between parallel plates with constant heat flux*, International Journal of Thermal Sciences 107, 1–12.

[22] Ali, N., Khan, S.U., Sajid, M., Abbas, Z. 2016. *MHD flow and heat transfer of couple stress fluid over an oscillatory stretching sheet with heat source/sink in porous medium*, Alexandria Engineering Journal 55 (2), 915-924.

[23] Anderson Jr., J.D. 2009. *Computational fluid dynamics*, National air and space museum, Smithsonian Institution, Washington DC. 3rd edition.

[24] Animasaun, I.L., Raju, C.S.K., Sandeep, N. 2016. *Unequal diffusivities case of homogeneous -heterogeneous reactions within viscoelastic fluid flow in the presence of induced magnetic-field and nonlinear thermal radiation*, Alexandria Engineering Journal 55, 1595–1606.

[25] Bashtovoi, V., Motsar, A., Reks, A. 2017. *Energy dissipation in a finite volume of magnetic fluid*, Journal of Magnetism and Magnetic Materials 43, 245–248.

[26] Bég, A.O., Ghosh, S.K., Ahmed, S., Bég, A.T. 2012. *Mathematical modeling of oscillatory magneto-convection of a couple-stress biofluid in an inclined rotating channel,* Journal of Mechanics in Medicine and Biology 12 (30), 1250050.

[27] Blanford, R.D., Thorne, K.S. 2005. *Applications of Classical Physics*, California Institute of Technology. www.pma.caltech.edu/courses/ph136. [Retrieved on 25 June 2016].

[28] Blazek, J. 2005. *Computational fluid dynamics: principle and applications,* 2nd Edition. Https://doi.org/10.1016/B978-008044506-9/50004-7. Chapter 2, 5-28.

[29] Branover, H., Unger, Y. 2020. *Metallurgical technologies, energy conversion and magnetohydrodynamics flows,* Progress in Astronautics and Aeronautics148, https:// public.ebookcentral.proquest.com.

[30] Casson, N. 1959. *A flow equation for pigment oil-suspensions of the printing ink type,* Rheology of Disperse Systems, C.C. Mill ed., Pergamon Press, London.

[31] Cogley, A.C., Vincenti, W.G., Gilles, S.E. 1968. *Differential approximation for radiative transfer in a non-grey gas near equilibrium,* AIAA J. 6, 551 - 553.

[32] Cortell, R. 2007. *MHD flow and mass transfer of an electrically conducting fluid of species*, Chemical Engineering and Processing 46 (8), 721-728.

[33] Das, S., Jana, R.N. 2014. *Entropy generation due to MHD flow in a porous channel with Navier slip*, Ain Shams Eng. J. 5, 575–584.

[34] Devakar, M., Sreenivasu, D., Shankar, B. 2014. *Analytical solutions of couple stress fluid flows with slip boundary conditions*, Alexandria Engineering Journal 53, 723 – 730.

[35] Devika, B., Satya Narayana, P.V., Venkataramana, S. 2013. *MHD oscillatory flow of a visco-elastic fluid in a porous channel with chemical reaction,* International Journal of Engineering Science Invention 2(2), 26 – 35.

[36] Djavareshkian, F.T., Talati, F., Ghasemi, A., Sohrabi, S. 2008. *Multidimensional combustion simulation and analytical solution of wall heat conduction in DI diesel engine*, Journal of Applied Sciences, 8(21): 3806-3816

[37] Dorch S.B.F. 2007. Magnetohydrodynamics, doi: 10.4249/scholarpedia.2295, 2(4).

[38] Duan, J.S., Rach, R. 2011. *A new modification of the Adomian decomposition method for solving boundary value problems for higher order differential equations*, Appl. Math. Comput. 218(8), 4090–4118.

[39] Eldabe, N.T.M., Hassan, A.A., Mohamed Mona, A.A. 2003. *Effect of couple stresses on the MHD of a non-Newtonian unsteady flow between two parallel porous plates*, Zeitschrift für Naturforschung, A, 58a: 204 - 210.

[40] Falade, A.J., Ukaegbu, J.C., Egere, A.C., Adesanya, S.O. 2017. *MHD oscillatory flow through a porous channel saturated with porous medium*, Alexandria Engineering Journal 56,147 – 152.

[41] Falade, J.A., Adesanya, S.O., Ukaegbu, J.C., Osinowo, M.O. 2016. *Entropy generation analysis for variable viscous couple stress fluid flow through a channel with non-uniform wall temperature*, Alexandria Engineering Journal 55, 69-75.

[42] Farlow, S.J. 1993. *Partial differential equations for scientists and engineers*, New York Dover Publications, Inc.

[43] Farooq M., Rahim M.T., Islam S., Siddiqui A.M. 2013. *Steady poiseuille flow and heat transfer of couple stress fluids between two parallel inclined plates with variable viscosity,* Journal of the association of Arab universities for basic applied sciences 14, 9-18.

[44] Foraboschi F.P., Federico I.D. 1964. *Heat transfer in laminar flow of non-Newtonian heat generating fluids*, Int. J. Heat Mass Transfer 7, 315

[45] Fosdick, R.L., Rajagopal, K.R. 1980. *Thermodynamics and stability of fluids of third grade*, Proceedings of the Royal Society of London, Series A, Mathematical and Physical Sciences 369(1738), 351 – 377.

[46] Fox, R.W., MacDonald, A.T., Pritchard, P.J. 2004. *Introduction to fluid mechanics*, 6th edition, John Wiley & Sons Inc, USA.

[47] Garg, B.P., Singh, K.D., Bansal, A.K. 2014. *An oscillatory MHD convective flow of visco-elastic fluid through porous medium filled in a rotating vertical porous channel with heat radiation*, IJEIT 3(12), 273 – 281.

[48] Ghosh, S.K., Anwar Bég, O., Zueco, J. 2010. *Hydromagnetic free convection flow with induced magnetic field effects*, Meccanica 45, 175–185.

[49] Gireesha, B.J., Mahanthesh, B., Shivakumara, I.S., Eshwarappa, K.M. 2016. *Melting heat transfer in boundary layer stagnation-point flow of nanofluid toward a stretching sheet with induced magnetic field*, Engineering Science and Technology, an International Journal 19, 313–321.

[50] Hartmann, J. 1937. *Theory of laminar flow of an electrically conducting liquid in a homogeneous field*, Hg-Dynamics I Math Fys Med 15, 1-28.

[51] Hassan, A.R. 2020. *The entropy generation analysis of a reactive hydromagnetic couple stress fluid flow through a saturated porous channel,* Applied Mathematics and Computation 369, 124843 (10 pages).

[52] Hassan, A.R., Fenuga, O.J. 2019. *The effects of thermal radiation on the flow of a reactive hydromagnetic heat generating couple stress fluid through a porous channel*, SN Applied Sciences 1,1278 https://doi.org/10.1007/s42452-019-1300-z.

[53] Hayat, T., Awais, M., Safdar, A., Hendi, A.A. 2012. *Unsteady three dimensional flow of couple stress fluid over a stretching surface with chemical reaction,* Nonlinear Analysis: Modelling and Control, 17(1), 47–59.

[54] Hayat, T., Muhammad, T., Alsaedi, A. 2017. *On three-dimensional flow of couple stress fluid with Cattaneo-Christov heat flux*, DOI: 10.1016/j.cjph.2017.03.003, to appear in: Chinese Journal of Physics.

[55] Hayat, T., Noreen, S., Shabab Alhothuali, M., Asghar, S., Alhomaidan, A. 2012. *Peristaltic flow under the effects of an induced magnetic field and heat and mass transfer, International Journal of Heat and Mass Transfer* 55 (1–3, 15), 443–452.

[56] Hayat, Y., Wang, K., Hutter, C. 2004. *Hall effects on the unsteady hydromagnetic oscillatory flow of a second-grade fluid*, International Journal of Non-Linear Mechanics 39 (6), 1027–1037.

[57] Hina, S., Mustafa, M., Hayat, T. 2015. *On the exact solution for peristaltic flow of couple-stress fluid with wall properties,* Bulgarian Chemical Communications, 47 (1), 30 – 37.

[58] Hussein A.M, Dawood H.K, Bakara R.A, Kadirgamaa K. 2017. *Numerical study on turbulent forced convective heat transfer using nanofluids TiO2 in an automotive cooling system*, Case studies in thermal engineering 9, 72-78.

[59] Ibrahim, W. 2016. *The effect of induced magnetic field and convective boundary condition on MHD stagnation point flow and heat transfer of upper-convected Maxwell fluid in the presence of nanoparticle past a stretching sheet,* Propulsion and Power Research 5,164–175.

[60] Iqbal, Z., Azhar, E., Maraj, E.N. 2017. *Transport phenomena of carbon nanotubes and bioconvection nanoparticles on stagnation point flow in presence of induced magnetic field*, Physica E 91, 128–135.

[61] Issa, B., Obaidat, I.M., Albiss, B.A., Haik, Y. 2013. *Magnetic Nanoparticles: Surface Effects and Properties Related to Biomedicine Applications*, Int. J. Mol. Sci. 14, 21266-21305.

[62] Jacobson, M.Z. 1998. *Fundamentals of atmospheric modelling*, Cambridge University Press, Cambridge.

[63] Jha, B.K., Ajibade, A.O. 2009. *Free convective flow of heat generating/absorbing fluid between vertical porous plates with periodic heat input*, International Communications in Heat and Mass Transfer 36, 624–631.

[64] Jha, B.K., Ajibade, A.O. 2010. *Free convective flow between vertical porous plates with periodic heat input,* ZAMM-Journal of applied mathematics, Z Angew Math Mech, 1–9. http://dx.doi.org/10.1002/zamm.200900268.

[65] Jha, B.K., Ajibade, A.O. 2012. *Effect of viscous dissipation on Natural convection flow between vertical parallel plates with time-periodic boundary conditions*, Communications in Nonlinear Science and Numerical Simulation 17, 1576-1587.

[66] Kaladhar, K. 2015. *Natural Convection Flow of Couple Stress Fluid in a Vertical Channel with Hall and Joule Heating Effects,* Procedia Engineering 127, 1071 – 1078.

[67] Kaladhar, K., Motsa, S.S., Srinivasacharya, D. 2016. *Mixed Convection Flow of Couple Stress Fluid in a Vertical Channel with Radiation and Soret Effects*, Journal of Applied Fluid Mechanics 9, 43-50.

[68] Kalpana, M., Bhuvana Vijaya, R. 2018. *Hall effects on MHD oscillatory flow on non-Newtonian fluid through porous medium in a vertical channel with suction/injection*, International Journal of Applied Engineering Research 14(21), 3960 – 3967.

[69] Kareem, S.O., Adesanya, S.O., Vincent, U.E. 2016. *Second law analysis for hydromagnetic couple stress fluid flow through a porous channel*, Alexandria Engineering Journal 55 (2), 925-931.

[70] Kataria, H.R., Patel, H.R., Rajiv, S. 2017. *Effect of magnetic field on unsteady natural convective flow of a micropolar fluid between two vertical walls*, Ain Shams Engineering Journal 8, 87–102.

[71] Khaled, A.R.A., Vafai, K. 2003. *The role of porous media in modelling flow and heat transfer in biological tissues*, Int. J. Heat and Mass Transfer 46, 4989 – 5003.

[72] Kumar, A., Singh, A.K. 2013. *Unsteady MHD free convective flow past a semi-infinite vertical wall with induced magnetic field,* Applied Mathematics and Computation 222, 462–471.

[73] Kumar, A., Singh, A.K. 2016. *Effects of heat source/sink and induced magnetic field on natural convective flow in vertical concentric annuli*, Alexandria Engineering Journal 55, 3125–3133.

[74] Landau, L.D., Lifshitz, E.M. 1987. *Fluid mechanics*, Institute of physical problems, USSR Academy of sciences, 2nd Edition.

[75] Lienhard IV, J.H., Lienhard V, J.H. 2019. *A heat transfer text book*, Massachusets Institute of Technology, Version 5.00, 784.

[76] Mahabaleshwar, U.S., Sarris, I.E., Hill, A.A., Giulio Lorenzini, Ioan Pop, 2017. *An MHD couple stress fluid due to a perforated sheet undergoing linear stretching with heat transfer*, International Journal of Heat and Mass Transfer 105,157–167.

[77] Makinde, O.D. 2011. *Similarity solution for natural convection from a moving vertical plate with internal heat generation and a convective boundary condition*, Therm. Sci. 15 (1), 137 – 143.

[78] Makinde, O.D., Eegunjobi, A.S. 2013. *Entropy generation in a couple stress fluid flow through vertical channel filled with saturated porous media*, Entropy 15, 4589-4606.

[79] Meade, D.B., Haran, B.S., White, R.E. 1996. *The Shooting Technique for the Solution of Two-point Boundary Value Problems*, Maple Tech 3(1), 85-93.

[80] Mehmood, A., Ali, A. 2007. *The effect of slip condition on unsteady MHD oscillatory flow of a viscous fluid in a planer channel*. Rom J Phys 52, 85–91.

[81] Mehmood, Z. Iqbal, Z. 2016. *Interaction of induced Magnetic Field and Stagnation Point Flow on Bioconvection Nanofluid Submerged in Gyrotactic Microorganisms*, doi:10.1016/j.molliq.2016.10.014, To appear in Journal of Molecular Liquids.

[82] Mekheimer, Kh.S. 2008. *Effect of the induced magnetic field on peristaltic flow of a couple stress fluid*, Physics Letters A 372, 4271-4278.

[83] Misra, J.C., Adhikary, S.D. 2016. *MHD oscillatory channel flow, heat and mass transfer in a physiological fluid in presence of chemical reaction,* Alexandria Engineering Journal 55, 287 – 297.

[84] Muthuraj, R., Srinivas, S., Immaculate, D.L. 2012. *Combined effects of chemical reaction and temperature dependent heat source on MHD mixed convective flow of a couple stress fluid in a vertical wavy porous space with travelling thermal waves*, CI&CEQ 18(2), 305 - 314.

[85] Nabil EL-Dabe, T.M., Salwa EL-Mohandis, M.G. 1995. *Effect of couple stresses on pulsatile hydromagnetic poiseuille flow,* Fluid Dynamics Research 15, 313 -324.

[86] Najeeb, A.K., Khan, H., Ali, S.A. 2016. *Exact solutions for MHD flow of couple stress fluid with heat transfer*, Journal of the Egyptian Mathematical Society 24, 125–129.

[87] Nandya, S.K. Tapas Ray Mahapatra, Loan Pop, 2015. *Unsteady separated stagnation-point flow over a moving porous plate in the presence of a variable magnetic field,* European Journal of Mechanics B/Fluids 53, 229–240.

[88] Nasir, A., Khan, S.U., Sajid, M., Abbas, Z. 2016. *MHD flow and heat transfer of couple stress fluid over an oscillatory stretching sheet with heat source/sink in porous medium*, Alexandria Engineering Journal 55, 915–924.

[89] Nayak, A., Dash, G.C. 2015. *Magnetohydrodynamic couple stress fluid flow through a porous medium in a rotating channel,* Journal of Engineering Thermophysics 24(3), 283 – 295.

[90] Noreen, S., Hayat, T., Alsaedi, A. 2011. *Study of slip and induced magnetic field on the peristaltic flow of pseudoplastic fluid,* International Journal of Physical Sciences 6(36), 8018-8026.

[91] Ojjela, O., Raju, A., Kashyap Kambhatla, P. 2017. *Influence of thermophoresis and induced magnetic field on chemically reacting mixed convective flow of Jeffrey fluid between porous parallel plates*, doi: 10.1016/j.molliq.2017.02.061. To appear in Journal of Molecular Liquids.

[92] Padma, G., Suneetha, S.V. 2018. *Hall effects on MHD flow through porous medium in a rotating parallel plate channel,* International Journal of Applied Engineering Research 13(11), 9772 – 9789.

[93] Parekh, K., Upadhyay, R.V. 2016. *The effect of magnetic field induced aggregates on ultrasound propagation in aqueous magnetic fluid*, http://dx.doi.org/10.1016/j. jmmm.2016.08.024i.

[94] Purusothaman, A., Chamkha, A.J. 2019. *Combined effects of mechanical vibration and magnetic field on the onset of buoyancy-driven convection in an anisotropic porous module,* J. Porous Media 22(11), 1411 – 1422.

[95] Rach, R. 1984. *A convenient computational form for the Adomian polynomials,* J. Math. Anal. Appl. 102(2), 415–419.

[96] Rach, R. 2008. *A new definition of the Adomian polynomials,* Kybernetes 37(7), 910–955.

[97] Rach, R. 2012. *A bibliography of the theory and applications of the Adomian decomposition method*, 1961-2011, Kybernetes 41(7/8), 1087–1148.

[98] Raju, C.S.K., Sandeep, N., Saleem, S. 2016. *Effects of induced magnetic field and homogeneous–heterogeneous reactions on stagnation flow of a Casson fluid*, Engineering Science and Technology, an International Journal 19, 875–887.

[99] Raju, M.C., Varma, S.V.K., Seshaiah, B. 2015. *Heat transfer effects on a viscous dissipative fluid flow past a vertical plate in the presence of induced magnetic field*, Ain Shams Engineering Journal 6, 333–339,

[100] Ramachandraiah, V., Nagaradhika, V., Sivaprasad, R., Subba Rao, A., Rajendra, P. 2018. *MHD effects on peristaltic flow of a couple stress fluid in a channel with permeable walls*, IJMTT 58(1), 24 – 37.

[101] Ramana Murthy, J.V., Srinivas, J., Sai, K.S. 2014. *Second law analysis of the flow of two immiscible couple stress fluids in four zones*, 10th International Conference on Heat Transfer, Fluid Mechanics and Thermodynamics, 1034 – 1043.

[102] Ramana Murthy, J.V., Srinivas, J. 2015. *First and second law analysis for the MHD flow of two immiscible couple stress fluids between two parallel plates*, Heat transfer-Asian Research, 44(5).

[103] Ravi Kumar, S. 2015. *The effect of the couple stress fluid flow on MHD peristaltic motion with uniform porous medium in the presence of slip effect*, JJMIE 9(4), 269 – 278.

[104] Rienstra, S.W., Hirschberg, A. 2004. *An introduction to acoustics*, Eindhoven University of Technology.

[105] Rimbault, B., Nguyen, C.T., Galanis, N. 2014. *Experimental investigation of CuO-water nanofluid flow and heat transfer inside a micro-channel heat sink*, Int. J. Therm. Sci. 84, 275 – 292

[106] Rundora, L., Makinde, O.D. 2018. *Buoyancy effects on unsteady reactive variable properties fluid flow in a channel filled with a porous medium*, J. Porous Media 21(8), 721 - 737.

[107] Saleem, N., Hayat, T., Alsaedi, A. 2012. *Effects of induced magnetic field and slip condition on peristaltic transport with heat and mass transfer in a non-uniform channel,* International Journal of the Physical Sciences 7(2),191 – 204.

[108] Salem, A.M., Abd El-Aziz, M., Abo-Eldahab, E.M., Abd-Elfatah I. 2009. *Effect of variable density on hydromagnetic mixed convection flow of non-Newtonian fluid past*

a moving vertical plate, Communications in Nonlinear Science and Numerical Simulation. 15, 1485-1493.

[109] Sankad, G.C., Nagathan, P.S. 2017. *Transport of MHD couple stress fluid through peristalsis in a porous medium under the influence of heat transfer and slip effects*, Int. J. Applied Mechanics and Engineering 22(2), 403 – 414.

[110] Saravanan, S., Brindha, D. 2011. *Global nonlinear stability of convection in a heat generating fluid filled channel with a moving boundary*, Appl. Math. Lett. 24, 487-493.

[111] Shehraz, A., Nehad, A.S. 2016. *Exact solutions for some unsteady flows of a couple stress fluid between parallel plates,* Engineering Physics and Mathematics, http://dx.doi.org/10.1016/j.asej.2016.05.008.

[112] Sheikholeslami, M. 2017. *Magnetic field influence on nanofluid thermal radiation in a cavity with tilted elliptic inner cylinder,* J. Mol. Liq. 229, 137 – 147.

[113] Sheikholeslami, M., Chamkha, A.J. 2017. *Influence of Lorentz forces on nanofluid forced convection considering Joule heating effect*, J. Mol. Liq. 225, 750 – 757.

[114] Sheikholeslami, M., Ganji, D.D. 2016. *Nanofluid hydrothermal behavior in existence of Lorentz forces considering Joule heating effect*, Journal of Molecular Liquids 224, 526–537.

[115] Sheikholeslami, M., Ganji, D.D. 2016. *Nanfluid convective heat transfer using semi analytical and numerical approaches: a review*, J. Taiwan Inst. Chem. Eng. 65, 43 – 77.

[116] Sheikholeslami, M., Ganji, D.D. 2015. *Entropy generation of nanofluid in presence of magnetic field using Lattice Boltzmann method*, Phys. A 417, 273 – 286.

[117] Sheikholeslami, M., Ganji, D.D. 2014. *Ferrohydrodynamic and magnetohydrodynamic effects on ferrofluid flow and convective heat transfer*, Energy 75, 400 – 410.

[118] Sheikholeslami, M., Ganji, D.D., Ashorynejad, H.R. 2013. *Investigation of squeezing unsteady nanofluid flow using ADM,* Powder Technol. 239, 259–265.

[119] Sheikholeslami, M., Ganji, D.D., Ashorynejad, H.R., Rokni, H.B. 2012. *Analytical investigation of Jeffery-Hamel flow with high magnetic field and nano particle by Adomian decomposition method,* Appl. Math. Mech.-Engl. Ed. 33(1), 1553-1564.

[120] Sheikholeslami, M., Ganji, D.D., Javed, M.Y., Ellahi, R. 2015. *Effect of thermal radiation on magnetohydrodynamics nanofluid flow and heat transfer by means of two phase model*, J. Magn. Magn. Mater. 374, 36 – 43.

[121] Sheikholeslami, M., Ganji, D.D., Rashidi, M.M. 2016. *Magnetic field effect on unsteady nanofluid flow and heat transfer using Buongiorno model*, J. Magn. Mater, 16, 164 – 173.

[122] Sheikholeslami, M., Rashidi, M.M., Hayat, T., Ganji, D.D. 2016. *Free convection of magnetic nanofluid considering MFD viscosity effect*, J. Mol. Liq. 218, 393 – 399.

[123] Sheikholeslami, M., Rokni, H.B. 2017. *Nanofluid two face model analysis in existence of induced magnetic field,* Int. J. Heat Mass Transf. 107, 288 – 299.

[124] Sheikholeslami, M., Shehzad, S.A. 2017. *Magnetohydrodynamics nanofluid convection in a porous enclosure considering heat flux boundary condition,* Int. J. Heat Mass Transf. 106, 1261 – 1269.

[125] Sheikholeslami, M., Zaigham Zia, Q. M., Ellahi, R. 2016. *Influence of Induced Magnetic Field on Free Convection of Nanofluid Considering Koo-Kleinstreuer-Li (KKL) Correlation,* Appl. Sci. 6, 324.

[126] Shih, Y.C. 2009. *Introduction to differential analysis of fluid motion*. Fluid mechanics, chapter 5.

[127] Siddiqui, A.M., Hameed, M., Siddiqui, B.M., Ghori, Q.K. 2010. *Use of Adomian decomposition method in the study of parallel plate flow of a third grade fluid,* Communications in Nonlinear Science and Numerical Simulation 15(9), 2388–2399.

[128] Sinha, A., Misra, J.C. 2014. *Effect of Induced Magnetic Field on Magnetohydrodynamic Stagnation Point Flow and Heat Transfer on a Stretching Sheet,* Journal of Heat Transfer, ASME 136 (11),112701 (11 pages).

[129] Sochi, T. 2010. *Non-Newtonian Flow in Porous Media*, Polymer 51 5007-5023.

[130] Srinivas, J., Adesanya, S.O., Falade, J.A., Gajjela, N. 2017. *Entropy generation analysis for a radiative micropolar fluid flow through a vertical channel saturated with*

non-Darcian porous medium, International Journal of Applied and Computational Mathematics 4, 3759.

[131] Srinivas, J., Adesanya, S.O., Ogunseye, H.A., Lebelo, R.S. 2018. *Couple stress fluid flow with variable properties*: *A second law analysis*, Mathematical Methods in Applied Sciences, DOI: 10.1002/mma.5325, 1-14

[132] Srinivas, J., Anwar Bég, O. 2018. *Homotopy study of entropy generation in magnetized micropolar flow in a vertical parallel plate channel with buoyancy effect*, Heat Transfer Research 49, 529-553

[133] Srinivas, J., Ramana Murthy, J.V. 2016. *Thermal analysis of a flow of immiscible couple stress fluids in a channel,* Journal of Applied Mechanics and Technical Physics 57(9), 97–1005.

134] Srinivas, J., Ramana Murthy, J.V., Ali J Chamkha, 2016. *Analysis of entropy generation in an inclined channel flow containing two immiscible micropolar fluids using HAM*, International Journal of Numerical Methods for Heat & Fluid Flow 26, 1027-1049.

[135] Srinivasacharya, D., Kaladhar, K. 2012. *Mixed convection flow of couple stress fluid between parallel vertical plates with Hall and Ion-slip effects*, Commun. Nonlinear Sci. Numer. Simulat. 17, 2447–2462.

[136] Srinivasacharya, D., Kaladhar, K. 2014. *Mixed Convection Flow of Chemically Reacting Couple Stress Fluid in a Vertical Channel with Soret and Dufour Effects,* International Journal for Computational Methods in Engineering Science and Mechanics 15, 413 - 421

[137] Srinivasacharya, D., Madhava Rao, G. 2016. *Computational analysis of magnetic effects on pulsatile flow of couple stress fluid through a bifurcated artery*, Computer Methods and Programs in Biomedicine 137, 269–279.

[138] Srinivasacharya D., Ram Reddy C.H., 2011. *Soret and Dufour effects on mixed convection in a non-Darcy porous medium saturated with micropolar fluid,* Nonlinear Analysis: Modelling and Control 16(1), 100–115.

[139] Srinivasacharya, D., Srikanth, D. 2008. *Effect of couple stresses on the pulsatile flow through a constricted annulus*, C. R. Mecanique 336, 820–827.

[140] Srinivasacharya, D., Srinivasacharyulu, N., Odelu, O. 2009. *Flow and heat transfer of couple stress fluid in a porous channel with expanding and contracting walls*, International Communications in Heat and Mass Transfer 36, 180–185.

[141] Stokes, V.K. 1966. *Couple stresses in fluid,* Physics of Fluids 9, 1709–1715.

[142] Tasawar, H., Iqbal, Z., Qasim, M., Aldossary, O.M. 2012. *Heat transfer in a Couple Stress Fluid over a Continuous Moving Surface with Internal Heat Generation and Convective Boundary Conditions*, Z. Naturforsch. 67a, 217 – 224 / DOI: 10.5560/ZNA.2012-0021.

[143] Torabi, M., Karimi, N., Zhang, K. 2015. *Heat transfer and second law analyses of forced convection in a channel partially filled by porous media and featuring internal heat sources*, Energy 93, 106 – 127

[144] Turner, J.S. 1973. *Buoyancy effects in fluids*, Cambridge University Press, UK.

[145] Vafai, K. 2015. *Handbook of porous media, 3rd ed.*, CRC Press Online.

[146] Veera Krishna, M., Chand Basha, S. 2016. *MHD Free Convection three dimensional flow through a porous medium between two vertical plates*, IOSR Journal of Mathematics 12(1), 88 – 105.

[147] Veera Krishna, M., Subba Reddy, G., Chamkha, A.J. 2018. *Hall effects on unsteady MHD oscillatory free convective flow of second grade fluid through porous medium between two vertical plates*, Phys. Fluids 30, 023106-1 – 9.

[148] Wang, C.Y. 1988a. *Buoyancy-Induced flows in porous media,* Computers and Mathematics with Applications 16 (4), 297 - 305.

[149] Wang, C.Y. 1988b. *Free convection between vertical plates with periodic heat input*. ASME J Heat Trans 110, 508–511.

[150] Wang, C.Y. 1988c. *Nonlinear streaming due to the oscillatory stretching of a sheet in a viscous*, Acta Mech. 72, 261–268.

[151] Xuan, Y., Li, Q. 2000. *Heat transfer enhancement of nanofluids,* International Journal of Heat and Fluid Flow, 21 (1), 58 – 64.

[152] Zueco, J., Bég, O.A. 2009. *Network numerical simulation applied to pulsatile non-Newtonian flow through a channel with couple stress and wall mass flux effects*, International Journal of Applied Mathematics and Mechanics 5(2), 1 - 16.